Doctoral Thesis

Particle Phenomenology of Compact Extra Dimensions

Henrik Melbéus

Theoretical Particle Physics, Department of Theoretical Physics,
School of Engineering Sciences
KTH Royal Institute of Technology, SE-106 91 Stockholm, Sweden

Stockholm, Sweden 2012

Typeset in LaTeX

Akademisk avhandling för avläggande av teknologie doktorsexamen (TeknD) inom ämnesområdet teoretisk fysik.

Scientific thesis for the degree of Doctor of Philosophy (PhD) in the subject area of Theoretical physics.

ISBN 978-91-7501-305-3

TRITA-FYS 2012:16
ISSN 0280-316X
ISRN KTH/FYS/--12:16--SE

Printed in Sweden by Universitetsservice US AB, Stockholm April 2012

Abstract

This thesis is an investigation of the subject of extra dimensions in particle physics. In recent years, there has been a large interest in this subject. In particular, a number of models have been suggested that provide solutions to some of the problem with the current Standard Model of particle physics. These models typically give rise to experimental signatures around the TeV energy scale, which means that they could be tested in the next generation of high-energy experiments, such as the LHC. Among the most important of these models are the universal extra dimensions model, the large extra dimensions model by Arkani-Hamed, Dimopolous, and Dvali, and models where right-handed neutrinos propagate in the extra dimensions.

In the thesis, we study phenomenological aspects of these models, or simple modifications of them. In particular, we focus on Kaluza–Klein dark matter in universal extra dimensions models, different aspects of neutrino physics in higher dimensions, and collider phenomenology of extra dimensions. In addition, we consider consequences of the enhanced renormalization group running of physical parameters in higher-dimensional models.

Key words: Higher-dimensional quantum field theories, universal extra dimensions, Arkani-Hamed–Dimopolous–Dvali (ADD) model, hierarchy problem, Kaluza–Klein dark matter, neutrino mass, seesaw mechanism, leptonic mixing, renormalization group running, collider phenomenology, Large Hadron Collider

Sammanfattning

Denna avhandling är en studie inom ämnet extra dimensioner i partikelfysik. Under senare år har det funnits ett stort intresse för detta ämne. I synnerhet har ett antal modeller föreslagits som tillhandahåller lösningar på några av problemen med den nuvarande standardmodellen för partikelfysik. Dessa modeller ger vanligtvis upphov till experimentella signaturer runt TeV-energiskalan, vilket innebär att de kan testas i nästa generation av högenergiexperiment, såsom LHC. Bland de viktigaste av dessa modeller är universella extra dimensioner, stora extra dimensioner, som har föreslagits av Arkani-Hamed, Dimopolous och Dvali, och modeller där högerhänta neutriner propagerar i de extra dimensionerna.

I avhandlingen studerar vi fenomenologiska aspekter av dessa modeller, eller enkla modifikationer av dem. Framför allt fokuserar vi på Kaluza–Klein-mörk materia i universella extra dimensioner, olika aspekter av neutrinofysik i högre dimensioner och acceleratorfenomenologi för extra dimensioner. Dessutom studerar vi konsekvenserna av det utökade renormeringsgruppslöpandet för fysikaliska parametrar i högredimensionella modeller.

Preface

This thesis is the result of my research at the Department of Theoretical Physics during the time period June 2007 to April 2012. The thesis is divided into two parts. The first part is an introduction to the subjects that form the basis for the scientific papers. These subjects include phenomenology of higher-dimensional field theories, dark matter, models of neutrino masses, and renormalization group running in extra dimensions. The second part consists of the eight scientific papers listed below.

List of papers

[1] Mattias Blennow, *Henrik Melbéus*, and Tommy Ohlsson
Neutrinos from Kaluza–Klein dark matter in the Sun
Journal of Cosmology and Astroparticle Physics **01**, 018 (2010)

[2] Johan Bonnevier, *Henrik Melbéus*, Alexander Merle, and Tommy Ohlsson
Monoenergetic gamma-rays from non-minimal Kaluza–Klein dark matter annihilations
Physical Review D **85**, 043524 (2012)

[3] *Henrik Melbéus*, Alexander Merle, and Tommy Ohlsson
Continuum photon spectrum from Z^1Z^1 annihilations in universal extra dimensions
Physics Letters B **706**, 329-332 (2012)

[4] *Henrik Melbéus*, Alexander Merle, and Tommy Ohlsson
Higgs Kaluza–Klein dark matter in universal extra dimensions
Manuscript

[5] Mattias Blennow, *Henrik Melbéus*, Tommy Ohlsson, and He Zhang
Signatures from an extra-dimensional seesaw model
Physical Review D **82**, 045023 (2010)

[6] Mattias Blennow, *Henrik Melbéus*, Tommy Ohlsson, and He Zhang
Renormalization group running of the neutrino mass operator in extra dimensions
Journal of High Energy Physics **04**, 052 (2011)

[7] Mattias Blennow, *Henrik Melbéus*, Tommy Ohlsson, and He Zhang
RG running in UEDs in light of recent LHC Higgs mass bounds
Submitted for publication.

[8] *Henrik Melbéus* and Tommy Ohlsson
Searches for hyperbolic extra dimensions at the LHC
Journal of High Energy Physics **08**, 077 (2008)

The thesis author's contribution to the papers

[1] I performed most of the analytical and numerical calculations. I also produced the figures and did most of the writing.

[2] The idea for this project was mine. The calculations were first performed by Johan Bonnevier and later independently checked by me, with some additions. I wrote most of the text.

[3] I provided the model-specific input and took part in the writing.

[4] I performed a part of the analytical calculations, some of which were also independently done by Alexander Merle. I also did the numerical computations, including the implementation of the relevant parts of the model, and did most of the writing.

[5] I performed the calculations of collider signatures in Sec. IV and did part of the writing.

[6] The analytical calculations were performed independently by me and He Zhang. I also did part of the writing.

[7] The work was divided equally among the authors. Specifically, I provided the input on the Higgs sector in the UED model, and I also did part of the writing.

[8] I performed the analytical and numerical calculations. I also produced the figures and did most of the writing.

List of acronyms

ACT	Air Cherenkov telescope
ADD	Arkani-Hamed–Dimopolous–Dvali
BLT	Boundary localized term
CDM	Cold dark matter
CL	Confidence level
CMBR	Cosmic microwave background radiation
DM	Dark matter
EFT	Effective field theory
EWPO	Electroweak precision observable
EWSB	Electroweak symmetry breaking
FLRW	Friedmann–Lemaître–Robertson–Walker
GWS	Glashow–Weinberg–Salam
KK	Kaluza–Klein
KKDM	Kaluza–Klein dark matter
LEP	Large electron-positron collider
LKP	Lightest Kaluza–Klein particle
LHC	Large hadron collider
MACHO	Massive compact halo object
MOND	Modified Newtonian dynamics
MUED	Minimal universal extra dimensions
NFW	Navarro–Frenk–White
PMNS	Pontecorvo–Maki–Nakagawa–Sakata
QCD	Quantum chromodynamics
QED	Quantum electrodynamics
QFT	Quantum field theory
RG	Renormalization group
RS	Randall–Sundrum
SM	Standard model
SSB	Spontaneous symmetry breaking
UED	Universal extra dimensions
UV	Ultraviolet
VEV	Vacuum expectation value
WIMP	Weakly interacting massive particle

Notation and conventions

Throughout this thesis, we use the Einstein summation convention, *i.e.*, we implicitly sum over pairs of indices, unless otherwise stated.

Ordinary four-dimensional spacetime indices are denoted by lower-case Greek letters, extra-dimensional spacetime indices by lower-case Roman letters, and general spacetime indices of the higher-dimensional spacetime by upper-case Roman letter.

The sign convention for the Minkowski metric and its generalization is given by $(g_{\mu\nu}) = \mathrm{diag}(1, -1, -1, -1)$.

We use natural units, setting $c = \hbar = 1$.

Acknowledgments

First of all, I would like to thank my supervisor Tommy Ohlsson for giving me the opportunity to do research in theoretical particle physics, for the collaboration that has resulted in the eight papers in this thesis, and for the careful proof-reading of the thesis. Thanks a lot for these past five years!

Special thanks are due to Alexander Merle, Johan Bonnevier, Mattias Blennow, and He Zhang for the fruitful collaborations that have resulted in the papers in this thesis. I also want to especially thank Mattias and Alex for inviting me to Munich and Heidelberg.

To my other friends and colleagues at the department, present and former, thank you for contributing to a nice working environment: Jonas, for the nice running company and all the related discussions (but not for beating my 10 km record time!); Stella, for introducing me to Sherlock and `oioioi.se`; Johannes, for the valuable advice on typesetting subscripts; Sofia, Farrokh, Edwin, Michal, and everyone else. I also have to thank our coffee machine, which has been invaluable during the time it has been with us.

Thanks also to Tomas Hällgren, who introduced me to the subject of extra dimensions when I did my diploma thesis at the department.

Moving outside the world of physics, I want to thank my friends—you know who you are.

Very special thanks to my family: my parents-in-law Sven and Tinna and sisters-in-law Malin and Jenny; my dog Yoshi, who is a constant source of love and laughter; my sister Johanna, who has always been a great friend; my parents, Ronny and Ulla, who have always supported me and encouraged me to do what I want with my life.

Finally, I want to express my warmest thanks to my wife Camilla, for all your invaluable support and love. I love you deeply.

Henrik Melbéus
Stockholm, April 2012

Contents

Part I

Introduction and background material

Chapter 1

Introduction

I'm a physicist. I have a working knowledge of the entire Universe and everything it contains.
— Sheldon Cooper

While few non-fictional physicists would claim to have such a full grasp of Nature, the above quote captures the essence of the subject of physics. Generally speaking, the aim of physics is to obtain a description of Nature under a large variety of different circumstances, ranging from the evolution of the Universe as a whole down to the very smallest distance scales. Such a description is obtained by making experiments and observations of different phenomena, finding patterns in the experimental data, and using these patterns to formulate mathematical models. These models must be able to make well-defined predictions, so that they can be tested against the results of other experiments in order to assess the validity of the models in different contexts. In this way, some models will be rejected, and others will have to be extended in order to expand their range of validity. Ultimately, any physical model is judged by its ability to properly describe the behavior of Nature.

In this thesis, we are interested in a description of Nature in terms of its fundamental building blocks and the interactions among them. These building blocks are the elementary particles, and the subject area is known as particle physics. According to the theory of quantum physics, high energies are needed in order to study small distance scales, and hence, particle physics also goes under the name high-energy physics.

One of the most successful ways of experimentally probing the regime of particle physics is to accelerate particles to very high energies and collide them. In such collisions, extremely high energy densities can be achieved, and these energies can be converted into mass, thus creating new particles. By studying the properties of these particles, information on high-energy physics can be obtained. In order to produce a particle in a collision, an energy at least large enough to create the rest mass of the particle is needed. Hence, in order to reveal increasingly heavy

particles, the energy available in accelerators has to be successively increased. Since interactions among elementary particles are also described in terms of particles, the same principle applies for finding new types of interactions. As technology is developed, the maximum energy that can be reached increases, and in this way, higher energy regimes in particle physics are successively probed.

A considerable experimental and theoretical effort during the 20th century led to the formulation of the so-called Standard Model of particle physics in the beginning of the 1970's. The Standard Model is one of the most successful physical models ever constructed. Remarkably, with few exceptions, it has remained unchanged for the last forty years. A number of particles that were predicted by the Standard Model but were not yet experimentally detected at the time when it was formulated have since been confirmed to exist and to have the expected properties. Some examples are the Z and W bosons, the top quark, and the tau neutrino. The only particle proposed by the Standard Model that has not yet been detected is the so-called Higgs boson, which emerges as a result of the way particles obtain their masses in the Standard Model.

In addition to particle collisions, particles are naturally created in high-energy environments in the Universe, such as stars and supernovae. Although heavy particles are typically unstable and decay long before reaching the Earth, important information could be obtained from the patterns of their stable decay products. These cosmic particles can be searched for in astrophysical experiments, and such methods are becoming increasingly important. The backside of astrophysical experiments is that it is not possible to control the sources of the particles, but only to make observations. Part of the experimental analysis then consists of determining the source of the observed particles, which introduces additional uncertainty. On the other hand, the energies available in the astrophysical context can be larger by far than what could be achieved in man-made accelerators, and in this sense, astrophysical experiments and accelerators are complementary to one another.

Also from the theoretical side, particle physics is becoming increasingly interconnected with the subject areas of astrophysics and cosmology. A particular example is the subject of dark matter, where cosmological observations imply that there exist massive particles that have not yet been detected [9]. Since none of the particles in the Standard Model can constitute this dark matter, these observations point towards new physics that lies beyond the Standard Model. Elementary particles can also be used as probes of celestial objects, such as stars and supernovae. In particular, neutrinos, which are weakly interacting and can escape the dense and hot environments of such objects, play an important role in this context.

Although the Standard Model successfully describes most observed particle physics phenomena up to the highest energy scales that have been reached, there are a number of important exceptions. The dark matter problem mentioned above is one such problem, and another problem is related to the properties of neutrinos. In the Standard Model, neutrinos are massless, but observations of neutrino flavor oscillations indicate that this is in fact not the case [10–13]. Hence, these observations point towards the need for an extension of the model. The Standard Model

also suffers from a number of problems from a theoretical point of view. Most importantly, it does not include the gravitational interaction, which is difficult to describe on a quantum physical level. Another problem, known as the hierarchy problem, is that the mass of the Higgs boson seems to be unnaturally small in relation to the high-energy scale where gravity becomes strong. Finally, the Standard Model includes a large number of parameters that are not determined by the model, but have to be experimentally measured. A more fundamental theory would be expected to reveal relations between these parameters, decreasing their number to only a few. After a more technical introduction to the Standard Model in Ch. 2, we will give a more detailed description of those problems with the model that are important for this thesis.

In order to resolve the problems with the Standard Model, a number of extensions of the model have been proposed. Two important examples are supersymmetric models [14], where each particle in the Standard Model is accompanied by a heavy so-called superpartner, and grand unified theories [15], which attempt to describe the different interactions in the Standard Model as manifestations of a single unified interaction, which emerges at very high energies. At present, a problem is that experimental data that could discriminate among these models have been lacking for many years. Interestingly, general considerations, as well as several of the suggested models, predict the existence of new physics close to the energy scale that the next generation of particle physics experiments will be able to probe.

The prime example of such an experiment is the Large Hadron Collider (LHC) at CERN in Geneva, Switzerland, which has been collecting data from high-energy proton collisions for one year. The LHC is quickly covering ground at energy scales beyond the current boundaries, and will help to bring new understanding to the field. In particular, the main goal of the LHC is the detection of the Higgs bosons. So far, no conclusive evidence for its existence has been obtained, but large ranges for its mass have been excluded, with only a small region remaining. A large effort is also being made to search for extensions of the Standard Model at the LHC.

In order to understand the implications of the data that the LHC and other experiments produce, it is of fundamental importance to work out the specific experimental signals that different models would give rise to. Most of the predicted new particles beyond the Standard Model are expected either to decay into other particles before they can be measured in detectors or to be extremely weakly interacting, so that they escape detection altogether. However, through measurements of other particles, that are produced at the same time, the existence of the new particles can be indirectly inferred. A major problem in this context is that it is not possible to "turn off" the well-known interactions of the Standard Model that are already well established. Hence, new physics signals are generally plagued by a large number of background events, and it is an important task to find signatures of the new physics phenomena that are as "clean" as possible. Finally, different models often give rise to very similar signatures, meaning that even if an observed event is established as a new physics signal, the problem still remains of determining which model that best describes the observation. Similar problems exist in astrophysical

experiments. The branch of particle physics working to bridge the gap between theoretical models and experimental results is known as phenomenology.

One way of extending the Standard Model is through the use of additional spatial dimensions. As we perceive the world, it is made up of three spatial and one temporal dimension, and no deviations from this notion have been experimentally observed. However, in principle, there could be more than three spatial dimensions, provided that, by some mechanism, the extra dimensions are hidden up to the energy scales that have been experimentally probed. Such a mechanism was proposed by Oskar Klein in 1926 [16]. He pointed out that if the extra dimensions are finite and small in size, large energies would be needed in order to resolve them. Klein, together with Theodor Kaluza [17], pioneered the subject of extra dimensions in the 1920's, and the subject generally goes under the name Kaluza–Klein theory.

In recent years, the subject of extra dimensions has received much attention, in large part inspired by string theory, which requires the existence of ten or eleven dimensions [18]. In particular, several models have been suggested which could be tested in the next generation of experiments, such as the LHC. These models provide solutions to different problems with the Standard Model, such as the dark matter problem and the hierarchy problem. In this thesis, we consider the phenomenology of a number of such extensions of the Standard Model in different contexts.

With the advent of the LHC, particle physics is finally being explored beyond the regime of the Standard Model. Hopefully, the coming years will provide answers to questions that have been asked in particle physics for a long time, and the nature of the extension of the Standard Model beyond its current limits will be revealed. Whether it will be extra dimensions, supersymmetry, or something completely different, it will surely be an exciting time for particle physicists.

1.1 Overview of the thesis

The rest of Part I of the thesis has the following structure. In Ch. 2, we give a more detailed description of the Standard Model of particle physics. In Ch. 3, we briefly introduce the subject of neutrino physics. Then, in Ch. 4, we discuss the general features of higher-dimensional quantum field theories. Next, in Ch. 5, we introduce the universal extra dimensions model, including the construction of a realistic models and its phenomenological consequences. In Ch. 6, we discuss the ADD model of large extra dimensions and models of neutrinos in extra dimensions. Then, in Ch. 7, we present the subject of dark matter, focusing on dark matter models in the context of extra dimensions. Finally, in Ch. 8, we summarize Part I of the thesis and discuss the main results of the scientific papers that are presented in Part II.

Chapter 2

The Standard Model of particle physics

The Standard Model (SM) of particle physics is currently the most well-established and accurate description of Nature on the smallest known distance scale. It describes three of the four known fundamental interactions in Nature—the strong, the weak, and the electromagnetic.

We begin this chapter with an overview of the particles and interactions in the SM. We specifically consider the Higgs sector, with a particular emphasis on the Higgs mechanism and the experimental bounds on the Higgs boson. Then, we discuss some of the problems of the SM that are of particular importance for this thesis. Finally, we discuss how the SM might be considered as an effective field theory (EFT), which is the low-energy approximation of some more fundamental theory.

2.1 Particles and interactions

The SM is a gauge theory, which is based on the gauge group $SU(3)_{\mathrm{c}} \otimes SU(2)_{\mathrm{L}} \otimes U(1)_{\mathrm{Y}}$. The $SU(2)_{\mathrm{L}} \otimes U(1)_{\mathrm{Y}}$ sector describes the Glashow–Weinberg–Salam (GWS) model of the electroweak interactions. Here, the subscript L stands for "left", indicating that the $SU(2)_{\mathrm{L}}$ sector acts only on left-handed fermions, and Y stands for the weak hypercharge, which is an Abelian quantum number. At energies lower than the electroweak scale, $M_{\mathrm{EW}} \simeq 246$ GeV, the GWS sector is broken by the Higgs mechanism to $U(1)_{\mathrm{Q}}$ of quantum electrodynamics (QED), where Q is the electric charge. Corresponding to the GWS sector, there is an Abelian gauge boson B_μ and a non-Abelian $SU(2)_{\mathrm{L}}$ triplet W^i_μ, $i = 1, 2, 3$, which act as mediators of the electroweak interactions. The $SU(3)_{\mathrm{c}}$ sector describes quantum chromodynamics (QCD), which is the theory of the strong interactions. The subscript c stands for "color", which is the name given to the quantum number of this non-Abelian gauge

group. The gauge bosons corresponding to this sector are the eight gluons g^a_μ, $a = 1, \ldots, 8$, which are $SU(3)_\mathrm{c}$ octets.

In addition to the twelve gauge bosons, the SM includes twelve spin-1/2 fermions and their corresponding antiparticles. These particles make up the matter content of the SM, and they are divided into six quarks,

$$\begin{pmatrix} u \\ d \end{pmatrix}, \quad \begin{pmatrix} c \\ s \end{pmatrix}, \quad \begin{pmatrix} t \\ b \end{pmatrix},$$

which interact strongly as well as electroweakly, and six leptons,

$$\begin{pmatrix} \nu_e \\ e^- \end{pmatrix}, \quad \begin{pmatrix} \nu_\mu \\ \mu^- \end{pmatrix}, \quad \begin{pmatrix} \nu_\tau \\ \tau^- \end{pmatrix},$$

which interact only electroweakly. As indicated above, the quarks and leptons are grouped into three generations, which are complete replicas of each other except for the masses of the particles.

Finally, the SM includes a complex scalar $SU(2)_\mathrm{L}$ doublet $\Phi = (H^+ \, H^0)^T$ known as the Higgs doublet. The role of the Higgs doublet in the SM is to dynamically generate the masses of all the particles, through the so-called Higgs mechanism. Of all the particles in the SM, the Higgs boson is the only one that has not been experimentally detected. In fact, there are a number of possible ways of generating the particle masses in the SM [19], and the Higgs mechanism as described here is only the simplest possibility. In this thesis, we will not consider any other possibility. The Higgs mechanism and the currently ongoing searches for the Higgs boson at the LHC and the Tevatron are described in Sec. 2.2.

The structure of the SM, *i.e.*, its particle content and the interactions among these particles, is strongly dictated by gauge invariance. Once the gauge group is specified, the only freedom left in the theory is the choice of the structure of the scalar sector, including the interactions between scalars and fermions, and the choices of gauge group representations for the fermions and scalars, which determine how these particles interact with the gauge bosons. In addition, the choices of fermion representations are highly restricted by quantum anomalies, which must cancel in order for the theory to be internally consistent [20]. In particular, once the left-handed quarks, which transform non-trivially under all sectors of the gauge group, are included, anomaly cancellations require the existence of all the other SM fermions [21].

We will describe the gauge interactions in terms of a general gauge field A^a_μ, where a is a gauge group index. The gauge sector is described by the Yang–Mills Lagrangian,

$$\mathcal{L}_\mathrm{YM} = -\frac{1}{4} F^a_{\mu\nu} F^{a,\mu\nu}, \tag{2.1}$$

where

$$F^a_{\mu\nu} = \partial_\mu A^a_\nu - \partial_\nu A^a_\mu - g f^{abc} A^b_\mu A^c_\nu \tag{2.2}$$

is the field-strength tensor. Here, g is the gauge coupling constant, and the symbols f^{abc} are the structure constants of the gauge group. The Yang–Mills Lagrangian

is determined by gauge invariance, and it describes all the interactions among the gauge fields. However, it does not describe the masses of the weak gauge bosons, which are dynamically generated by interactions of these fields with the Higgs field.

The interactions between the gauge bosons and a fermion ψ is given by the term

$$\mathcal{L}_{\text{fermion}} = \mathrm{i}\overline{\psi}\gamma^{\mu}D_{\mu}\psi, \tag{2.3}$$

which is obtained by replacing the derivative ∂_μ in the kinetic term for a free fermion field by the so-called covariant derivative,

$$D_{\mu} = \partial_{\mu} + \mathrm{i}gA^{a}_{\mu}T^{a}_{\psi}, \tag{2.4}$$

in order to preserve gauge invariance. Here, T^a_ψ are the generators of the gauge group in the representation that ψ belongs to. This replacement gives rise to an interaction term of the form

$$\mathcal{L}_{\text{fermion-gauge}} = -g\overline{\psi}\gamma^{\mu}A^{a}_{\mu}T^{a}_{\psi}\psi. \tag{2.5}$$

Hence, the interactions between fermions and gauge bosons are completely determined once the gauge structure and fermion representations have been chosen.

A particular feature of the fermion interactions in the SM is that they are chiral, *i.e.*, the left- and right-handed parts of each fermion have different interactions with the gauge bosons. Specifically, the left-handed fermions are $SU(2)_{\text{L}}$ doublets, while the right-handed ones are singlets. Written in terms of the $SU(2)_{\text{L}}$ structure, the fermions are

$$Q_{i\text{L}} = \begin{pmatrix} u_{i\text{L}} \\ d_{i\text{L}} \end{pmatrix}, \quad u_{i\text{R}} \quad , d_{i\text{R}}, \quad L_{i\text{L}} = \begin{pmatrix} \nu_{i\text{L}} \\ l^{-}_{i\text{L}} \end{pmatrix}, \quad e_{i\text{R}},$$

where $i = 1, 2, 3$ is a generation index. Note that there are no right-handed neutrinos in the SM, which implies that neutrinos are massless.

The Higgs sector is given by

$$\mathcal{L}_{\text{Higgs}} = |D_{\mu}\Phi|^2 - V(\Phi), \tag{2.6}$$

where, as for the fermions, the partial derivative has been replaced by a covariant derivative in order to preserve gauge invariance. The Higgs potential $V(\Phi)$ is given by

$$V(\Phi) = -\mu^2|\Phi|^2 + \frac{\lambda}{2}|\Phi|^4. \tag{2.7}$$

This is the most general renormalizable form of the potential for a complex scalar field.

Finally, the interactions between the Higgs field and the fermions are Yukawa interactions, which are given by the Lagrangian

$$\mathcal{L}_{\text{Yukawa}} = -Y_u^{ij}\overline{Q_{i\text{L}}}\tilde{\Phi}u_{j\text{R}} - Y_d^{ij}\overline{Q_{i\text{L}}}\Phi d_{j\text{R}} - Y_e^{ij}\overline{L_{i\text{L}}}\Phi e_{j\text{R}} + \text{h.c.}, \tag{2.8}$$

where $\tilde{\Phi} = \mathrm{i}\tau_2\Phi^*$ is the conjugate of the Higgs field, and τ_2 is the second Pauli matrix.

Together, Eqs. (2.1), (2.3), (2.6), and (2.8) describe all the interactions in the SM. It is noteworthy that these interactions constitute all the possible renormalizable interactions among scalars, spin-1/2 fermions, and gauge bosons in four space-time dimensions [20].

2.2 The Higgs sector

2.2.1 The Higgs mechanism

The Higgs potential (2.7) has its minimum at

$$|\Phi| = \sqrt{\frac{\mu^2}{\lambda}} \equiv v \simeq 246 \text{ GeV}. \tag{2.9}$$

This minimum defines the vacuum expectation value (VEV) of the Higgs field, and the physical states are the excitations of the field around this point. Using standard conventions, we have

$$\Phi = \begin{pmatrix} H^+ \\ \frac{1}{\sqrt{2}}(H + v + \mathrm{i}A^0) \end{pmatrix} = \begin{pmatrix} H^+ \\ \frac{1}{\sqrt{2}}(H + \mathrm{i}A^0) \end{pmatrix} + \begin{pmatrix} 0 \\ \frac{v}{\sqrt{2}} \end{pmatrix}. \tag{2.10}$$

Here, the lower component has been written in terms of two real scalar fields, and the real part $H+v$ is chosen in such a way that H is the excitation from the ground state given by the VEV v. Since the VEV picks out a particular component of the Higgs field, it is not $SU(2)_{\mathrm{L}}$ symmetric. A symmetry which is respected by the Lagrangian, but not by the ground state of a system, is said to be spontaneously broken, and the system is said to undergo a spontaneous symmetry breaking (SSB).

As an example which is more easily analyzed, yet contains the essential features of the Higgs mechanism, we consider a complex scalar field Φ interacting with an Abelian gauge field A_μ. Giving Φ the real VEV $\langle\Phi\rangle = v$, we write $\Phi = (H + v + \mathrm{i}\phi)/\sqrt{2}$, and obtain from the Higgs Lagrangian in Eq. (2.6)

$$\begin{aligned} \mathcal{L}_{\text{Higgs}} &= \frac{1}{2}(D_\mu\phi)^\dagger(D^\mu\phi) \\ &= \frac{1}{2}(\partial_\mu - \mathrm{i}gA_\mu)(H + v - \mathrm{i}\phi)(\partial^\mu + \mathrm{i}gA^\mu)(H + v + \mathrm{i}\phi) \\ &= \frac{1}{2}\partial_\mu H\partial^\mu H + \frac{1}{2}\partial_\mu\phi\partial^\mu\phi + \frac{1}{2}(gv)^2 A_\mu A^\mu - \mathrm{i}gvH\partial_\mu A^\mu \\ &\quad + \text{interaction terms}. \end{aligned} \tag{2.11}$$

The last of the quadratic terms in in Eq. (2.11) is a bilinear term mixing A_μ and the scalar ϕ. It can be removed by adding to the Lagrangian a gauge-fixing term of the form

$$\begin{aligned} \mathcal{L}_{\text{gf}} &= -\frac{1}{2\xi}\left(\partial_\mu A^\mu - \xi gv\phi\right)^2 \\ &= -\frac{1}{2\xi}\left(\partial_\mu A^\mu\right)^2 + gv\phi\partial_\mu A^\mu - \frac{1}{2}\left(\sqrt{\xi}gv\right)^2\phi^2. \end{aligned} \tag{2.12}$$

Gauge-fixing terms of this form, parametrized by ξ, define the so-called R_ξ gauges [20]. Adding the terms in Eqs. (2.11) and (2.12) to the Yang–Mills Lagrangian in Eq. (2.1), we obtain

$$\begin{aligned}\mathcal{L}_{\mathrm{YM}} + \mathcal{L}_{\mathrm{Higgs}} + \mathcal{L}_{\mathrm{gf}} &= -\frac{1}{4}F_{\mu\nu}F^{\mu\nu} + \frac{1}{2}m_A^2 A_\mu A^\mu - \frac{1}{2\xi}\left(\partial_\mu A^\mu\right)^2 \\ &\quad + \frac{1}{2}\partial_\mu H \partial^\mu H + \frac{1}{2}\partial_\mu \phi \partial^\mu \phi - \frac{1}{2}\left(\sqrt{\xi} m_A\right)^2 \phi^2 \\ &\quad + \text{interaction terms}, \end{aligned} \tag{2.13}$$

where $m_A \equiv gv$. Through the SSB, the gauge field A_μ has obtained a mass which is proportional to the VEV of the scalar field, and the imaginary part ϕ of the complex field Φ has obtained a gauge-dependent mass $m_\phi = \sqrt{\xi} m_A$. It is the Goldstone boson corresponding to the SSB, and it can be removed from the particle spectrum by choosing the unitary gauge, $\xi \to \infty$.

This generation of gauge boson masses through a SSB is known as the Higgs mechanism. After the SSB, only one of the two real components of the Higgs field remains as a physical scalar particle. The other component is said to be "eaten" by the gauge boson that gains a mass through the Higgs mechanism. Since a massive gauge boson has one more degree of freedom than a massless one, the total number of degrees of freedom is preserved by the SSB.

In the SM, the SSB that occurs when the Higgs field obtains its VEV gives rise to more complicated mass terms for the electroweak gauge bosons,

$$\mathcal{L}_{\mathrm{mass,gauge}} = \frac{1}{2}\frac{v^2}{4}\left[g^2 (W_\mu^1)^2 + g^2 (W_\mu^2)^2 + (-g W_\mu^3 + g' B_\mu)^2\right], \tag{2.14}$$

where g and g' are the $SU(2)_{\mathrm{L}}$ and $U(1)_{\mathrm{Y}}$ coupling constants, respectively. The two components W^1 and W^2 of the $SU(2)_{\mathrm{L}}$ gauge bosons obtain equal masses $m_W = gv/2$, and the linear combination

$$Z_\mu \equiv \frac{1}{\sqrt{g'^2 + g^2}}\left(-g W_\mu^3 + g' B_\mu\right), \tag{2.15}$$

known as the Z boson, obtains the mass $m_Z = \sqrt{g^2 + g'^2}\, v/2$. The orthogonal combination

$$A_\mu \equiv \frac{1}{\sqrt{g'^2 + g^2}}\left(g' W_\mu^3 + g B_\mu\right), \tag{2.16}$$

which remains massless, is identified as the photon. Corresponding to the three gauge bosons that obtain masses, three real components of the Higgs field are eaten, and a single real scalar field, the Higgs boson H, remains as a physical scalar. In terms of gauge groups, the VEV of the Higgs field breaks $SU(2)_{\mathrm{L}} \otimes U(1)_{\mathrm{Y}}$ to the Abelian gauge group $U(1)_{\mathrm{Q}}$, and the photon is the gauge boson corresponding to

this gauge group. Here, Q stands for ordinary electric charge. The electric charge is related to the quantum numbers of the unbroken gauge group by the relation

$$Q = T_3 + Y, \tag{2.17}$$

where T_3 is the third component of the weak isospin of $SU(2)_{\mathrm{L}}$.

The transformation of the gauge fields from the $\{W^3, B\}$ basis to the mass eigenstate basis $\{Z, A\}$ is given by

$$\begin{pmatrix} Z \\ A \end{pmatrix} = \begin{pmatrix} \cos\theta_{\mathrm{W}} & -\sin\theta_{\mathrm{W}} \\ \sin\theta_{\mathrm{W}} & \cos\theta_{\mathrm{W}} \end{pmatrix} \begin{pmatrix} W^3 \\ B \end{pmatrix}, \tag{2.18}$$

where the Weinberg angle θ_{W} is defined by $\tan\theta_{\mathrm{W}} = g'/g$. The W^1 and W^2 bosons are usually rotated into the states $W^{\pm}$, which are defined as

$$W_\mu^{\pm} = \frac{1}{\sqrt{2}}(W_\mu^1 \mp \mathrm{i}W_\mu^2). \tag{2.19}$$

Due to the chiral structure of the SM, fermion mass terms of the type

$$\mathcal{L}_{\mathrm{mass,fermion}} = m_\psi \overline{\psi_{\mathrm{L}}}\psi_{\mathrm{R}} + \mathrm{h.c.}, \tag{2.20}$$

where h.c. denotes the Hermitian conjugate, are not allowed by gauge invariance. However, similarly to the gauge bosons, masses for the fermions can be generated dynamically through their couplings to the Higgs doublet. When the Higgs field acquires its VEV, the Yukawa interactions given in Eq. (2.8) give rise to mass terms of the form

$$\mathcal{L}_{\mathrm{mass,fermion}} = m^{ij}\overline{\psi_{\mathrm{L}i}}\psi_{\mathrm{R}j} + \mathrm{h.c.}, \tag{2.21}$$

where

$$m^{ij} = \frac{1}{\sqrt{2}}Y^{ij}v. \tag{2.22}$$

Note that this mass matrix is generally not diagonal. This means that the weak eigenstates differ from the mass eigenstates, and induces mixing among the SM quarks.

2.2.2 Collider Higgs searches and bounds

The experimental verification of the existence of the Higgs boson is the last missing piece of the SM, and the main physics objective of the LHC. The only degree of freedom left in the SM Higgs sector, once the VEV has been measured, is the mass of the Higgs boson. Hence, the results of searches for the Higgs boson are presented as exclusion intervals for m_H. Using approximately 5 fb^{-1} of data each, the ATLAS [22] and CMS [23] experiments have explored the range 110 GeV $\leq m_H \leq$ 600 GeV without finding conclusive evidence for the Higgs boson. The main production

Analysis	$\mathcal{L}_{\text{int}}$	**Excluded regions** (95 % CL)
ATLAS search [22]	4.9 fb^{-1}	112.9 GeV $\leq m_H \leq$ 115.5 GeV 131 GeV $\leq m_H \leq$ 238 GeV 251 GeV $\leq m_H \leq$ 466 GeV
CMS search [23]	4.8 fb^{-1}	127 GeV $\leq m_H \leq$ 600 GeV
CDF / DØ [24]	10 fb^{-1}	100 GeV $\leq m_H \leq$ 106 GeV 147 GeV $\leq m_H \leq$ 179 GeV
LEP search [26]	2.5 fb^{-1}	114 GeV $\leq m_H$
LEP / Tevatron EWPO [25]		$m_H \leq$ 158 GeV

Table 2.1. Summary of the experimental bounds on the SM Higgs boson mass. Here, $\mathcal{L}_{\text{int}}$ denotes the total integrated luminosity used in each analysis.

channels for the Higgs boson at hadron colliders are gluon fusion, vector boson fusion, associated vector boson production, and production in association with top quarks. Among the decay products of the Higgs boson, the $\gamma\gamma$, $\tau^+\tau^-$, $b\overline{b}$, W^+W^-, and ZZ modes have been searched for.

In their analyzes, both ATLAS and CMS have found small excesses of events in the region around 125 GeV, which could be a first hint for the existence of the Higgs boson. In addition, in a combined analysis of 10 fb^{-1} of Tevatron collision data, the CDF and DØ collaborations found a similar excess in the range 115 GeV $\lesssim m_H \lesssim$ 135 GeV [24]. However, more data are needed to clarify whether or not the origin of these excesses is actually due to a SM Higgs boson.

In addition to the direct collider searches, the mass of the Higgs boson can be constrained by its contribution to well-measured electroweak precision observables (EWPOs), in particular the W and Z boson masses. A combined analysis of LEP and Tevatron data from 2010 gives the 95 % CL upper limit $m_H \leq$ 158 GeV [25]. However, it should be noted that these indirect constraints may be modified in extensions of the SM. This is the case in the universal extra dimensions (UED) model (see Ch. 5), where the contributions from additional particles are opposite to those from a heavy Higgs boson, relaxing the constraints.

In Table 2.1, we summarize the most important direct and indirect constraints on m_H.

2.3 Problems with the Standard Model

The SM is a very successful model of particle interactions up to energies at least of the order of 100 GeV. Below this energy scale, it successfully describes most observed particle physics phenomena, with a few important exceptions. However, it does suffer from a number of problems, of theoretical as well phenomenological nature. Most particle physicists do not believe the SM to be the final story, but rather the low-energy limit of some more fundamental theory. Such a theory should

provide solutions to the problems with the SM. Most extensions of the SM that are proposed aim to solve, or at least alleviate, one or more of these problems. Here, we mention only the problems that are of the most importance for this thesis.

2.3.1 Dark matter

Cosmological observations strongly indicate that the ordinary matter that is observed makes up only 5 % percent of the total energy in the Universe. Another 23 % consists of some unknown form of matter [9]. The hypothesis that conforms in the best way with the full body of experimental evidence for this anomaly is that this matter is due to one or more new particle species, known as dark matter (DM). Since none of the particles in the SM fit the experimental constraint on such a DM particle, this problem points towards new physics, beyond the SM. DM is described in more detail in Ch. 7.

2.3.2 Neutrino oscillations and masses

As mentioned above, the fact that there are no right-handed neutrinos in the SM implies that neutrinos are massless in this model. However, in 1998, the Super-Kamiokande experiment provided the first evidence for neutrino oscillations [10]. Since the standard oscillation mechanism demands that neutrinos are massive, this is another observation that points towards the need for an extension of the SM. We discuss neutrino physics, including oscillations and mass models, in Ch. 3.

2.3.3 Quantum gravity

Perhaps the most obvious sign that the SM is not a complete theory is that it completely neglects the gravitational interactions. In order to extend the SM to include this fourth interaction, a quantized description of gravity would be necessary. However, at energies around the electroweak scale, gravity is far weaker than the SM interactions. It is expected to become strong only for energies around the so-called Planck scale, $M_{\mathrm{Pl}} \simeq 10^{19}$ GeV, which is far from the energy scales that any experiment will be able to probe in the foreseeable future. This means that it is generally very difficult to experimentally test quantum theories of gravity, such as string theory. On the other hand, the fact that gravity is so weak means that it is a good approximation to neglect it in most particle physics contexts. In Sec. 6.1, we describe a model where the influence of gravity becomes important at energy scales much lower than generally expected.

2.3.4 The hierarchy problem

A problem of a more theoretical kind is related to the SM Higgs boson. All particles in an interacting quantum field theory (QFT) receive contributions to their bare masses, due to radiative corrections. For fermions and gauge bosons, these

corrections are mild, but for the Higgs boson, which is an elementary scalar field, this is not the case. If new physics appears at a high-energy scale Λ, the radiative corrections to the squared mass of a scalar field, δm^2, are expected to be proportional to Λ^2. Hence, the most natural value for the mass of such a field is of the same order of magnitude as Λ. For the SM, Λ is supposed to be no larger than the Planck scale. The so-called hierarchy problem can be formulated as the question of why the mass of the Higgs field is separated from the Planck scale by 17 orders of magnitude. In technical terms, this would mean that its bare mass m_{B}^2 would need to cancel the radiative correction δm^2 to a precision of 38 significant digits. Though not technically impossible, such a precise "fine-tuning" of the parameters seems highly unnatural, and a fundamental reason for this cancellation would be desirable. The most popular solution to this problem is provided by supersymmetric extensions of the SM [14], where new degrees of freedom cancel the quadratic contributions to scalar masses. Another possible solution is discussed in Sec. 6.1.

2.3.5 Fermion generations

As mentioned in the beginning of this chapter, the SM contains three generations of fermions, which are identical except for their masses. Within each generation, all particles are necessary in order to cancel quantum anomalies in the SM, but there is no clear reason why there should be more than one generation. It is believed by many physicists that this issue could be clarified in an extension of the SM. In one version of the UED model, which is described in Ch. 5, the existence of three generations is required by the cancellation of six-dimensional anomalies [27].

2.4 The Standard Model as an effective field theory

As mentioned above, all the interactions in the SM are renormalizable. In practical terms, this means that all the divergences appearing in the calculations of physical observables can be absorbed into a finite number of counterterms. Hence, only a finite number of measurements are needed in order to experimentally fix the parameters of a renormalizable model, and any additional measurements serve as tests of predictions of the model.

Historically, non-renormalizable theories have been considered as being unpredictive and useless. However, from a more modern point of view, non-renormalizability is seen only as a sign that a theory cannot naively be extrapolated to arbitrarily high energies. Such a theory is called an effective field theory (EFT). From this point of view, an EFT is perfectly acceptable within its range of validity. At some energy scale, known as the cutoff scale of the EFT, the theory breaks down, and has to be replaced by some more fundamental theory, known as the ultraviolet (UV) completion of the EFT. Typically, the UV completion includes new degrees of freedom.

From the EFT point of view, the SM Lagrangian is actually expected to contain higher-dimensional, non-renormalizable terms due to heavy degrees of freedom. Formally, this statement can be expressed as

$$\mathcal{L} = \mathcal{L}^{(d=4)} + \frac{c^{(5)}}{\Lambda}\mathcal{L}^{(d=5)} + \frac{c^{(6)}}{\Lambda^2}\mathcal{L}^{(d=6)} + \dots, \tag{2.23}$$

where Λ is a high-energy scale related to the fundamental theory, the constants $c^{(n)}$ are numerical coefficients, and d denotes the dimensionality of each term. The dimension-four term $\mathcal{L}^{(d=4)}$ is the ordinary SM Lagrangian. Since the operators of higher dimensions are suppressed by successively higher powers of the inverse of Λ, the importance of these operators decreases with increasing dimensionality, provided that the relevant coefficients are of a similar size. Although there are infinitely many terms in the expansion (2.23), only a finite number of them are relevant at a given energy scale, and hence, the theory can be renormalized order-by-order.

An example of a dimension-five operator, which is important for models of neutrino mass generation, is given in Ch. 3.

Chapter 3

Neutrino physics

Neutrino physics has emerged as one of the most interesting topics within the subject of particle physics. In particular, neutrino oscillations imply that neutrinos are massive, pointing to new physics beyond the SM. Considerable experimental and theoretical effort has been put into finding the answers to questions such as the origin of the light-neutrino masses, the Dirac or Majorana nature of neutrinos, and the absolute neutrino mass scale.

In this chapter, we give a basic introduction to this subject. We begin with a description of the phenomenon of neutrino oscillations, including experimental evidence and implications for neutrino masses. Next, we discuss neutrino mass terms and mechanisms that could generate small neutrino masses. Finally, we give an introduction to so-called non-unitarity effects in neutrino oscillations.

3.1 Neutrino oscillations

The first evidence for neutrino oscillations, *i.e.*, flavor transitions during propagation, was the so-called solar neutrino problem, the fact that measurements of the electron neutrino flux from the Sun did not agree with predictions from the well-established solar model [28]. Since the measured flux was smaller than expected, it was proposed that the deficit could be due to part of the emitted electron neutrinos oscillating into other flavors, which were not experimentally observed.

The first experiment providing strong evidence for neutrino oscillations was the Super-Kamiokande experiment, which in 1998 reported a deficit in the flux of atmospheric neutrinos which is in agreement with predictions taking neutrino oscillations into account [10]. In 2001, the results from the SNO experiment provided conclusive evidence for neutrino oscillations as the source of the solar neutrino problem [11]. Subsequently, a number of experiments, such as KamLAND [12, 13], MINOS [29], T2K [30], Daya Bay [31], and RENO [32] have confirmed these results and constrained the oscillation parameters.

Neutrinos are produced in weak interactions in the flavor eigenstates ν_e, ν_μ, and ν_τ. Oscillations between these flavors occur if neutrinos are massive and the mass eigenstates are rotated with respect to the flavor eigenstates, *i.e.*, if there is mixing in the lepton sector. Neutrino oscillations are described in terms of transition probabilities, $P(\nu_\alpha \to \nu_\beta, L)$, or simply $P_{\alpha\beta}$, which give the probability for a neutrino initially measured in the flavor state α to be measured in the flavor state β after traveling a distance L. In a simplified model, with two neutrino flavors, e and μ, the transition probabilities are symmetric between the two flavors, and are given by (see, for example, Refs. [33, 34])

$$P(\nu_e \to \nu_\mu, L) = P(\nu_\mu \to \nu_e, L) = \sin^2(2\theta)\sin^2\left(\frac{\Delta m^2 L}{4E}\right), \tag{3.1}$$

$$P(\nu_e \to \nu_e, L) = P(\nu_\mu \to \nu_\mu, L) = 1 - \sin^2(2\theta)\sin^2\left(\frac{\Delta m^2 L}{4E}\right). \tag{3.2}$$

Here, E is the energy of the neutrino, θ is the leptonic mixing angle and $\Delta m^2 \equiv m_2^2 - m_1^2$, where m_1 and m_2 are the mass eigenvalues. From this expression, it is clear that neutrino oscillations cannot occur if either the mixing angle or the mass-squared difference vanishes. In particular, the mass-squared difference is zero for massless neutrinos, and hence, the observation of neutrino oscillations implies that neutrinos are massive.

In the SM, there are three lepton generations, and hence, corresponding to the three mass eigenstates, there are two mass-squared differences, which are conventionally taken to be Δm^2_{21} and Δm^2_{31}. The full three-flavor mixing in the leptonic sector is described by the Pontecorvo–Maki–Nakagawa–Sakata (PMNS) matrix, U, which defines the transformation from mass to flavor basis,

$$\nu_\alpha = \sum_{i=1}^{3} U_{\alpha i}\nu_i, \quad \alpha = e, \mu, \tau. \tag{3.3}$$

In terms of U and the mass-squared differences, the neutrino transition probabilities can be written as [35]

$$\begin{aligned} P_{\alpha\beta} = \delta_{\alpha\beta} \quad &- \quad 4\sum_{i<j} \mathrm{Re}(U_{\beta i}U^*_{\alpha i}U^*_{\beta j}U_{\alpha j})\sin^2\left(\frac{\Delta_{ij}}{2}\right) \\ &+ \quad 2\sum_{i<j} \mathrm{Im}(U_{\beta i}U^*_{\alpha i}U^*_{\beta j}U_{\alpha j})\sin\left(\Delta_{ij}\right), \end{aligned} \tag{3.4}$$

where $\Delta_{ij} \equiv \Delta m^2_{ij} L/(2E)$. It is easy to show that $P_{\alpha\beta} = \delta_{\alpha\beta}$ if either $\Delta m^2_{ij} = 0$ or $U_{\alpha i} = \delta_{\alpha i}$. Hence, the conclusion that the mass-squared differences must be non-zero and the mixing non-trivial holds also in the three-flavor case.

The PMNS matrix can be parametrized as

$$
\begin{aligned}
U &= \begin{pmatrix} 1 & 0 & 0 \\ 0 & c_{23} & s_{23} \\ 0 & -s_{23} & c_{23} \end{pmatrix} \begin{pmatrix} c_{13} & 0 & s_{13}\mathrm{e}^{-\mathrm{i}\delta} \\ 0 & 1 & 0 \\ -s_{13}\mathrm{e}^{\mathrm{i}\delta} & 0 & c_{13} \end{pmatrix} \\
&\times \begin{pmatrix} c_{12} & s_{12} & 0 \\ -s_{12} & c_{12} & 0 \\ 0 & 0 & 1 \end{pmatrix} \begin{pmatrix} 1 & 0 & 0 \\ 0 & \mathrm{e}^{\mathrm{i}\rho} & 0 \\ 0 & 0 & \mathrm{e}^{\mathrm{i}\sigma} \end{pmatrix}, \qquad (3.5)
\end{aligned}
$$

where $s_{ij} = \sin\theta_{ij}$ and $c_{ij} = \cos\theta_{ij}$. Here, there are three mixing angles, θ_{12}, θ_{13}, and θ_{23}, and in contrast to the two-flavor case, there is also a complex CP-violating so-called Dirac phase, δ. In addition, in the case that neutrinos are Majorana fermions (see Sec. 3.2.1), there are two Majorana phases, ρ and σ.

A global analysis of neutrino oscillation data gives the current best-fit values for the three-flavor oscillation parameters $\Delta m^2_{21} = 7.59 \cdot 10^{-5}$ eV^2, $|\Delta m^2_{31}| = 2.50 \cdot 10^{-3}$ eV^2, $\sin^2\theta_{23} = 0.52$, $\sin^2\theta_{12} = 0.312$, and $\sin^2\theta_{13} = 0.013$ [36,37]. However, this analysis does not take into account recent data from the Daya Bay [31] and RENO [32] experiments, which both indicate that $\theta_{13} \simeq 9^\circ$. There is yet no experimental value for the Dirac phase.

From a theoretical point of view, much effort has been put into building models that describe the observed mixing parameters in the neutrino sector. The so-called tri-bimaximal mixing pattern [38], where $\theta_{12} = \sin^{-1}(1/\sqrt{3}) \sim 35.3^\circ$, $\theta_{13} = 0$, and $\theta_{12} = 45^\circ$, has until recently been compatible with all neutrino oscillation data. However, the Daya Bay measurement of $\theta_{13} \simeq 9^\circ$ [31] now seems to rule out tri-bimaximal mixing, at least at low energies. On the other hand, predictions for the mixing patterns are usually valid at some high-energy scale, such as a grand unification scale. Hence, comparison to experimental data has to take into account the renormalization group (RG) running of the physical neutrino parameters from this high-energy scale to the low-energy scales at which the measurements are made. In particular, the running effects could be significant in higher-dimensional models, as discussed in Sec. 4.3 and in Paper 6.

Since the transition probabilities depend only on the mass-squared differences, neutrino oscillation experiments are not sensitive to the absolute neutrino mass scale. There are currently a number of running and planned experiments aiming to determine this scale, *e.g.*, the KATRIN experiment, which will attempt to measure the neutrino mass scale by studying the energy spectrum of the electron in beta decay processes [39].

Currently, the best upper bound on the neutrino masses comes from cosmological considerations, giving $\sum_i m_i < 0.58$ eV at the 95 % CL [40]. However, this upper limit is sensitive to assumptions regarding the cosmological model.

3.2 Neutrino mass models

3.2.1 Dirac vs. Majorana neutrinos

In the SM, the charged fermions receive masses through the Higgs mechanism. These are so-called Dirac masses, which are of the form

$$\mathcal{L}_{\text{Dirac}} = m_{\text{D}}(\overline{\psi_{\text{L}}}\psi_{\text{R}} + \overline{\psi_{\text{R}}}\psi_{\text{L}}). \tag{3.6}$$

Dirac mass terms involve both the left- and right-handed components of the fermion, and hence, it is not possible to construct such mass terms for neutrinos without adding right-handed neutrinos to the SM. In such an extension of the SM, neutrino masses could, in principle, be generated in the same way as the masses of the other fermions, through their Yukawa couplings to the Higgs field. However, in order for the neutrino masses to be of the order of 0.1 eV, which is a factor of about 10^6 smaller than the electron mass, the Yukawa couplings would have to be extremely small in comparison to those of the other fermions. This problem has led to the development of different mechanisms that could naturally generate small neutrino masses.

Since neutrinos are electrically neutral, they could be their own antiparticles. Spin 1/2-fermions that are their own antiparticles are known as Majorana fermions. On the level of the chiral components, the condition that a fermion is its own antiparticle can be written as $\psi_{\text{R}} = (\psi_{\text{L}})^c$, where $(\psi_{\text{L}})^c$ denotes the conjugate of ψ_{L}. This means that the left- and right-handed chiral components of a Majorana fermion are not independent. Hence, while a Dirac fermion has two independent chiral components, a Majorana fermion has only one.

The Majorana or Dirac nature of neutrinos is one of the most important issues in neutrino physics, and it has important consequences for the possible ways of generating neutrino masses. A Majorana fermion ψ_{M} can have a mass term of the form

$$\mathcal{L}_{\text{Majorana}} = -\frac{1}{2}\overline{(\psi_{\text{M}})^c}M\psi_{\text{M}} + \text{h.c.} \tag{3.7}$$

This term breaks the conservation of all the charges of ψ_{M} by two units, and hence, charged fermions cannot have Majorana masses, or electric charge conservation would be violated. This also means that Majorana masses for neutrinos necessarily break the conservation of lepton number. Note that the mass term in Eq. (3.7) with $\psi_{\text{M}} = \nu_{\text{L}}$ would break the SM gauge invariance, and hence, it is not possible to introduce Majorana mass terms in the SM using only the left-handed neutrinos.

Majorana neutrinos, but not Dirac neutrinos, allow for so-called neutrinoless double beta decay, which makes it possible to experimentally test the Majorana / Dirac nature of neutrinos. In this process, two unstable nuclei decay simultaneously, while exchanging a neutrino. The rate for the process is proportional to the square of the so-called effective neutrino mass

$$m_{ee} = \left|\sum_{i=1}^{3} m_i U_{ei}^2\right|, \tag{3.8}$$

and hence, it is suppressed by the smallness of the light-neutrino masses. On the other hand, neutrinoless double beta decay experiments also give information on the neutrino masses. The current bound on the effective mass is $m_{ee} \lesssim 0.5$ eV [41]. There is a number of experiments searching for neutrinoless double beta decay; see, for example, the review [41].

3.2.2 Seesaw mechanisms and the Weinberg operator

A Majorana mass term for the left-handed neutrinos is not allowed by the SM gauge invariance. Although such a term could be generated by a non-renormalizable coupling to the Higgs field, the problem still remains that the coupling constants would have to be unnaturally small. On the other hand, right-handed neutrinos would be completely neutral with respect to the SM gauge group, and hence, they could have a bare Majorana mass $M_{\rm R}$. If the neutrinos are also given a Dirac mass $m_{\rm D}$, the neutrino mass matrix in $\{\nu_{\rm L}, \nu_{\rm R}\}$ basis is given by

$$\mathcal{M} = \begin{pmatrix} 0 & m_{\rm D} \\ m_{\rm D}^T & M_{\rm R} \end{pmatrix}, \tag{3.9}$$

i.e., the Dirac mass induces a mixing between the left- and right-handed neutrinos. In general, $M_{\rm R}$ and $m_{\rm D}$ are matrices in generation space. In the case of a single generation, $M_{\rm R}$ and $m_{\rm D}$ are numbers, and the eigenvalues of the mass matrix $\mathcal{M}$ are given by

$$m_{1,2} = \frac{M_{\rm R} \pm \sqrt{M_{\rm R}^2 + 4m_{\rm D}^2}}{2}. \tag{3.10}$$

Since the Majorana mass $M_{\rm R}$ is not related to the SM gauge interactions, it could naturally be much larger than the electroweak scale. If the Dirac mass is generated through the Higgs mechanism, in the same way as the other fermion masses, it is expected to be of the order of $m_{\rm D} \simeq 100$ GeV. Then $M_{\rm R} \gg m_{\rm D}$, and the masses are approximately[1]

$$m_1 \simeq -m_{\rm D}^2/M_{\rm R}, \quad m_2 \simeq M_{\rm R}. \tag{3.11}$$

Hence, the mass m_1 is suppressed relative to the electroweak scale by the small number $m_{\rm D}/M_{\rm R}$. In the general case, with an arbitrary number of fermion generations, the light-neutrino mass matrix is given by

$$m_\nu \simeq -m_{\rm D} M_{\rm R}^{-1} m_{\rm D}^T. \tag{3.12}$$

The mechanism described above is not the only possible way of generating small neutrino masses through the coupling to heavy degrees of freedom. Generally, one

[1] The minus sign in front of the small mass is removed by a rephasing of the corresponding fermion field.

can consider a Majorana mass term for the left-handed neutrinos given by the dimension-five operator

$$\mathcal{L}_{\text{Weinberg}} = -\frac{1}{2}\frac{(\overline{L_{\text{L}}}\phi)(\phi^T L_{\text{L}}^c)}{\Lambda}, \tag{3.13}$$

where Λ is the energy scale corresponding to the heavy degrees of freedom. When the Higgs field obtains its VEV, a Majorana mass which is proportional to v^2/Λ is generated. The introduction of heavy right-handed neutrinos is the first example of such a mechanism, and it is known as the type-I seesaw mechanism [42, 43]. In addition, the operator (3.13) could be generated by an $SU(2)_{\text{L}}$ scalar triplet or an $SU(2)_{\text{L}}$ fermion triplet. These two mechanisms are known as the type-II [44–47] and type-III [48, 49] seesaw mechanisms, respectively.

Given the light-neutrino masses, the mass scale M_{R} can be estimated, using the expression (3.12). Taking $m_\nu = 0.1$ eV and $m_{\text{D}} = 100$ GeV, we obtain the mass $M_{\text{R}} \simeq 10^{14}$ GeV. Hence, in order to generate the observed light-neutrino masses, the right-handed neutrinos must be very heavy. This means that it is hard to experimentally test the conventional seesaw models.

Recently, much attention has been directed to alterations of the conventional seesaw models that could possibly be tested at the LHC, *e.g.*, the so-called inverse seesaw model [50]. In Sec. 6.2, we describe an observable seesaw model in the context of extra dimensions.

3.3 Non-unitarity effects

If the light neutrinos mix only among themselves, the transition probabilities in Eq. (3.4) should fulfill the relations

$$\sum_\alpha P_{\alpha\beta} = \sum_\beta P_{\alpha\beta} = 1 \tag{3.14}$$

in order to conserve probability. On the level of the PMNS matrix U, these conditions correspond to the unitarity condition $U^\dagger U = 1$.

However, in many models, it is the case that the light neutrinos mix also with additional degrees of freedom, for example right-handed neutrinos or the scalar triplet in the seesaw models. If this is the case, the matrix U (as defined in Eq. (3.3)) is not the matrix governing the neutrino oscillations. Instead, we have

$$\nu_\alpha = \sum_{i=1}^{3} V_{\alpha i}\nu_i + \sum_{i=1}^{n} X_{\alpha i}\xi_i, \tag{3.15}$$

where ξ_i, $i = 1, \ldots, n$, are the additional degrees of freedom. Here, V is the upper 3×3 sub-matrix of the unitary matrix that diagonalizes the mass matrix for the light neutrinos as well as the additional degrees of freedom. In general, V is

non-unitarity, implying that probability is not conserved in transitions within the subsystem consisting only of the light neutrinos.

General non-unitarity effects are conventionally parametrized as $V = (1 - \varepsilon)U$, where ε is a Hermitian matrix [51]. Hence, $V^\dagger V = 1 - 2U^\dagger \varepsilon U + \mathcal{O}(\varepsilon^2)$. In a given model, ε can, at least in principle, be related to the parameters of the model. In general, the elements of ε can be bounded by their contributions to processes such as $e \to \mu\gamma$, giving

$$|\varepsilon| < \begin{pmatrix} 2.0 \times 10^{-3} & 6.0 \times 10^{-5} & 1.6 \times 10^{-3} \\ \sim & 8.0 \times 10^{-4} & 1.1 \times 10^{-3} \\ \sim & \sim & 2.7 \times 10^{-3} \end{pmatrix} \tag{3.16}$$

at 90 % CL [52]. Hence, these limits can be used to constrain the parameters of models inducing non-unitarity effects. In many models, such as the conventional seesaw models, the mixing between the light neutrinos and the heavy degrees of freedom is small, and hence, so are the non-unitarity effects. In Paper 5, we investigated a model where extra dimensions give rise to large non-unitarity effects (see also Sec. 6.2).

Chapter 4

Quantum field theory in extra dimensions

In this chapter, we present the formalism of higher-dimensional quantum field theories. We begin by describing a number of basic concepts that are of major importance for such theories. Then, we discuss the fact that higher-dimensional quantum field theories are in general non-renormalizable and what their UV completions could be. Next, we describe the features of RG running in extra dimensions. Finally, we summarize a number of TeV-scale higher-dimensional models that have emerged in recent years.

4.1 Kaluza–Klein decomposition

4.1.1 Compactification

The most obvious question that any theory including extra spatial dimensions must be able to answer is why the extra dimensions have not been observed. Clearly, any additional dimensions have to differ from the ordinary three spatial dimensions in some way. The most common solution to this problem was provided by Oskar Klein in 1926 [16]. He suggested that the reason why the extra dimensions have not been observed is that they are small. More specifically, the extra dimensions are compact, having for example the geometry of a circle with a small radius. In order to probe such compact dimensions, particles with small wavelengths would be needed, and by quantum mechanics, the wavelength of a particle is inversely proportional to its energy. Hence, in measurements performed at an energy scale smaller than that corresponding to the size of the extra dimensions, these dimensions would effectively be hidden.

The space that is spanned by the compact extra dimensions is usually referred to as the internal space, and the full higher-dimensional spacetime is called the bulk.

4.1.2 Kaluza–Klein tower

These statements can be treated in a more precise way through the important technique known as the Kaluza–Klein (KK) decomposition of a higher-dimensional field. This idea provides a mathematical reformulation of a higher-dimensional field theory as a four-dimensional theory, where the existence of the extra dimensions is encoded in the structure of the particles and their interactions. The procedure is most easily demonstrated in the simple setting of a complex scalar field in a single extra dimension that is compactified on a circle with a radius R. The action for this model is given by

$$\mathcal{S} = \int \mathrm{d}^5 x \left(\partial_M \phi^* \partial^M \phi - m^2 \phi^* \phi \right). \tag{4.1}$$

Since the fifth dimension is a circle, ϕ must be periodic in the coordinate x^5 along this direction, *i.e.*, $\phi(x^\mu, x^5) = \phi(x^\mu, x^5 + 2\pi R)$. This means that, without loss of generality, the field can be expanded in a Fourier series in x^5, *i.e.*,

$$\phi(x^\mu, x^5) = \frac{1}{\sqrt{2\pi R}} \sum_{n=-\infty}^{\infty} \phi^{(n)}(x^\mu) \mathrm{e}^{\frac{\mathrm{i}nx^5}{R}}. \tag{4.2}$$

Using this explicit x^5-dependence, we can integrate out the fifth dimension in Eq. (4.1). Then, we obtain the action

$$\mathcal{S} = \sum_{n=-\infty}^{\infty} \int \mathrm{d}^4 x \left[\partial_\mu \phi^{(n)*} \partial^\mu \phi^{(n)} - \left(m^2 + \frac{n^2}{R^2} \right) \phi^{(n)*} \phi^{(n)} \right], \tag{4.3}$$

which describes a four-dimensional field theory with an infinite number of scalar fields $\phi^{(n)}$, which are known as the KK modes of the field ϕ. These fields are labeled by the integer n, and the mass of the field $\phi^{(n)}$ is $m_n = \sqrt{m^2 + n^2/R^2}$. The set of these fields is known as the KK tower corresponding to the higher-dimensional scalar field. Within the KK tower, the only difference between the modes is their masses. The $n = 0$ mode, known as the zero mode, is the lightest mode in the tower, and it corresponds to a field which has no momentum along the extra dimension.

The physics behind this so-called dimensional reduction can be understood in a simple way by considering the relativistic energy-momentum relation,

$$E^2 = \mathbf{p}^2 + m^2 = (p_1^2 + p_2^2 + p_3^2) + p_5^2 + m^2. \tag{4.4}$$

Here, the squared momentum has been divided into two terms: the ordinary three-dimensional part $p_1^2 + p_2^2 + p_3^2$ and the extra contribution p_5^2 from the fifth dimension.

From a five-dimensional point of view, these two parts of the momentum are on an equal footing, at least locally. However, from a four-dimensional point of view, where the possibility of motion along the fifth dimension is unknown, measurements of the energy and momentum of a particle would lead us to interpret the five-dimensional part of the momentum as part of the squared mass. This means that a particle with mass m in a five-dimensional spacetime is considered to have a four-dimensional mass equal to $\sqrt{m^2 + p_5^2}$. Since the internal space is compact, the momentum along the extra dimension is quantized, *i.e.*, it is only allowed to take on a discrete set of specific values. In the case that we consider, the momentum can take on the values $p_5^{(n)} = n/R$, for $n \in \mathbb{Z}$. Hence, the effective four-dimensional mass is also quantized, as $m_n = \sqrt{m^2 + n^2/R^2}$. The momentum eigenstates are interpreted as an infinite KK tower of distinct particles, as illustrated in Fig. 4.1

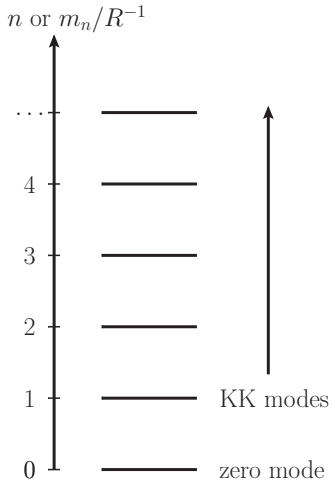

Figure 4.1. Illustration of the KK tower, for the case $m = 0$.

In the beginning of this section, it was stated that the existence of small extra dimensions would be hidden at low energies. The example given above demonstrates the general features of how this mechanism works in practice, from a particle physics point of view. The quantization of the momentum along the extra dimension implies that, in order for a particle to move along this dimension, its momentum must be larger than R^{-1}. Equivalently, from the four-dimensional viewpoint, R^{-1} is the threshold energy for production of excited KK modes. Below this energy scale, only the zero modes of the fields are observed. At energies of the order of R^{-1}, the effects of the extra dimension start to become important, and as the energy increases, the higher-dimensional structure successively emerges through the higher-level KK modes.

While the above discussion focused on the simple example of a scalar field in a single extra dimension, the generalization to other fields and internal spaces is

in principle straightforward. The KK spectrum, *i.e.*, the set of particle masses in each tower, depends on the geometry of the internal space. Mathematically, the KK spectrum for the example given above is the spectrum of the Laplace operator on the circle, *i.e.*, the set of values m allowing for periodic solutions to the equation $\Delta\phi = \partial_5^2\phi = -m^2\phi$. For other internal spaces, *e.g.*, curved spaces, the Laplace operator generalizes to a more complicated operator, and the KK spectrum is modified accordingly. In general, the KK modes are not evenly distributed, in the way that they are for a flat internal space. KK expansions for fermions and gauge bosons are discussed in Secs. 5.1 and 5.2, respectively.

Higher-dimensional models are generally constrained by direct searches for excited KK modes at colliders as well as by their contributions to the EWPOs. The constraints on R^{-1} depend on the specific model under consideration, but are typically of the order of several TeV (see, for example, Refs. [53, 54]). The models that we consider in Ch. 5 and 6 include different mechanisms that relax these general constraints, enabling potential discoveries in the next generation of experiments.

4.1.3 Matching of parameters

Using the KK decomposition, we can relate the parameters of a higher-dimensional field theory to the effective parameters of the low-energy theory. As an example, we add a self-interaction term to the action (4.1),

$$\mathcal{S}_{\text{int}} = -\int \mathrm{d}^5x\lambda_5|\phi|^4. \tag{4.5}$$

In the low-energy limit, $E \ll R^{-1}$, we can insert the KK expansion given in Eq. (4.2) into Eq. (4.5), keep only the zero mode, and integrate over x^5. Then, we obtain the effective action

$$\mathcal{S}_{\text{int}}^{(0)} = -2\pi R\int \mathrm{d}^4x\lambda_5\frac{1}{(2\pi R)^2}|\phi^{(0)}|^4 = -\int \mathrm{d}^4x\frac{\lambda_5}{2\pi R}|\phi^{(0)}|^4. \tag{4.6}$$

Comparing this expression to the corresponding action for a four-dimensional theory,

$$\mathcal{S}_{\text{int}} = -\int \mathrm{d}^4x\lambda_4|\phi|^4, \tag{4.7}$$

and identifying the four-dimensional field ϕ with the zero mode $\phi^{(0)}$, we obtain the relation

$$\lambda_5 = 2\pi R\lambda_4 \tag{4.8}$$

between the parameters. Hence, given the radius of the extra dimension, the value of the five-dimensional coupling constant can be inferred from the effective four-dimensional one. Since λ_4 is a dimensionless quantity, this relation implies that the five-dimensional coupling constant has mass dimension equal to -1. In general, interacting quantum field theories where the coupling constants have negative mass dimensions are non-renormalizable [20]. We will now show that this is a general feature of higher-dimensional quantum field theories.

4.2 Non-renormalizability

An important and general property of quantum field theories in more than four spacetime dimensions is that they are non-renormalizable. A straightforward way to observe this is to write down the action for an interacting field theory in D spacetime dimensions,

$$\mathcal{S} = \int \mathrm{d}^D x \; \mathcal{L}, \tag{4.9}$$

and analyze the mass dimensions of the coupling constants. We denote the mass dimension of a quantity by square brackets, $[\ldots]$. In natural units, the action is dimensionless, and hence, the Lagrangian density must have the mass dimension D in order to balance the integration measure, which has mass dimension $-D$. The mass dimensions for the different fields in the SM are determined by the kinetic terms given in Eqs. (2.1), (2.3), and (2.6). Using $[\partial] = 1$, we obtain the result

$$[\phi] = [A] = \frac{D-2}{2}, \tag{4.10}$$

$$[\psi] = \frac{D-1}{2}. \tag{4.11}$$

The interactions in the SM are gauge boson interactions, Yukawa interactions, and scalar self-interactions, given in Eqs. (2.1), (2.5), and (2.6); Eq. (2.8); and Eq. (2.7), respectively. The coupling constants appearing in these interactions have the mass dimensions

$$[g] = [Y] = \frac{4-D}{2}, \tag{4.12}$$

$$[\lambda] = 4 - D. \tag{4.13}$$

While these coupling constants are all dimensionless for $D = 4$, they have negative mass dimension for $D > 4$. This means that all the SM interactions are non-renormalizable for $D > 4$. Notice that this property of higher-dimensional quantum field theories depends only on the number of spacetime dimensions, and not on the geometry of these dimensions.

In the higher-dimensional picture, the non-renormalizability of the theory is manifest from the negative mass dimensions of the coupling constants. However, in the four-dimensional picture, the coupling constants are dimensionless, and it would seem that the theory is in fact renormalizable. However, the KK towers are infinite and there is no upper bound on the masses of the KK modes. This is how the non-renormalizability manifests in the four-dimensional picture, and hence, in any renormalizable UV completion, the KK tower has to be truncated in some way above a certain energy scale.

4.2.1 Ultraviolet completions

Since the non-renormalizability of higher-dimensional quantum field theories depends only on the dimensionality of spacetime, it is hard to construct well-defined

UV completions of such models. By far, the most common alternative is string theory, which is not a QFT, but a theory of extended objects. In string theory, the so-called string tension provides a natural cutoff close to the Planck scale, and hence, the theory is well-defined for high energies. An alternative to string theory in this context is provided by so-called dimensional deconstruction models [55, 56]. In these models, spacetime is fundamentally four-dimensional, but appears higher-dimensional in a certain energy range. This effect is due to a special structure of the gauge group, which is a direct product of a number of copies of the same group.

4.3 Renormalization group running

The existence of extra dimensions would have a large impact on the RG running of physical parameters. In general, the RG equations at a given energy scale μ are sensitive to the particle mass spectrum below μ. This means that, below the first-level KK scale, the beta function for any physical quantity is the same as in the SM. This means that the beta function for an observable $\mathcal{O}$ can be divided into two terms,

$$16\pi^2 \frac{\mathrm{d}\mathcal{O}}{\mathrm{d}\ln\mu} = \beta_{\mathcal{O}}^{\mathrm{SM}} + \beta_{\mathcal{O},\mathrm{tot}}^{\mathrm{ED}}, \tag{4.14}$$

where $\beta_{\mathcal{O}}^{\mathrm{SM}}$ is the contribution from diagrams involving only SM particles and $\beta_{\mathcal{O},\mathrm{tot}}^{\mathrm{ED}}$ is the contributions from diagrams involving KK modes. Furthermore, the KK mass spectrum is approximately degenerate at each KK level in comparison to the mass difference between successive levels. This means that we can approximate the contributions from all the particles within a given KK level to become relevant at a common energy scale. Finally, it is often the case that the particle spectrum at each excited KK level is identical, except for the particle masses. In the case of a single extra dimension, we can write

$$\beta_{\mathcal{O},\mathrm{tot}}^{\mathrm{ED}} = \sum_n \beta_{\mathcal{O},n}^{\mathrm{ED}} = s\beta_{\mathcal{O}}^{\mathrm{ED}}, \tag{4.15}$$

where $s = \lfloor \mu/R^{-1} \rfloor$ and $\beta_{\mathcal{O}}^{\mathrm{ED}}$ is the contribution from a single KK level. Here, $\lfloor x \rfloor$ denotes the largest integer that is smaller than x. For energy scales that are large in comparison to R^{-1}, an approximate power-law behavior is obtained for the RG running. Thus, the running could be significantly enhanced in comparison to four-dimensional models, where it is often approximately logarithmic in the energy scale.

In general, models with d extra dimensions give rise to an RG running which is of the form

$$16\pi^2 \frac{\mathrm{d}\mathcal{O}}{\mathrm{d}\ln\mu} = X_d \left(\frac{\mu}{R^{-1}}\right)^d \beta_{\mathcal{O}}^{\mathrm{ED}}, \tag{4.16}$$

where $X_d = 2\pi^{d/2}/[\delta\Gamma(d/2)]$. Hence, the power-law running is a general feature of higher-dimensional theories, with the power-law exponent given by the dimensionality of the internal space.

The non-renormalizability of higher-dimensional theories has important consequences for the interpretation of the RG running in such theories. An effective theory must have an explicit cutoff scale Λ, and hence, within the effective theory, the physical quantities are finite, but depend on the value of Λ. This means that the renormalized quantities cannot be considered to run with the energy scale μ, but rather to depend on the fixed energy scale Λ. The problem is that it is in general not clear whether or not it is possible to associate Λ with the mass scale for the UV completion of the effective theory [57]. However, as was noted in Sec. 4.2, the non-renormalizability of higher-dimensional theories manifests itself in the four-dimensional picture through the infinite KK towers. Since the RG equations depend only on the particle spectrum below the energy scale being considered, the theory can, at any given energy scale, be replaced by a theory with finite, truncated KK towers, while giving the same results as the higher-dimensional theory. Such a truncated theory is renormalizable, and hence, from a practical point of view, the normal interpretation of the RG equations is valid. Then, the cutoff scale can be identified with the mass scale for the UV completion, without any ambiguity.

In Paper 6, the RG running of neutrino parameters in higher-dimensional models was investigated. The large running could affect the high-energy mixing patterns, giving connections to the mixing patterns that were discussed in Sec. 3.1. In Paper 7, we considered the impact of higher-dimensional RG running on the Higgs self-coupling constant in light of recent LHC Higgs bounds.

4.4 Higher-dimensional models at the TeV scale

Inspired by string theory, several models of extra dimensions, which could potentially solve some of the problems with the SM, have been suggested. A common feature of many of these models is that their effects become relevant at energy scales close to 1 TeV, which means that they could potentially be tested at the LHC. The most important models include the UED model [58], which has received much attention in connection to the field of DM, and the ADD model [59, 60] as well as the Randall–Sundrum (RS) model [61, 62], which both aim to solve the hierarchy problem of the SM. In Ch. 5, we will describe the UED model, which was studied in Papers 1, 2, 3, 4, 6, and 7. Then, in Ch. 6, we will describe a number of models, including the ADD model, where a subset of the particles are constrained to a lower-dimensional brane. These models were studied in Papers 5, 6, and 8.

Chapter 5

Universal extra dimensions

UEDs were first proposed by Appelquist, Cheng, and Dobrescu in the year 2000 [58]. In these models, all of the fields in the SM are promoted to higher-dimensional fields. There are a number of versions of UED models, differing with respect to the number of extra dimensions and the geometry of the internal space. The particle content is usually chosen in the minimal way that reproduces the SM in the low-energy limit. However, for reasons that will be made clear in this chapter, there are necessarily additional degrees of freedom at the non-zero KK levels, compared to the SM ones. The motivations for UED models include the existence of a DM candidate particle [63, 64], the need for three fermion generations in order to cancel gauge anomalies [27], and proton stability [65].

We begin this chapter with a discussion on the properties of fermions and gauge bosons in higher-dimensional models. In order to reproduce the phenomenology of the SM at low energies, the models must be compactified on so-called orbifolds. We discuss the consequences of the orbifolding, including the important concept of KK parity conservation. Then, we discuss realistic UED models. Finally, we summarize the experimental constraints on such models.

5.1 Fermions and orbifolding

Promoting fermions to higher-dimensional fields is not as straightforward as doing so with scalars, since the properties of fermions depend drastically on the dimensionality of spacetime. In the SM, the $SU(2)_{\mathrm{L}}$ gauge interactions of the fermions are chiral, *i.e.*, their left- and right-handed parts have different gauge group transformation properties. This structure is made possible by the fact that the Dirac representation is reducible in four dimensions. A Dirac fermion can be decomposed into two irreducible representations of definite chirality, so-called Weyl fermions. This decomposition is not possible for an arbitrary space-time dimensionality. In particular, the Dirac representation is irreducible in an odd number of dimensions,

and in that case, there is no concept of chiral representations. This means that, on the level of the five-dimensional Lagrangian, the fermions have non-chiral interactions, and the same holds for the zero modes, which represent the SM fields. This is known as the chirality problem.

In an odd number of dimensions $D = 2k + 1$, spinors are 2^k-component objects [18], and hence, for $D = 5$, spinors have four components, as in four dimensions. The key to resolving the chirality problem is to remove one of the chiral components of the zero mode of each fermion. In this way, the zero modes behave as chiral fermions, and the theory is effectively chiral for energies below R^{-1}. In general, the zero mode of a field can be removed by replacing the circle S^1 by the orbifold[1] $S^1/\mathbb{Z}_2$, which is obtained from S^1 by identifying the opposite points x^5 and $-x^5$, as illustrated in Fig. 5.1. In order for the action to be invariant under the parity transformation $x^5 \to -x^5$, the five-dimensional fields have to be either even or odd under this transformation. Writing the KK expansion given in Eq. (4.2) in terms of trigonometric functions, the expansion of an even field is given by

$$\phi_{\text{even}}(x^\mu, x^5) = \frac{1}{\sqrt{\pi R}}\left[\phi^{(0)}(x^\mu) + \sqrt{2}\sum_{n=1}^{\infty}\phi^{(n)}(x^\mu)\cos\left(\frac{nx^5}{R}\right)\right], \tag{5.1}$$

while that of an odd field is given by

$$\phi_{\text{odd}}(x^\mu, x^5) = \sqrt{\frac{2}{\pi R}}\sum_{n=1}^{\infty}\phi^{(n)}(x^\mu)\sin\left(\frac{nx^5}{R}\right). \tag{5.2}$$

The important property is that, whereas an even expansion series includes a zero mode, an odd one does not.

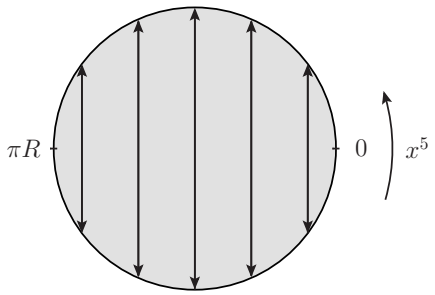

Figure 5.1. Illustration of the construction of the orbifold $S^1/\mathbb{Z}_2$ from a circle with radius R. The points x^5 and $-x^5$ are identified, giving an interval with length πR.

Alternatively, the orbifold can be seen as an interval with length πR. From this point of view, the different KK expansions depend on the boundary conditions of a field on this interval.

[1]Simply put, an orbifold is a generalization of a manifold that allows for the existence of singular points.

Fermions transform under $x^5 \to -x^5$ as

$$\Psi(x^\mu, x^5) \to \Psi'(x^\mu, x^5) = \gamma_5 \Psi(x^\mu, -x^5), \tag{5.3}$$

or, in terms of the would-be chiral components,

$$\begin{pmatrix} \psi_{\rm L}(x^\mu, x^5) \\ \psi_{\rm R}(x^\mu, x^5) \end{pmatrix} \to \begin{pmatrix} -\psi_{\rm L}(x^\mu, -x^5) \\ \psi_{\rm R}(x^\mu, -x^5) \end{pmatrix}. \tag{5.4}$$

Thus,

$$\begin{aligned} \Psi \text{ even} &\Leftrightarrow \psi_{\rm L} \text{ odd and } \psi_{\rm R} \text{ even}, \\ \Psi \text{ odd} &\Leftrightarrow \psi_{\rm L} \text{ even and } \psi_{\rm R} \text{ odd}, \end{aligned}$$

i.e., $\psi_{\rm L}$ and $\psi_{\rm R}$ necessarily have opposite transformation properties, so that fermions on $S^1/\mathbb{Z}_2$ are always effectively chiral at the level of the zero modes. Now, the chirality problem can be solved by introducing two five-dimensional Dirac fermions for each Dirac fermion Ψ in the SM. One of these, $\Psi_{\rm D}$ (D for doublet), has the quantum numbers of $\psi_{\rm L}$, while the other one, $\Psi_{\rm S}$ (S for singlet), has the quantum numbers of $\psi_{\rm R}$. In order to reproduce the SM correctly in the low-energy limit, $\Psi_{\rm D}$ has to be odd and $\Psi_{\rm S}$ even, *i.e.*,

$$\begin{aligned} \Psi_{\rm D}(x^\mu, x^5) &= \frac{1}{\sqrt{\pi R}} \left[P_{\rm L} \Psi_{\rm D}^{(0)}(x^\mu) + \sqrt{2} \sum_{n=1}^{\infty} P_{\rm L} \Psi_{\rm D}^{(n)}(x^\mu) \cos\left(\frac{n x^5}{R}\right) \right. \\ &\qquad \left. + \sqrt{2} \sum_{n=1}^{\infty} P_{\rm R} \Psi_{\rm D}^{(n)}(x^\mu) \sin\left(\frac{n x^5}{R}\right) \right], \end{aligned} \tag{5.5}$$

$$\begin{aligned} \Psi_{\rm S}(x^\mu, x^5) &= \frac{1}{\sqrt{\pi R}} \left[P_{\rm R} \Psi_{\rm S}^{(0)}(x^\mu) + \sqrt{2} \sum_{n=1}^{\infty} P_{\rm R} \Psi_{\rm S}^{(n)}(x^\mu) \cos\left(\frac{n x^5}{R}\right) \right. \\ &\qquad \left. + \sqrt{2} \sum_{n=1}^{\infty} P_{\rm L} \Psi_{\rm S}^{(n)}(x^\mu) \sin\left(\frac{n x^5}{R}\right) \right]. \end{aligned} \tag{5.6}$$

Here, $P_{\rm R/L} = (1 \pm \gamma_5)/2$ are the four-dimensional projection operators, and we identify the chiral SM fermions as $\psi_{\rm L} = P_{\rm L} \Psi_{\rm D}^{(0)}$ and $\psi_{\rm R} = P_{\rm R} \Psi_{\rm S}^{(0)}$.

At each non-zero KK level, the two Dirac spinors $\Psi_{\rm D}$ and $\Psi_{\rm S}$ receive contributions to their masses from the momentum along extra dimensions, as well as from the Higgs mechanism. The contributions from the extra dimensions come from the kinetic terms in the five-dimensional Lagrangian, and therefore, they are diagonal. On the other hand, the contributions from the Higgs mechanism necessarily involve a mixing of the two Dirac fermions. The fermion mass matrix at the nth KK level, in $\{\Psi_{\rm S}^{(n)}, \Psi_{\rm D}^{(n)}\}$ basis, is given by

$$\mathcal{M}_\Psi^{(n)} = \begin{pmatrix} -n/R & m_\Psi \\ m_\Psi & n/R \end{pmatrix}, \tag{5.7}$$

where $m_\Psi = Y_\Psi v/\sqrt{2}$. The eigenvalues of this matrix are

$$M_\Psi^{(n)} = \pm\sqrt{\frac{n^2}{R^2} + m_\Psi^2}. \tag{5.8}$$

Since the mass matrix in flavor basis is not diagonal, the Dirac fermions Ψ_D and Ψ_S generally mix with each other. The mixing angle $\alpha^{(n)}$ at the nth KK level is given by

$$\tan 2\alpha^{(n)} = \frac{m_\Psi}{n/R}, \tag{5.9}$$

i.e., it is suppressed at all KK levels if $R^{-1} \gg m_\Psi$.

For an even number of dimensions, $D = 2k$, spinors are 2^k-component objects [18]. Hence, spinors in six dimensions have eight components. A reduction into states of definite chirality is possible, but this higher-dimensional chirality is not the same as the one in four dimensions. The chiral representations, which are referred to as states of $+/-$ chirality, carry half of the degrees of freedom of the Dirac representations, *i.e.*, they are four-component objects. These fermion representations are irreducible, and clearly, the chiral fermions cannot represent the SM fermions in the low-energy limit. However, since they have four components, the situation is similar to the five-dimensional case, and an analogous solution to the problem is possible, provided only that the internal space is chosen in such a way that the zero modes of fields can be projected out. Thus, for each Dirac fermion in the SM, the model must include two six-dimensional fermions with definite six-dimensional chirality and with quantum numbers corresponding to the left- and right-handed parts of the SM fermion. The six-dimensional fermion chiralities are constrained by the requirement of anomaly cancellation, and the structure is given by $Q_+ = (u_+, d_+)$, u_-, d_-, $L_+ = (\nu_+, e_+)$, e_-, and ν_- [27, 66]. It is interesting to note that, in sharp contrast to the SM, the anomaly cancellations demand the existence of a sterile fermion ν_-.

In six dimensions, the number of possible internal spaces is increased. One of the most studied cases is the so-called chiral square, $T^2/\mathbb{Z}_4$ [67, 68]. This orbifold can be constructed from a square with side length L by identifying the sides $(y, 0)$ and $(0, y)$ as well as (y, L) and (L, y), for $0 \leq y \leq L$, *i.e.*, folding the square along the diagonal, as illustrated in Fig. 5.2. In contrast to the two possible choices for the boundary conditions of a field on the orbifold $S^1/\mathbb{Z}_2$, the chiral square admits four different consistent choices. With $n = 1, 2, 3, 4$ denoting the choice of boundary conditions, the expansion of a field on this orbifold is given by [67]

$$A_n(x^\mu, x^5, x^6) = \frac{1}{L}\left[\delta_{n,0} A^{(0,0)}(x^\mu) + \sum_{j\geq 1}\sum_{k\geq 0} f_n^{(j,k)}(x^5, x^6) A^{(j,k)}(x^\mu)\right], \tag{5.10}$$

where

$$f_n^{(j,k)}(x^5, x^6) = \mathrm{e}^{-\mathrm{i}n\pi/2}\cos\left(\frac{jx^5 + kx^6}{R} + \frac{n\pi}{2}\right) + \cos\left(\frac{kx^5 - jx^6}{R} + \frac{n\pi}{2}\right) \tag{5.11}$$

and we have defined $R = L/\pi$. The squared mass for a KK mode with indices (j, k) is $m^2_{j,k} = (j^2 + k^2)/R^2$. Note that only the $n = 0$ fields have zero modes, and that there is no $(0, 1)$ mode. This means that, for each field, there is a single lightest KK mode, with indices $(1, 0)$ and mass $m_{1,0} = R^{-1}$. We call this mode the first KK mode.

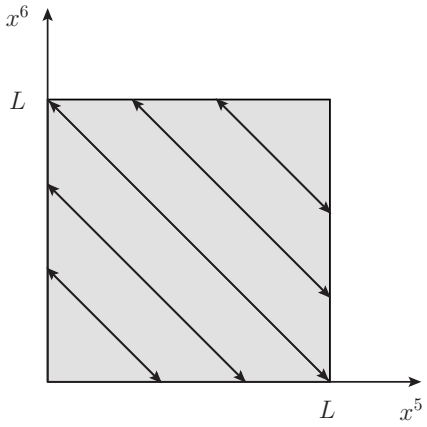

Figure 5.2. Illustration of the construction of the orbifold $T^2/\mathbb{Z}_2$ from a square with side length L. The sides $(y, 0)$ and $(0, y)$ as well as (y, L) and (L, y), for $0 \leq y \leq L$, are identified.

5.2 Gauge bosons

Next, we turn to the properties of gauge bosons in higher-dimensional quantum field theories. Since the number of components of any vector field is equal to the dimensionality of spacetime, these gauge bosons will have additional components, compared to the four-dimensional case. The correct choice of orbifold transformation properties of each of the components is an important issue, which affects the phenomenology of the models.

In order to simplify the treatment, we consider in the following only Abelian gauge bosons. The calculations can be straightforwardly extended to the case of non-Abelian ones. The same conclusions hold for that case, with the addition of self-interactions among the different components of the gauge field.

In five dimensions, the kinetic term for an Abelian gauge boson is given by

$$\begin{aligned}
\mathcal{L}_{\rm YM}^{\rm 5D} &= -\frac{1}{4}F_{MN}F^{MN} \\
&= -\frac{1}{4}\left(F_{\mu\nu}F^{\mu\nu} + 2F_{\mu 5}F^{\mu 5}\right) \\
&= -\frac{1}{4}F_{\mu\nu}F^{\mu\nu} - \frac{1}{2}\partial_\mu A_5 \partial^\mu A^5 - \frac{1}{2}\partial_5 A_\mu \partial^5 A^\mu + \partial_\mu A^5 \partial_5 A^\mu \\
&= -\frac{1}{4}F_{\mu\nu}F^{\mu\nu} + \frac{1}{2}\partial_\mu a \partial^\mu a + \frac{1}{2}\partial_5 A_\mu \partial_5 A^\mu - \partial_\mu a \partial_5 A^\mu, \qquad (5.12)
\end{aligned}$$

where we have defined $a \equiv A_5 = -A^5$. Since the partial derivatives transform under the orbifold $\mathbb{Z}_2$ transformation $x^5 \to -x^5$ as

$$\begin{aligned}
\partial_\mu &\to \partial_\mu, \qquad (5.13) \\
\partial_5 &\to -\partial_5, \qquad (5.14)
\end{aligned}$$

the first three terms of Eq. (5.12) are invariant under this transformation, irrespective of the transformation properties of the components of A_M. The last term, on the other hand, is invariant only if the fifth component A_5 has transformation properties opposite to those of the four-dimensional part A_μ. Requiring that the four-dimensional part has a zero mode gives

$$\begin{aligned}
A_\mu(x^\mu, x^5) &= \frac{1}{\sqrt{\pi R}}\left[A_\mu^{(0)} + \sqrt{2}\sum_{n=1}^{\infty} A_\mu^{(n)} \cos\left(\frac{nx^5}{R}\right)\right], \qquad (5.15) \\
a(x^\mu, x^5) &= \sqrt{\frac{2}{\pi R}}\sum_{n=1}^{\infty} a^{(n)} \sin\left(\frac{nx^5}{R}\right). \qquad (5.16)
\end{aligned}$$

Using these KK expansions, it is easy to show that the four-dimensional Lagrangian corresponding to Eq. (5.12) is given by

$$\begin{aligned}
\mathcal{L}_{\rm YM} = \sum_{n=0}^{\infty}\Bigg[&-\frac{1}{4}F_{\mu\nu}^{(n)}F^{\mu\nu(n)} + \frac{1}{2}\left(\frac{n}{R}\right)^2 A_\mu^{(n)}A^{\mu(n)} \\
&+ \frac{1}{2}\partial_\mu a^{(n)}\partial^\mu a^{(n)} + \frac{n}{R}A^{\mu(n)}\partial_\mu a^{(n)}\Bigg]. \qquad (5.17)
\end{aligned}$$

This form of the Lagrangian makes it clear that, from the four-dimensional point of view, the KK modes $a^{(n)}$ of the fifth component a of the gauge field appear as scalars. The last term in Eq. (5.17), which is a bilinear term mixing $A_\mu^{(n)}$ and $a^{(n)}$, can be removed by adding to the Lagrangian the gauge-fixing term

$$\begin{aligned}
\mathcal{L}_{\rm gf} &= \int_0^{\pi R} {\rm d}x^5 \left[-\frac{1}{2\xi}\left(\partial_\mu A^\mu - \xi\frac{n}{R}a\right)^2\right] \\
&= \sum_{n=0}^{\infty}\left[-\frac{1}{2\xi}\left(\partial_\mu A^\mu\right)^2 + \frac{n}{R}a^{(n)}\partial_\mu A^{\mu(n)} - \frac{1}{2}\left(\sqrt{\xi}\frac{n}{R}\right)^2 (a^{(n)})^2\right]. \qquad (5.18)
\end{aligned}$$

Note that this term is not five-dimensionally Lorentz invariant, since it contains the four-dimensional Lorentz scalar $\partial_\mu A^\mu$, rather than $\partial_M A^M$. However, five-dimensional Lorentz invariance is already explicitly broken by the orbifolding procedure. Adding Eq. (5.18) to Eq. (5.17), we finally obtain

$$\mathcal{L}_{\rm YM} + \mathcal{L}_{\rm gf} = \sum_{n=0}^{\infty} \Bigg[-\frac{1}{4} F_{\mu\nu}^{(n)} F^{\mu\nu(n)} + \frac{1}{2} m_{A^{(n)}}^2 A_\mu^{(n)} A^{\mu(n)} - \frac{1}{2\xi} \left(\partial_\mu A^\mu\right)^2 + \frac{1}{2} \partial_\mu a^{(n)} \partial^\mu a^{(n)} - \frac{1}{2} (\sqrt{\xi} m_{A^{(n)}})^2 (a^{(n)})^2 \Bigg], \quad (5.19)$$

where $m_{A^{(n)}} \equiv n/R$. Comparing this Lagrangian to Eq. (2.13), one observes that the four-dimensional gauge fields $A_\mu^{(n)}$, for $n \geq 1$, obtain masses by eating the fields $a^{(n)}$, which are interpreted as Goldstone bosons. Finally, note that if a was not restricted to be odd by the orbifolding procedure, there would be a massless scalar $a^{(0)}$ in the particle spectrum. Such a massless scalar, with gauge-strength interactions, is ruled out by experiments, and this is a second potential problem of the model that the orbifolding solves.

In the six-dimensional case, the situation concerning the gauge bosons is more complicated than in the five-dimensional case. In five dimensions, the KK modes of the fifth component of each gauge boson are eaten, in order to give masses to the corresponding KK modes of the four-dimensional part of the gauge boson. In six dimensions, there are two extra components for each gauge boson, and one linear combination of these is eaten, in the same way as in five dimensions, while the orthogonal combination appears as a physical scalar in the spectrum. This particle is known as the adjoint scalar. The extra components of a gauge field have to be assigned boundary conditions in such a way that the adjoint scalar has no zero mode, which means that it appears only starting from the first excited KK level.

5.3 Boundary localized terms and Kaluza–Klein parity

While resolving the chirality problem and removing the zero modes of the extra components of the gauge bosons, the orbifolding procedure also complicates the model. The orbifold $S^1/\mathbb{Z}_2$ has two fixed points under the $\mathbb{Z}_2$ transformation, $y = 0$ and $y = \pi R$, *i.e.*, the boundary points of the interval. At such points, the symmetries of the theory allow for localized terms in the Lagrangian, so-called boundary localized terms (BLTs). These terms could modify the mass spectrum as well as the interactions among the particles.

The BLTs are generated by radiative corrections [69], which means that it is inconsistent not to include them. In contrast to the bulk parameters in the UED Lagrangian, the BLTs are not determined by the SM parameters, and hence, they are separate inputs to the theory. In the most general case, all the BLTs that are

allowed by the SM gauge invariance should be included, and the coefficients of these operators can only be constrained by experiments. In the literature, the ansatz is often made that the BLTs vanish at the cutoff scale, Λ, of the higher-dimensional theory.[2] This ansatz defines the minimal UED (MUED) model. Although the BLTs are assumed to vanish at the energy scale Λ, the running of the parameters induces non-zero terms at lower energies.

In UED models, there are two different sources breaking translational invariance in the fifth dimension, and hence, conservation of the fifth component of the momentum. The BLTs explicitly do so, and in addition, there are contributions to the breaking from loop-processes wrapping around the compact dimension. The latter are intrinsically loop-suppressed, and in the MUED model, the BLTs are generated only by radiative corrections, so that those contributions are also loop-suppressed. On the level of the four-dimensional theory, this means that KK number is not conserved, but it is broken only at loop-level.

In the important case that the BLTs at the two fixed points are equal, the Lagrangian is invariant under a translation by πR, which maps the fixed points onto one another. This discrete translation defines a $\mathbb{Z}_2$ transformation on the orbifold $S^1/\mathbb{Z}_2$. Correspondingly, there should be a conserved quantity. Indeed, under the translation $x^5 \to x^5 + \pi R$, the KK wavefunctions transform as

$$\cos\left(\frac{nx^5}{R}\right) \quad \to \quad (-1)^n \cos\left(\frac{nx^5}{R}\right), \tag{5.20}$$

$$\sin\left(\frac{nx^5}{R}\right) \quad \to \quad (-1)^n \sin\left(\frac{nx^5}{R}\right). \tag{5.21}$$

If the Lagrangian is to be invariant under this transformation, the condition

$$(-1)^{\sum_i n_i} = 1 \tag{5.22}$$

has to hold for every vertex. Hence, the conservation of KK number is broken, but the total KK number in each vertex has to be even. In other words, on the four-dimensional level, there is a multiplicatively conserved quantum number, which can be defined as $(-1)^n$. The assumption that the BLTs appear symmetrically is consistent, in the sense that they evolve in the same way with the energy scale. This means that if they are equal at some energy scale, then this is true for all energies.

KK parity is analogous to R-parity, which is a discrete symmetry that appears in supersymmetric extensions of the SM. In such models, the supersymmetric partners of the SM particles are charged under R-parity, which implies that all vertices include an even number of such supersymmetric partners. The consequences of the two symmetries are similar.

In the six-dimensional UED model on the chiral square, the situation is similar. Like the $S^1/\mathbb{Z}_2$ orbifold, the chiral square has fixed points, at $(x^5, x^6) = (0, 0)$,

[2] The situation is analogous to the case of the minimal supersymmetric Standard Model, where an ansatz for the supersymmetry breaking terms is made at the scale of grand unification [14].

(L, L), and $(0, L)$.[3] These points induce BLTs and break the conservation of KK number. If the BLTs at the points $(0, 0)$ and (L, L) are identical[4], the Lagrangian is invariant under a rotation by π around the center of the square, *i.e.*,

$$x^5 \rightarrow L - x^5, \tag{5.23}$$
$$x^6 \rightarrow L - x^6. \tag{5.24}$$

Under this rotation, the KK wavefunctions given in in Eq. (5.11) transform as

$$\begin{aligned} f_n^{(j,k)}(x^5, x^6) &\rightarrow f_n^{(j,k)}(L - x^5, L - x^6) \\ &= \mathrm{e}^{-\mathrm{i}n\pi/2} \cos\left(-\frac{jx^5 + kx^6}{R} + (j+k)\pi + \frac{n\pi}{2}\right) \\ &\quad + \cos\left(-\frac{kx^5 - jx^6}{R} + (k-j)\pi + \frac{n\pi}{2}\right) \\ &= \mathrm{e}^{-\mathrm{i}n\pi/2} \cos\left(\frac{jx^5 + kx^6}{R} + \frac{n\pi}{2} - (j+k+n)\pi\right) \\ &\quad + \cos\left(\frac{kx^5 - jx^6}{R} + \frac{n\pi}{2} - (k-j+n)\pi\right) \\ &= (-1)^{j+k+n} \mathrm{e}^{-\mathrm{i}n\pi/2} \cos\left(\frac{jx^5 + kx^6}{R} + \frac{n\pi}{2}\right) \\ &\quad + (-1)^{-j+k+n} \cos\left(\frac{kx^5 - jx^6}{R} + \frac{n\pi}{2}\right) \\ &= (-1)^{j+k+n} f_n^{(j,k)}(x^5, x^6). \end{aligned} \tag{5.25}$$

where we have used the fact that $(-1)^j = (-1)^{-j}$. It can be shown that there are additional symmetries in the model that enforce the constraint $(-1)^n$ for each vertex [67]. Hence, there is again a conserved KK parity, which is given by $(-1)^{j+k}$.

To summarize, in the MUED models, KK parity is always conserved, while KK number is conserved at tree-level, but broken at loop-level. These constraints on the interactions of the KK particles have important consequences for the constraints on and phenomenology of the model.

5.3.1 Stability of the lightest Kaluza–Klein particle

An important consequence of the conservation of KK parity is that the lightest Kaluza–Klein particle (LKP), *i.e.*, the lightest first-level KK mode, is completely stable. By definition, the only particles that are lighter than the LKP are the SM particles, and by conservation of energy, these are the only particles that the LKP could decay into. Hence, any decay vertex of the LKP would have a net KK

[3] The fourth point, $(L, 0)$, is identified with $(0, L)$.

[4] The points at $(0, L)$ and $(L, 0)$ are identified on the orbifold, and hence, they have to be identical.

number $n = 1$, which is forbidden by KK parity. The fact that the LKP is stable means that it could potentially be a DM candidate. This kind of DM is known as Kaluza–Klein dark matter (KKDM), and was first proposed in Refs. [63, 64]. The situation is completely analogous to supersymmetric models where R-parity is conserved. The viability of the LKP as a DM candidate, and the corresponding phenomenology, is discussed in more detail in Sec. 7.5.

5.4 Mass corrections

At tree level, the mass for a given field with zero-mode mass m_0 is given by

$$m_n = \sqrt{m_0^2 + \frac{n^2}{R^2}} \tag{5.26}$$

in the five-dimensional case, and

$$m_{j,k} = \sqrt{m_0^2 + \frac{j^2 + k^2}{R^2}} \tag{5.27}$$

in the six-dimensional case. If the zero-mode contributions to the particle masses are ignored, all of the KK modes at a given level are degenerate, and processes such as $e^{(2)} \to e^{(1)} + \gamma^{(1)}$ would marginally be kinematically allowed. Although the issue would seem to be resolved by the zero-mode masses, these contributions could be completely irrelevant in comparison to radiative corrections to the masses [70]. This means that radiative corrections play a major role in determining the decay patterns of KK particles in UED models. Also, the identity of the LKP is sensitive to radiative corrections, and could have a large impact on studies of KKDM, where the LKP is the potential DM candidate.

Since the contributions to the masses of the KK modes coming from the extra dimensions are really parts of the momenta, these parts would seem to be protected by Lorentz invariance, and hence not obtain any corrections. However, due to the compactification of the fifth dimension on a circle, Lorentz invariance is broken at loop-level by virtual particles wrapping around this dimension. Since this is a long-distance effect, it gives rise only to finite, well-defined corrections to the mass spectrum. These corrections are present for any model of compactified extra dimensions.

A second source of radiative corrections is the orbifolding of the internal space, which induces BLTs that break Lorentz invariance locally. In MUED models, these corrections can be uniquely determined. In this case, they evolve from zero at the cutoff scale Λ, and are proportional to $\ln \Lambda$.

5.5 Minimal universal extra dimensions

We are now in a position to discuss the particle content and the phenomenology of realistic MUED models. We begin with the five-dimensional model, followed by the six-dimensional model on the chiral square.

5.5.1 Five dimensions

At each KK level, the electroweak gauge bosons $B^{(n)}$ and $W^{3(n)}$ mix to form mass eigenstates, in the same way as in the SM. The mass matrix at the nth KK level, in $\{B^{(n)}, W^{3(n)}\}$ basis, is given by [70]

$$\mathcal{M}^{(n)}_{\text{gauge}} = \begin{pmatrix} \frac{n^2}{R^2} + \delta m^2_{B^{(n)}} + \frac{1}{4}g'^2v^2 & \frac{1}{4}g'gv^2 \\ \frac{1}{4}g'gv^2 & \frac{n^2}{R^2} + \delta m^2_{W^{3(n)}} + \frac{1}{4}g^2v^2 \end{pmatrix}, \tag{5.28}$$

where $\delta m^2_{B^{(n)}}$ and $\delta m^2_{W^{3(n)}}$ are corrections to the tree-level masses. Due to the difference between these corrections, the mixing is small for $n > 0$. For $R^{-1} \geq 300$ GeV, the first-level Weinberg angle is bounded as $\sin\theta^{(1)}_{\text{W}} \lesssim 0.05$, and for larger values of n, it is even smaller. This means that we can make the approximation $B^{(n)} \simeq A^{(n)}$ and $W^{3(n)} \simeq Z^{(n)}$. In order to conform with the most commonly used notation in the literature, we will call these fields $B^{(n)}$ and $Z^{(n)}$. In the context of DM, we will use the simplified notation B^1 and Z^1 for the level-one KK excitations.

In the SM, each of the weak gauge bosons obtains a mass by eating a component of the Higgs field. In a five-dimensional gauge theory, the masses of the non-zero KK modes of a gauge boson can be understood as being due to the gauge boson eating its fifth component at each KK level, in a completely analogous way. In the case of the weak gauge bosons in the five-dimensional model, each KK mode receives mass terms from both of these sources[5], ad hence, the corresponding mechanism is more complicated. The fifth component of the gauge boson and the corresponding component of the Higgs field mix at each KK level to form two scalar particles. One of these is eaten by the gauge boson in order to generate a mass, and the other one appears as a physical scalar in the particle spectrum. The mixing angle $\beta^{(n)}$ at the nth KK level is given by

$$\tan\beta^{(n)} = \sqrt{\frac{m^2_A}{(n/R)^2 + \delta m^2_{A^{(n)}} + m^2_A}}, \tag{5.29}$$

where $A = W, Z$. Since $m^2_A \ll (n/R)^2 + \delta m^2_{A^{(n)}}$, the physical scalar is mainly composed of the Higgs field. Since one of the four components of the Higgs field is physical already in the SM, there are three new scalars at each KK level. Two of these, $H^{\pm(n)}$, are charged and the third, $A^{0(n)}$, is a pseudoscalar.

[5] Since the excited KK modes of the Higgs field obtain large positive contributions to the mass parameter $-\mu^2$, only the zero mode acquires a VEV.

For simplicity, the effects of electroweak symmetry breaking (EWSB) are usually ignored in comparison to the mass scale R^{-1}, *i.e.*, terms of order $(vR)^2$ are neglected. Using this approximation, the particle content of the model is summarized in Table 5.1.

The mass spectrum, including both sources of radiative corrections, was determined in Ref. [70]. In Fig. 5.3, the mass spectrum for the five-dimensional model with these corrections is shown for $R^{-1} = 500$ GeV, $\Lambda R = 20$ and $m_H = 125$ GeV. The LKP is the first KK excitation of the B boson, the B^1. In general, the identity of the LKP in the MUED model depends on the value of the compactification scale as well as the Higgs mass [71]. In some parts of the parameter space, the LKP could be the first-level KK mode of the graviton or the charged Higgs boson, $H^{\pm(1)}$. However, taking the current constraints on the MUED model into account (see Sec. 5.7), the $H^{\pm(1)}$ LKP is ruled out, and in most of the remaining parameter space, the B^1 is the LKP. Another important feature of the spectrum is that the heaviest level-one modes are the strongly interacting ones, *i.e.*, the KK quarks and gluons. These are the particles that have the largest production rates in hadron colliders such as the Tevatron and the LHC, and the fact that they have many kinematically open decay channels is important for the resulting phenomenology.

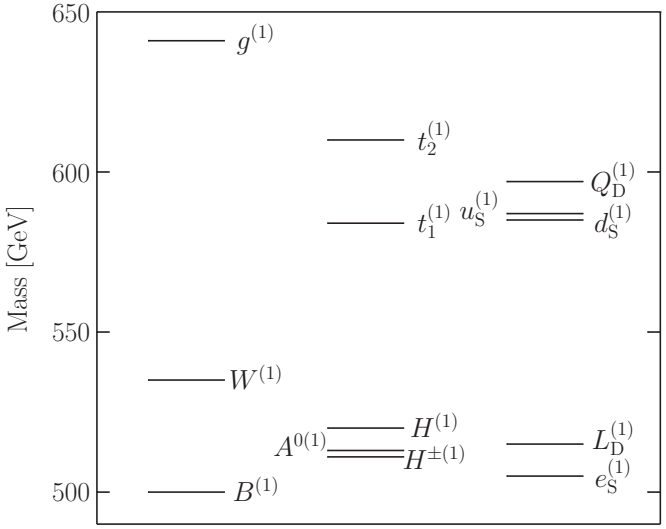

Figure 5.3. The mass spectrum of the five-dimensional MUED model, including radiative corrections.

5.5.2 Six dimensions

In general, the two extra components of each of the weak gauge bosons are mixed with the components of the Higgs field. In the limit that the inverse of the radius

Zero modes	$S^1/\mathbb{Z}_2$	$T^2/\mathbb{Z}_4$
$n = 0$ / $(j,k) = (0,0)$	$n \geq 1$	$(j,k) \neq (0,0)$
Gauge bosons		
A_μ	$B_\mu^{(n)} \simeq A_\mu^{(n)}$	$B_\mu^{(j,k)} \simeq A_\mu^{(j,k)}$
Z_μ	$W_\mu^{3(n)} \simeq Z_\mu^{(n)}$	$W_\mu^{3(j,k)} \simeq Z_\mu^{(j,k)}$
$W_\mu^\pm$	$W_\mu^{\pm(n)}$	$W_\mu^{\pm(j,k)}$
g_μ^a	$g_\mu^{a(n)}$	$g_\mu^{a(j,k)}$
Fermions		
$Q_{\rm L} = \begin{pmatrix} u_{\rm L} \\ d_{\rm L} \end{pmatrix}$	$Q_{\rm D}^{(n)} = \begin{pmatrix} u_{\rm D}^{(n)} \\ d_{\rm D}^{(n)} \end{pmatrix}$	$Q_{\rm D}^{(j,k)} = \begin{pmatrix} u_{\rm D}^{(j,k)} \\ d_{\rm D}^{(j,k)} \end{pmatrix}$
$u_{\rm R}$	$u_{\rm S}^{(n)}$	$u_{\rm S}^{(j,k)}$
$d_{\rm R}$	$d_{\rm S}^{(n)}$	$d_{\rm S}^{(j,k)}$
$L_{\rm L} = \begin{pmatrix} \nu_{\rm L} \\ e_{\rm L} \end{pmatrix}$	$L_{\rm D}^{(n)} = \begin{pmatrix} \nu_{\rm D}^{(n)} \\ e_{\rm D}^{(n)} \end{pmatrix}$	$L_{\rm D}^{(j,k)} = \begin{pmatrix} \nu_{\rm D}^{(j,k)} \\ e_{\rm D}^{(j,k)} \end{pmatrix}$
$e_{\rm R}$	$e_{\rm S}^{(n)}$	$e_{\rm S}^{(j,k)}$
		$\nu_{\rm S}^{(j,k)}$
Scalars		
H	$H^{(n)}$	$H^{(j,k)}$
	$A^{0(n)}$	$A^{0(j,k)}$
	$H^{\pm(n)}$	$H^{\pm(j,k)}$
		$B_{\rm H}^{(j,k)}$
		$W_{\rm H}^{3(j,k)}$
		$W_{\rm H}^{\pm(j,k)}$
		$g_{\rm H}^{a(j,k)}$

Table 5.1. The particle content in the two UED models described in this chapter, neglecting EWSB effects. For the six-dimensional model, the allowed values of the KK indices are $(j,k) = (0,0)$ and $j \geq 1$, $k \geq 0$, *i.e.*, there are no $(0,1)$ modes. The non-zero KK modes of the fermions are Dirac particles, and S and D denotes $SU(2)_{\rm L}$ singlets and doublets, respectively. The subscript H on the scalars in the six-dimensional model denotes adjoint scalars.

of the internal space is much larger than the VEV of the Higgs field, one of the physical combinations is mainly composed of the Higgs field, while the other is mainly a combination of the extra components of the weak gauge boson. In total, there are 15 new scalars at each KK level.

The particle content, neglecting EWSB effects, is summarized in Table 5.1. The mass spectrum for the six-dimensional MUED model on the chiral square, which was calculated in Refs. [72–74], is shown in Fig. 5.4. In this model, the LKP is the adjoint scalar $B^1_{\rm H}$, rather than B^1. Hence, the phenomenology of the model is quite different from the five-dimensional case. In addition, the relative mass splittings among the first-level KK modes are larger than in the five-dimensional case.

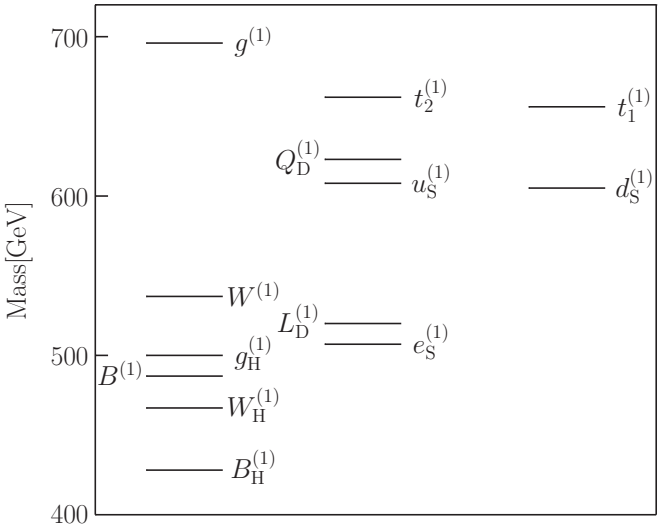

Figure 5.4. The mass spectrum of the six-dimensional MUED model on the chiral square, including radiative corrections. The masses of the Higgs fields depend quadratically on the cutoff scale, and hence, no reliable values can be given for those masses.

5.5.3 Collider phenomenology

In colliders, conservation of KK parity implies that first-level KK modes can only be produced in pairs. Once such a KK mode has been produced, it will decay in a chain where KK parity is conserved, ending in the production of the LKP. At each step in this decay chain, a SM particle is emitted, giving signals including jets, leptons, photons, and missing energy. Since the first-level KK mass spectrum is relatively degenerate, these SM particles will be soft, which means that it could be difficult to separate them from the background. For jets, the background is large at the LHC, and a better search strategy is to look for leptons [75]. The

most promising channel is the four leptons plus missing energy, for which the LHC should be able to probe to compactification radius up to about 1.5 TeV.

An alternative strategy, which could also be used to distinguish UED models from supersymmetric models at the LHC, is to search for signals from the second-level KK modes. The production of a single second-level KK particle is consistent with conservation of KK parity, but not KK number. Hence, such a process can occur at loop-level in MUED models. Since the masses of second-level particles are about twice as large as those of the first-level modes, a second-level particle can decay into SM particles or into a pair of first-level KK particles. In Ref. [76], it was found that the second-level KK modes of the γ and Z gauge bosons provide the best prospects for detection at the LHC. These particles can be detected as resonances in the invariant mass distributions of electron and muon pairs.

In the six-dimensional UED model on the chiral square, the situation regarding the second-level modes is different [73]. In this case, the second KK level consists of the $(1,1)$ states, which have masses of about $\sqrt{2}R^{-1}$. This has two important consequences for the phenomenology of these modes. First, for a given value for R^{-1}, the second-level modes are much lighter than in the five-dimensional model, enhancing their production cross sections. Second, decays into first-level modes, which have masses of about R^{-1}, are kinematically forbidden. This means that the second-level modes can only decay into SM particles, enhancing the resonant production of fermion pairs from decays of heavy gauge bosons.

5.6 Non-minimal universal extra dimensions

Going beyond the MUED models, *i.e.*, dropping the assumption that the BLTs vanish at the cutoff scale Λ, means that the parameters of the model are modified. In particular, this is true for the mass spectrum. Thus, non-minimal models could have a phenomenology differing quite significantly from the corresponding MUED models. As the number of BLTs allowed by the gauge symmetries of the SM is large, it is difficult to make a general analysis of the impact of BLTs on the phenomenology of UED models. The studies that have been performed in the literature have focused on a subset of the possible BLTs, or have taken a more phenomenological approach by assuming that the mass spectrum is modified in some specific way without considering the detailed mechanisms in terms of BLTs.

The BLTs give rise to modifications of precision observables already at tree-level, and hence, they can be experimentally constrained. However, these constraints are relatively weak, leaving significant room for phenomenologically relevant modifications in UED models. In Ref. [77], it was shown that experimentally allowed BLTs in the electroweak sector could modify the mass spectrum in such a way that the $Z^{(1)}$ or $H^{(1)}$ becomes the LKP. The consequences of this fact in the context of KKDM is discussed in Sec. 7.5.

In addition to the identity of the LKP, BLTs would modify the rest of the parameter space. This means that the decay patterns of the first-level KK modes could

change, modifying the collider phenomenology compared to the minimal models. Studies of collider signals in non-minimal UED models are much more dependent on the full first-level spectrum than DM studies, where the most important aspect is the LKP. Hence, it is difficult to perform robust studies of such signals.

5.7 Constraints on the models

UED models can by constrained by direct searches for KK particles at colliders as well as the contribution from the KK modes to different precision observables. At present, the limits from the collider and indirect searches give similar lower limits on the compactification scale. In addition, one of the strongest motivations for UED models is the possibility to obtain a DM candidate. Hence, the models are also indirectly constrained by the requirement of obtaining the correct relic abundance for the DM particle. The DM constraints are reviewed in Sec. 7.5.

5.7.1 Collider constraints

So far, the only analysis related to UED models performed by the LHC experiments treats a variation of the five-dimensional MUED model, which is embedded in an even higher-dimensional spacetime, where the additional dimensions are of the ADD type (see Sec. 6.1). In this model, the B^1 can decay into a KK graviton and a SM photon, giving rise to a diphoton plus large missing energy signal. The lower bound on the compactification of this model is given by $R^{-1} \geq 1.23$ TeV [78].

In Ref. [79], the results of the LHC searches for the SM Higgs boson were used to constrain the five-dimensional MUED model, as well as a number of six-dimensional models. The contributions from the KK modes to the production processes for the Higgs boson were used to constrain the compactification scale. In particular, the contributions from KK top quarks to the gluon fusion process are large in the UED model. The resulting lower limits on R^{-1} depend on the Higgs mass, with the limit increasing with m_H. For the five-dimensional UED model, the bound ranges from $R^{-1} \gtrsim 200$ GeV at $m_H = 120$ GeV to $R^{-1} \gtrsim 950$ GeV at $m_H = 140$ GeV. Below $m_H = 120$ GeV, no bound is obtained. For the six-dimensional UED model on the chiral square, the bound ranges from $R^{-1} \gtrsim 250$ GeV at $m_H = 115$ GeV to $R^{-1} \gtrsim 1300$ GeV at $m_H = 140$ GeV.

In Ref. [80], this idea was developed further, taking into account the UED contributions to the processes $gg \to H \to \gamma\gamma$ and $gg \to H \to W^+W^-$. Combining the LHC Higgs bounds with EWPO constraints and the requirement of having a DM candidate with the correct abundance, the authors found that only a small region of the MUED parameter space remains. However, this analysis is more sensitive to the specific MUED assumptions.

The direct search for KK modes at the Tevatron has also been used to place constraints on the compactification scale in the five-dimensional UED model. The

analysis performed in Ref. [81] gives the lower limit $R^{-1} \gtrsim 300$ GeV, using the multilepton channel.

5.7.2 Constraints from precision observables

The UED model can also be constrained by the contributions from the KK modes to the EWPOs, in particular to the self-energies of the gauge bosons. The leading KK contributions to the most important EWPOs are opposite to those of a heavy Higgs boson, and thus, the indirect EWPO bounds on the Higgs boson mass given in Table 2.1 are not valid in the UED model. Instead, the bounds on R^{-1} and m_H are correlated, with the upper limit on R^{-1} becoming weaker with an increasing Higgs mass.

The strongest constraint on the five-dimensional UED model from EWPOs was obtained by the Gfitter group [82], using results from Refs. [83, 84]. The result is shown in Fig. 5.5. For a low Higgs boson mass $m_H = 115$ GeV, the lower bound on the compactification scale is $R^{-1} \gtrsim 700$ GeV, which is comparable to the limit obtained from the LHC Higgs search described above, and for a heavy Higgs boson, $m_H = 700$ GeV, 300 GeV $\lesssim R^{-1} \lesssim 450$ GeV. The largest allowed value for the Higgs boson mass in the five-dimensional MUED model is 800 GeV.

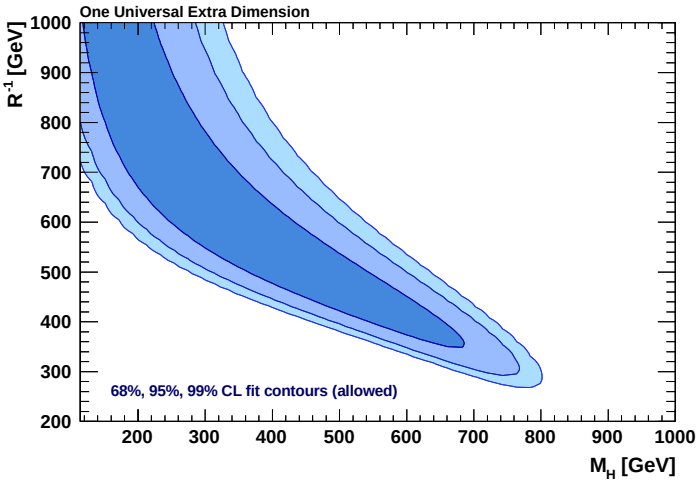

Figure 5.5. Constraints on the five-dimensional UED model from fits to EWPOs. The allowed 68 %, 95 %, and 99 % contours in the (m_H, R^{-1}) plane are shown. Figure taken from Ref. [82].

By considering the contributions from the KK modes to the $b \to s\gamma$ vertex in the five-dimensional MUED model, the authors of Ref. [85] obtained the lower limit $R^{-1} \gtrsim 600$ GeV at 95 % CL. This limit is independent of the Higgs mass, but depends on the MUED assumptions. A similar analysis for the six-dimensional

MUED model on the chiral square, which was carried out in Ref. [86], gives the lower limit $R^{-1} \gtrsim 650$ GeV at 95 % CL. However, in six-dimensional models, the sums over internal KK particles diverge, and hence, this result depends explicitly on the cutoff scale Λ.

In addition, constraints from the contributions of the KK modes to the $Zb\overline{b}$ vertex give lower limits on the compactification scale of the order of 300 GeV. [58, 87, 88].

5.7.3 Limits on the cutoff scale

An upper limit on the cutoff scale can be determined by considering the loop-expansion parameters corresponding to the gauge coupling constants, which are given by [89]

$$\varepsilon_i = N_i \frac{\alpha_i(\Lambda)}{4\pi} \Lambda R, \quad i = 1, 2, 3, \tag{5.30}$$

where $\alpha_i(\Lambda)$ is the fine-structure constant corresponding to the coupling constant g_i and N_i is the number of colors of the gauge group i. The non-renormalizability of the theory results in the linear Λ-dependence in this expression, and the upper bound on Λ is given by the solution to the equation $\varepsilon_i = 1$, *i.e.*, it is the energy scale where the coupling becomes non-perturbative. The strongest limit is set by the $SU(3)_c$ sector of the SM gauge group, giving an upper bound of the order of $\Lambda R \simeq 10$.

In Paper 7, a similar method was applied to the Higgs sector of the five-dimensional MUED model. The enhanced running induced by the extra dimensions could cause the Higgs self-interaction coupling constant λ to either diverge or become negative, in which case the Higgs potential would become unstable. The fate of λ depends on the initial conditions, *i.e.*, its low-energy value, which has not been experimentally measured. However, λ is related to the Higgs boson mass m_H through the relation $\lambda = m_H^2/v^2$, where v is the VEV of the Higgs field. Thus, the running behavior of λ is affected by the LHC Higgs mass bounds (see Sec. 2.2.2). For the allowed low-mass region, λ runs rapidly to negative values in the five-dimensional MUED model. Hence, the bound $\Lambda R < 6$ could be imposed for $m_H = 130$ GeV and $R^{-1} = 1$ TeV, with an even more restrictive bound for a smaller Higgs mass and/or a larger compactification scale.

Chapter 6

Brane models

An alternative way to avoid the problems related to fermions and gauge bosons in extra dimensions is to postulate that only some of the particles in the model propagate through the higher-dimensional spacetime. Typically, this is motivated by restricting the remaining particles to a lower-dimensional brane residing in the bulk. The particles that reside on the brane are effectively lower-dimensional, and have no corresponding KK towers. Since it is the excited KK modes that give rise to the constraints on higher-dimensional models, these constraints may be weakened by assuming that some particles are confined to a brane.

In this chapter, we describe two models that are based on this idea. First, we describe the so-called ADD model of large extra dimensions, where only gravity propagates in the bulk. Then, we consider a model where sterile fermions propagate in the bulk, giving rise to a mechanism for generating small neutrino masses.

6.1 Large extra dimensions—The ADD model

The standard example of a brane model is the ADD model, [59, 60], named after its originators Arkani-Hamed, Dimopolous, and Dvali, who proposed the model in 1998. In the ADD model, all the SM particles are confined to a brane. On the other hand, gravity, which is not a part of the SM, probes the full higher-dimensional spacetime. Because of the weakness of the gravitational interactions, the constraints on this sector are far less stringent than those on the SM.

6.1.1 The model

In the ADD model, the extra dimensions are assumed to be flat and compactified on the d-dimensional torus T^d. For simplicity, the radii of the extra dimensions are usually assumed to have a common value R. The number of extra dimensions d is a free parameter; however, if the model is considered as a low-energy limit of

string theory, where the total number of dimensions is ten or eleven, the maximum possible value is $d = 7$.

There are a number of different possible origins for the brane and the confining mechanism that restricts the SM to this subspace. One possible scenario was described in the original ADD paper [59], and other possibilities have been suggested in the literature, *e.g.*, in Ref. [90]. At sufficiently low energies, the thickness and dynamics of the brane can be neglected, which means that it has no other effect than to localize the SM fields. This is most commonly assumed in the literature, although studies of the effects of a dynamical brane have also been performed [91].

The existence of the brane breaks translational invariance along the extra dimensions, in the same way as the BLTs do in UED models. Therefore, momentum conservation is broken along these dimensions, enabling the production of single excited KK modes. In a more fundamental model, where the dynamics of the brane are taken into account, the recoiling momentum is provided by the brane itself. In the ADD model, there is no KK parity.

The only dynamical degrees of freedom in the bulk are the fluctuations of the metric tensor. According to the general theory of relativity, in the absence of matter and a cosmological constant, its dynamics are given by the Einstein field equations,

$$G_{\mu\nu} \equiv R_{\mu\nu} - \frac{1}{2} g_{\mu\nu} R = 0. \tag{6.1}$$

Here, $R_{\mu\nu}$ is the Ricci tensor, R is the Ricci scalar, and $\bar{M}_{\mathrm{Pl}}$ is the (reduced) Planck scale. The Planck scale is defined as $M_{\mathrm{Pl}} \equiv 1/\sqrt{G_{\mathrm{N}}}$, where G_{N} is Newton's gravitational constant. It is the energy scale where the gravitational interaction becomes strong. At this scale, quantum effects for gravity are expected to become important, and general relativity has to be replaced by a full quantum theory of gravity, which has not yet been found. The reduced Planck scale $\bar{M}_{\mathrm{Pl}} \equiv M_{\mathrm{Pl}}/\sqrt{8\pi}$ is introduced in order to simplify equations by removing numerical constants.

Equation (6.1) can be obtained by applying the principle of stationarity to the Einstein–Hilbert action

$$\mathcal{S}_{\mathrm{EH}} = \bar{M}_{\mathrm{Pl}}^2 \int \sqrt{|g|}\mathrm{d}^4 x R. \tag{6.2}$$

This formulation of the theory has the advantage that it is straightforward to generalize it to an arbitrary number of dimensions. Notice that, since the mass dimension of the Ricci scalar $[R] = 2$, the first term in the action must be multiplied by a constant of mass dimension two in order to be dimensionless. The Planck scale is the relevant energy scale for general relativity, and the overall numerical coefficient is determined by comparing the equations of motion to classical Newtonian mechanics in the low-energy limit.

Generalizing the Einstein–Hilbert action to D dimensions, we obtain

$$\mathcal{S}_{\mathrm{EH}}^{(D)} = \bar{M}_D^{d+2} \int \sqrt{|g|}\mathrm{d}^D x R. \tag{6.3}$$

The quantity $\bar{M}_D$ is analogous to $\bar{M}_{\rm Pl}$ and the factor $\bar{M}_D^{d+2}$ makes the action dimensionless.

The main motivation for the ADD model is to provide a solution to the hierarchy problem, which was described in Sec. 2.3.4. In the ADD model, the quantity M_D replaces the Planck scale $M_{\rm Pl}$ as the fundamental mass scale for gravity. Hence, the cutoff scale that appears in the hierarchy problem is M_D, rather than $M_{\rm Pl}$. If the volume of the internal space is sufficiently large, this new fundamental scale can be significantly closer to the electroweak scale.

At low energies, the higher-dimensional Einstein–Hilbert action (6.3) can be approximated by the expression

$$\mathcal{S}_{\rm EH}^{(D)} \simeq \bar{M}_D^{d+2} V_d \int \sqrt{|g|}\mathrm{d}^4 x R^{(0)}, \tag{6.4}$$

which is obtained by neglecting the excited KK modes of the Ricci scalar and integrating out the extra dimensions, giving the volume factor $V_d = (2\pi R)^d$. Comparing Eq. (6.4) to the four-dimensional Einstein–Hilbert action (6.2) we obtain the relation

$$\bar{M}_{\rm Pl}^2 = \bar{M}_D^{d+2} V_d = \bar{M}_D^{d+2} (2\pi R)^d = M_D^{d+2} R^d. \tag{6.5}$$

In the last step, we have introduced the quantity $M_D = (2\pi)^{d/(2+d)} \bar{M}_D$, following Ref. [92]. By appropriately choosing the size of the radius R, the new fundamental Planck scale M_D can be lowered down to the electroweak scale. Assuming $M_D =$ 1 TeV gives

$$R = M_D^{-1} \left(\frac{\bar{M}_{\rm Pl}}{M_D} \right)^{2/d} \simeq 10^{32/d}\ \mathrm{TeV}^{-1} \simeq 2 \cdot 10^{\frac{32-19d}{d}}\ \mathrm{m}. \tag{6.6}$$

Numerical values of R for $d = 1, \ldots, 7$ are given in Table 6.1. From the point of view of the higher-dimensional theory, the weakness of gravity can be understood as the suppression of Newton's gravitational constant by the large volume of the extra dimensions. Although gravity could be of the same strength as the SM interactions, it is spread out in a large internal space, and hence, it seems weak from the four-dimensional point of view.

However, there is a problem with the solution to the hierarchy problem in the ADD model. Although the fundamental Planck scale M_D can be lowered to the electroweak scale, a new energy scale is introduced through the radius R. For $M_D = 1$ TeV, the relation between R and M_D is

$$R^{-1} = 10^{-32/d} M_D \ll M_D. \tag{6.7}$$

Hence, the hierarchy problem is simply reformulated as the question of why the size of the extra dimensions is so large compared to the Planck scale. This problem can possibly be resolved by considering an analogue of the ADD model, where the extra dimensions are hyperbolic rather than flat [93]. The volume of a hyperbolic space depends exponentially on its radius, and hence, a large volume suppression

d	R	R^{-1}
1	$2 \cdot 10^{13}$ m	10^{-20} eV
2	2 mm	0.1 meV
3	9 nm	20 eV
4	$2 \cdot 10^{-11}$ m	10 keV
5	$5 \cdot 10^{-13}$ m	400 keV
6	$4 \cdot 10^{-14}$ m	5 MeV
7	$7 \cdot 10^{-15}$ m	30 MeV

Table 6.1. The radii R of the extra dimensions and the mass splittings R^{-1} in the ADD model, assuming $M_D = 1$ TeV.

can possibly be obtained while keeping the size of the extra dimensions closer to the fundamental Planck scale. The collider phenomenology of such a model was considered in Paper 8.

6.1.2 The graviton

Like the SM, general relativity can be seen as a gauge theory. The gauge transformations are the general coordinate transformations, and the gauge field is a spin-2 boson known as the graviton. However, since the coupling constant $M_{\rm Pl}^{-1}$ has negative mass dimension, quantizing the general theory of relativity gives a non-renormalizable theory. At energies lower than $M_{\rm Pl}$, such a theory can be used as an effective theory.

The graviton is treated as a perturbation around a background metric, *i.e.*,

$$g_{\mu\nu} = \eta_{\mu\nu} + \frac{h_{\mu\nu}}{M_{\rm Pl}}. \tag{6.8}$$

Here, $g_{\mu\nu}$ is the full metric, $\eta_{\mu\nu}$ is the background metric, and $h_{\mu\nu}$ is the graviton field. The normalization factor $M_{\rm Pl}^{-1}$ gives the graviton the correct mass dimension. Since $h_{\mu\nu}$ is symmetric, it has ten degrees of freedom, which is twice the number expected for a spin-2 particle. However, five of these degrees of freedom are unphysical and can be removed by choosing a gauge.

The linearized equations of motion for the graviton are obtained by inserting the expression given in Eq. (6.8) into the Einstein field equations, and expanding to first order in $M_{\rm Pl}^{-1}$. In the case that the background metric $\eta_{\mu\nu}$ is the flat Minkowski metric, the resulting equations in the so-called harmonic gauge [94] are

$$\Box h_{\mu\nu} = 0, \tag{6.9}$$

where $\Box \equiv \partial^\mu \partial_\mu$ is the d'Alembert operator. Equation (6.9) is the wave equation for a particle traveling at the speed of light.

In the ADD model, the d'Alembert operator is generalized to $\Box = \partial^K \partial_K$, and with this replacement, the analogue of Eq. (6.9) is

$$\partial^K \partial_K h_{MN} = (\Box_4 + \partial^m \partial_m) h_{MN} = 0, \tag{6.10}$$

where $\Box_4$ is the four-dimensional d'Alembert operator. The field h_{MN} can be expanded in a Fourier series

$$h_{MN}(x^\mu, y) = \frac{1}{(2\pi R)^{d/2}} \sum_{n=-\infty}^{\infty} h_{MN}^{(n)}(x^\mu) \mathrm{e}^{\frac{\mathrm{i}n\cdot y}{R}}. \tag{6.11}$$

The equation of motion for the nth KK mode is

$$\left(\Box_4 + \frac{|n|^2}{R^2}\right) h_{MN}^{(n)} = 0, \tag{6.12}$$

which is the Klein–Gordon equation for a field with mass $m_n = |n|/R$.

6.1.3 Graviton interactions

In order to make predictions for processes involving KK gravitons, the interactions between the graviton and the SM fields have to be determined. These interactions are given by adding to the Einstein–Hilbert action the term

$$\mathcal{S}_{\mathrm{int}} = \int \sqrt{|g|} \mathrm{d}^4 x \mathcal{L}_{\mathrm{matter}}. \tag{6.13}$$

Here, $\mathcal{L}_{\mathrm{matter}}$ is the SM Lagrangian, modified to include interactions with the graviton. Hence, the graviton couples to all SM fields through the factor $\sqrt{|g|}$ in the integration measure. In addition, there are gauge interactions between the SM fields and the graviton, which are given by additional terms in the covariant derivatives, in the same way as for the SM gauge bosons.

In order to determine the coupling of the graviton field $h_{\mu\nu}$ to the SM fields, we use Eq. (6.8), and expand the Lagrangian to first order in $\bar{M}_{\mathrm{Pl}}^{-1}$, which gives

$$\sqrt{|g|}\mathcal{L} = \mathcal{L} + \frac{1}{\bar{M}_{\mathrm{Pl}}} T^{\mu\nu} h_{\mu\nu} + \mathcal{O}(\bar{M}_{\mathrm{Pl}}^{-2}), \tag{6.14}$$

where we have introduced the energy-momentum tensor

$$T^{\mu\nu} = \frac{\delta\left(\sqrt{|g|}\mathcal{L}_{\mathrm{matter}}\right)}{\delta g_{\mu\nu}}. \tag{6.15}$$

To lowest order, the graviton couples to the energy-momentum tensor $T^{\mu\nu}$, with the interaction suppressed by the factor $\bar{M}_{\mathrm{Pl}}^{-1}$.

It is straightforward to generalize these results to the ADD model, for which the interaction is given by

$$\mathcal{S}_{\rm int} = \frac{1}{M_D^{\frac{d+2}{2}}} \int \mathrm{d}^D x \; T^{MN}(x^\mu, y^a) h_{MN}(x^\mu, y^a). \tag{6.16}$$

Since the SM fields are confined to the brane at $y = y_0$, the energy-momentum tensor has the form

$$T^{MN}(x^\mu, y) = \delta^M_\mu \delta^N_\nu T^{\mu\nu}(x^\mu) \delta^{(d)}(y - y_0), \tag{6.17}$$

where $\delta^{(d)}(y)$ is the Dirac distribution in d dimensions and $T^{\mu\nu}$ is the ordinary four-dimensional energy-momentum tensor. Using this result and the KK expansion of the graviton field given in Eq. (6.11), we obtain the action

$$\begin{aligned} \mathcal{S}_{\rm int} &= \frac{1}{M_D^{\frac{d+2}{2}}} \sum_n \int \mathrm{d}^4 x \; T^{\mu\nu}(x^\mu) \frac{1}{(2\pi R)^{d/2}} h^{(n)}_{\mu\nu}(x^\mu) \mathrm{e}^{\frac{\mathrm{i}n \cdot y_0}{R}} \\ &= \frac{1}{\bar{M}_{\rm Pl}} \sum_n \int \mathrm{d}^4 x \; T^{\mu\nu}(x^\mu) h^{(n)}_{\mu\nu}(x^\mu). \end{aligned} \tag{6.18}$$

In the last equality, we have used the relation $\bar{M}_{\rm Pl}^2 = M_D^{d+2} R^d$ to eliminate R. We have also used the fact that the value of y_0 only determines the phase of $h_{\mu\nu}$, which does not affect any physical results, so that we can set $y_0 = 0$ without loss of generality. Hence, similarly to gravity in four dimensions, each KK mode couples to the energy-momentum tensor with the coupling suppressed by $\bar{M}_{\rm Pl}^{-1}$. The difference induced by the extra dimensions is that there is a KK tower of gravitons.

6.1.4 Collider signatures

We can now turn to the possible collider signatures of the ADD model. The graviton could be directly produced as a real particle, or indirectly studied by measuring contributions to SM processes from gravitons in virtual intermediate states. Both of these kinds of signatures of the ADD model have been studied in the literature [92, 95–103].

Since cross sections involving a graviton are suppressed by the inverse square of the Planck scale, the production rates for single graviton modes are very low. However, in the ADD model, the mass splitting R^{-1} between the KK modes is typically small, and hence, a large number $E_{\rm cm} R$ of KK modes are available. By searching for the production of *any* graviton mode together with a detectable SM particle, a sufficiently large total cross section could potentially be obtained. From the five-dimensional point of view, this corresponds to the production of a graviton

with any momentum along the extra dimensions. The cross section for such a process is given by

$$\sigma_{\rm tot} = \sum_n \sigma_m \simeq \int {\rm d}m \rho(m) \sigma_m, \tag{6.19}$$

where σ_m is the cross section for the production of a KK mode with mass m in the given process. In the last step, we have used the fact that the mass splittings between the states are small, compared to the experimental energy resolution, in order to approximate the sum as an integral. The function $\rho(m)$ is the density of states, which is given by

$$\rho(m) = S_{d-1} \frac{\bar{M}_{\rm Pl}^2}{M_D^{2+d}} m^{d-1}, \tag{6.20}$$

where S_{d-1} is the area of the unit sphere in d dimensions.

Due to its very weak interaction with matter, a produced graviton will escape detection, giving missing energy signals. The best detection prospects are given by two-body processes, where the graviton is produced together with one additional particle. In Ref. [92], it was concluded that, in direct production processes, graviton production together with a photon or a single jet gives the best prospects for detection.

6.1.5 Constraints

There are a number of ways of constraining the parameter space of the ADD model. In addition to collider searches, the model predicts modifications to Newton's law for sufficiently small distance scales, and the existence of a large number of light gravitons could potentially be problematic in high-temperature astrophysical contexts. Which constraint is the most important depends heavily on the number of extra dimensions. Below, we discuss each of the important constraints in turn.

Deviations from Newton's law

In a theory where gravity propagates in d extra dimensions with radii R, the gravitational potential is given by

$$V(r) = -G_{\rm N} \frac{m_1 m_2}{r^{1+d}} \tag{6.21}$$

for $r \lesssim R$, while the ordinary expression holds for $r \gtrsim R$. Hence, the extra dimensions give rise to deviations from this law at distance scales given by the size of the extra dimensions. If the radius R is too large, the deviations could be in conflict with experimental results. For $d = 1$, deviations would be observed already at the

scale of the solar system, which is clearly ruled out. Constraints on deviations from Newton's law of the general form

$$V(r) = -G_{\mathrm{N}} \frac{m_1 m_2}{r} \left(1 + \alpha \mathrm{e}^{-r/\lambda}\right) \tag{6.22}$$

are shown in Fig. 6.1 [104]. Using these constraints, the upper limit on the radius of the largest extra dimension is $R \leq 44\ \mu$m. Comparing this limit to the radii given in Table 6.1 shows that $d = 2$ is also ruled out for $M_D = 1$ TeV, but allowed for $M_D > 3.2$ TeV. For $d \geq 3$, the deviations occur on small enough distances scales to avoid detection.

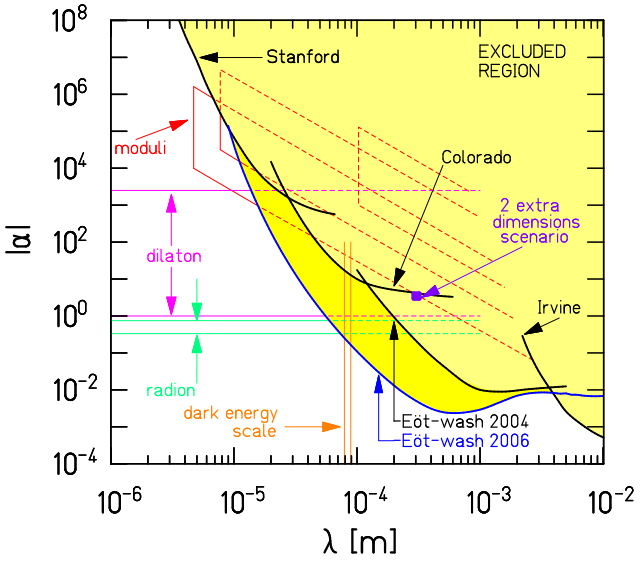

Figure 6.1. Constraints on deviations from Newton's law of the form given in Eq. (6.22). Figure taken from Ref. [104].

Astrophysical constraints

Even stronger constraints can be placed on the model by considering its impact on astrophysical systems. In particular, as pointed out in Ref. [105], KK gravitons which are produced in supernovae and subsequently bound to neutron stars would give rise to photons through $G^{(n)} \to \gamma\gamma$ decays. Using data from the EGRET satellite, the authors were able to obtain bounds on M_D. Recently, the Fermi-LAT collaboration performed a more detailed analysis along the same lines [106], obtaining the bounds $M_D \gtrsim 230$ TeV, 16 TeV, and 2.5 TeV for $d = 2$, 3, and 4.

For $d = 2$ and 3, these are currently the strongest bounds available on the ADD model, whereas for $d = 4$, the result is comparable to collider limits. However, it should be noted that these results rely on all the extra dimensions having the same size, and could be much less restrictive in more general cases. For example, in the model of hyperbolic large extra dimensions that is studied in Paper 8, there is a mass gap at the lower end of the spectrum. If this gap is larger than the supernova temperature, these bounds will be evaded completely.

In addition, weaker constraints on the model are obtained by considering the accelerated cooling of supernovae due to the emission of light KK gravitons. The strongest constraints of this kind come from the supernova SN1987A. For $d = 2$, 3, and 4, the lower bound on M_D obtained in this way is 50 TeV, 4 TeV, and 1 TeV, respectively [107].

Collider constraints

The ATLAS and CMS collaborations have searched for signals of the ADD model in the diphoton, dilepton, and monojet plus large missing energy channels. The constraints on the fundamental mass scale M_D obtained through these searches are summarized in Table. 6.2, for the number of extra dimensions $d = 2, \ldots, 7$. The signal in the monojet plus missing energy channel is due to the direct production of KK gravitons, which is sensitive to M_D. On the other hand, the diphoton and dilepton channels receive contributions from virtual KK gravitons. Since the sums over KK modes for $d \geq 2$ diverge, these results are sensitive to the cutoff scale Λ, rather than M_D. It is not clear what the exact relation between Λ and M_D is. The limits quoted in Table. 6.2 are obtained using the relation given in Ref. [95].

Analysis			$d =$	2	3	4	5	6	7
Monojet + missing energy									
ATLAS	1 fb^{-1}	[108]†		3.2	2.6	2.3	2.1	2.0	
ATLAS	33 pb^{-1}	[109]		2.3	2.0	1.8			
CMS	1.1 fb^{-1}	[110]†		4.0	3.2	2.8	2.6	2.4	
CMS	36 pb^{-1}	[111]		2.6	2.1	1.9	1.7	1.7	
Diphotons									
ATLAS	2.12 fb^{-1}	[112]			3.1	2.9	2.7	2.6	2.4
CMS	2.2 fb^{-1}	[113]		2.6	3.3	3.1	2.9	2.8	2.6
Dileptons									
CMS	2 fb^{-1}	[114]		2.7	3.3	3.1	2.9	2.8	2.6

† Preliminary results

Table 6.2. The ATLAS and CMS 95 % CL lower bounds on the fundamental mass scale M_D (measured in TeV) in the ADD model.

Constraints from precision observables

The virtual exchange of KK gravitons contributes to EWPOs as well as the muon anomalous magnetic moment. Using the results from Ref. [115], the Gfitter group [82] has used the experimental bounds on these parameters to put constraints on the ADD model. As for the collider processes, the results depend explicitly on the cutoff scale Λ, and the results are given as functions of Λ/M_D. The resulting allowed regions are shown in Fig. 6.2.

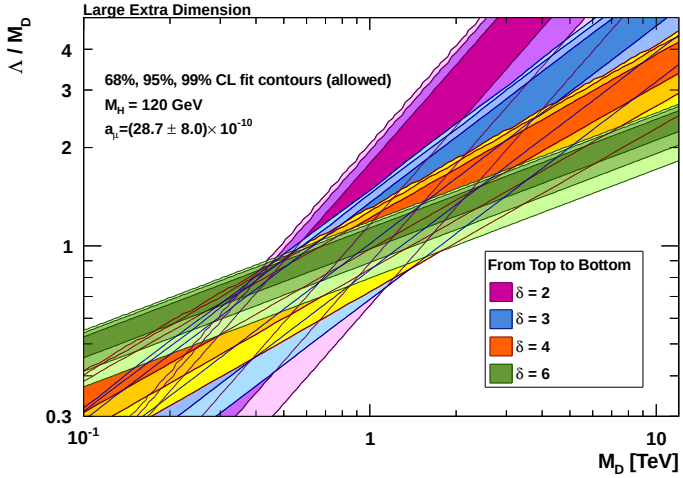

Figure 6.2. Constraints on the ADD model from a combination of electroweak precision data and the muon anomalous magnetic moment. The allowed 68 %, 95 %, and 99 % contours in the $(M_D, \Lambda/M_D)$ plane are shown for a number of extra dimensions $\delta = 2$, 3, 4, and 6. Figure taken from Ref. [82].

6.1.6 Limits on the cutoff scale

The cutoff scale of the model can be estimated in the same way as for the UED model, by considering the loop-expansion parameter. For the ADD model, it is given by [92]

$$\varepsilon = \frac{S_{D-1}}{2(2\pi)^D} \left(\frac{\Lambda}{M_D}\right)^{D-2}. \tag{6.23}$$

The upper limit thus obtained for Λ is

$$\Lambda = [\Gamma(2 + d/2)]^{\frac{1}{2+d}} \, (4\pi)^{\frac{4+d}{d+2d}} \, M_D. \tag{6.24}$$

However, since M_D is the fundamental energy scale for gravity, unknown quantum gravitational effects are expected to become important at this scale, making any predictions above M_D uncertain.

6.2 Higher-dimensional neutrino mass models

In the spirit of the ADD model, it is natural to consider the possibility of only SM singlet particles probing the bulk. In particular, if right-handed neutrinos were added to the SM following the patterns of the other fermions, they would be SM singlets. As discussed in Sec. 5.1, two-component chiral fermions do not exist in higher-dimensional models, and instead, the right-handed neutrinos would be replaced by SM singlet Dirac fermions with right-handed zero modes. In order for the theory to be effectively chiral at the level of the zero modes, it has to be compactified on a properly chosen orbifold. Here, we consider the simplest possibility, $S^1/\mathbb{Z}_2$. The model resembles the type-I seesaw model (see Ch. 3), except that the zero modes of the sterile fermions are accompanied by towers of massive KK modes, which could be responsible for the suppression of the light-neutrino masses.

The KK expansions of the sterile fermions $\Psi = (\xi\, \eta^c)^T$ are given in Eq. (5.6). The relevant parts of the action are given by

$$\begin{aligned} \mathcal{S} &= \int \mathrm{d}^5x \left[\mathrm{i}\overline{\Psi}\Gamma^M D_M \Psi - \frac{1}{2}\left(\overline{\Psi^c} M_\mathrm{R} \Psi + \mathrm{h.c.}\right)\right] \\ &\quad + \int_{y=0} \mathrm{d}^4x \left(-\frac{1}{\sqrt{M_\mathrm{S}}} \overline{\nu_\mathrm{L}} \hat{m}^c \Psi - \frac{1}{\sqrt{M_\mathrm{S}}} \overline{\nu_\mathrm{L}^c} \hat{m} \Psi + \mathrm{h.c.} \right), \end{aligned} \tag{6.25}$$

where M_S is the higher-dimensional mass scale. The five-dimensional mass term M_R leads to Majorana mass terms for the KK modes of Ψ, and there are also two four-dimensional Dirac mass terms, $\hat{m}$ and $\hat{m}^c$, localized on the brane where the left-handed neutrinos live. It is useful to introduce the linear combinations

$$X^{(n)} = \frac{1}{\sqrt{2}}(\xi^{(n)} - \eta^{(n)}), \tag{6.26}$$

$$Y^{(n)} = \frac{1}{\sqrt{2}}(\xi^{(n)} + \eta^{(n)}). \tag{6.27}$$

In the basis $\{\nu_{\rm L}, \xi^{(0)}, X^{(1)}, Y^{(1)}, \ldots\}$, the action (6.25) gives rise to the infinite-dimensional mass matrix

$$\mathcal{M} = \begin{pmatrix} 0 & m_{\rm D} & m_{\rm D} & m_{\rm D} & \cdots & m_{\rm D} & m_{\rm D} & \ldots \\ m_{\rm D}^T & M_{\rm R} & 0 & 0 & \cdots & 0 & 0 & \ldots \\ m_{\rm D}^T & 0 & M_{\rm R} - \dfrac{1}{R} & 0 & \cdots & 0 & 0 & \ldots \\ m_{\rm D}^T & 0 & 0 & M_{\rm R} + \dfrac{1}{R} & \cdots & 0 & 0 & \ldots \\ \vdots & \vdots & \vdots & \vdots & \ddots & 0 & 0 & \ldots \\ m_{\rm D}^T & 0 & 0 & 0 & 0 & M_{\rm R} - \dfrac{n}{R} & 0 & \ldots \\ m_{\rm D}^T & 0 & 0 & 0 & 0 & 0 & M_{\rm R} + \dfrac{n}{R} & \ldots \\ \vdots & \vdots & \vdots & \vdots & \vdots & \vdots & \vdots & \ddots \end{pmatrix} . \tag{6.28}$$

An approximate solution to the eigenvalue equation for this mass matrix with respect to the small ratio $m_{\rm D}/M_{\rm R}$ gives the light-neutrino mass matrix

$$m_\nu \simeq m_{\rm D} \left(M_{\rm R}^{-1} + \sum_{n=1}^{\infty} \frac{2M_{\rm R}}{M_{\rm R}^2 - n^2/R^2} \right) m_{\rm D}^T = m_{\rm D} \frac{\pi R}{\tan{(\pi R M_{\rm R})}} m_{\rm D}^T . \tag{6.29}$$

In the case that the Majorana mass $M_{\rm R}$ takes on one of the values $(n + 1/2)R^{-1}$, where n is an integer, this mass vanishes identically. Although such an apparent fine-tuning seems unnatural, it is motivated in the context of string theory by the Scherk–Schwartz decomposition, which requires $M_{\rm R} = (n + 1/2)R^{-1}$, due to topological constraints [116]. If this relation would hold exactly, the light-neutrino masses would vanish. However, small perturbations could result in neutrino masses which are naturally light.

In Paper 5, we have investigated an alternative seesaw mechanism in the context of extra dimensions. Since higher-dimensional theories are generally non-renormalizable, the KK tower must be cut off at some energy scale Λ. In the case that the tower is cut at some maximal KK number N, the massive eigenstates pair to form Dirac neutrinos, except for the top of the KK tower, where a single Majorana neutrino with mass N/R remains. This heavy mode is responsible for the generation of the light-neutrino masses. In the case $N \gg RM_{\rm R}$, the light-neutrino masses are given by

$$m_\nu \simeq (R/N) m_{\rm D} m_{\rm D}^T . \tag{6.30}$$

Mixing among the left-handed neutrinos and the sterile fermions induces non-unitarity effects in the neutrino mixing matrix, as discussed in Sec. 3.3. Due to the tower of sterile fermions, we have

$$\nu_{\rm L} \simeq V \nu_{m{\rm L}} + K^{(0)} \xi^{(0)} + \sum_{n=1}^{N} \left[K^{(-n)} X^{(n)} + K^{(n)} Y^{(n)} \right] , \tag{6.31}$$

where the coefficients $K^{(n)} = m_{\rm D}(M_{\rm R} + n/R)^{-1}$ and V is the upper-left 3×3 sub-matrix of the unitary matrix diagonalizing the complete mass matrix including the sterile fermions. The non-unitarity matrix ε is related to the parameters of the model through the expression

$$\varepsilon \simeq \frac{1}{2}\pi^2 R^2 m_{\rm D} m_{\rm D}^{\dagger}, \tag{6.32}$$

and hence, the non-unitarity bounds can be used to constrain the parameter space of the model. As an example, for $R^{-1} = 1$ TeV and $m_{\rm D} = 100$ GeV, the non-unitarity matrix is of the order of 10^{-2}, which is larger than allowed by the constraints given in Eq. (3.16).

6.2.1 Collider signatures

The production of KK modes of the sterile fermions, followed by their decays into the final states $\ell_\alpha W^+$, $\nu_\alpha Z$, and $\nu_\alpha H$, gives rise to possible collider signatures. In general, multi-lepton final states at the LHC are promising channels for seesaw models [117]. Also, a particularly striking feature of seesaw models is the breaking of lepton number. However, in the higher-dimensional models described here, the lepton number breaking occurs only at a high-energy scale, and hence, it is not relevant for collider searches. Instead, lepton number conserving multi-lepton and missing energy searches provide the best prospects. In Ref. [118], where the LHC signals of the higher-dimensional seesaw model without a cutoff were considered, the most promising channel was found to be three leptons and large missing energy. It was found that the LHC would be able to probe the parameter space up to R^{-1} of the order of a few hundred GeV.

In Paper 5, we considered the three leptons and large missing energy channel for the truncated model that is described above. From the collider signal point of view, this model is very similar to the model studied in Ref. [118]. However, in contrast to the result of that work, we found that the constraints imposed on the model from contributions to the non-unitarity parameters are sufficiently strong to rule out the part of the parameter space of the model that could possibly be probed at the LHC.

Chapter 7

Dark matter

The subject of DM was born in 1933 with the observation by Zwicky that the measured light emitted from the Coma galaxy cluster did not correspond to the inferred total mass of the cluster [119]. Since then, an increasing amount of observations giving further support to the DM hypothesis has been obtained, and today, the concept of a DM sector of the Universe is well-established. Although the need for DM is realized through cosmological observations, it has strong implications for particle physics, in particular for models beyond the SM. The fact that DM has not been directly observed provides one of the major challenges for particle physics today. The subject is one of the strongest links between the descriptions of Nature on the smallest and largest scales. It is currently one of the most active areas of research in particle physics, astrophysics, and cosmology.

We begin the chapter with a short overview of the standard model of cosmology and the need for a DM sector in the Universe. This is followed by a discussion on the general properties of DM candidate particles. Then, we consider KKDM, which is the most important class of DM candidates for this thesis. Finally, we discuss the issue of detection of DM, focusing in particular on the detection prospects for KKDM candidates.

7.1 Standard cosmology

The standard model of cosmology, the Hot big bang model, is based on the cosmological principle, stating that the Universe is homogeneous and isotropic on large-distance scales. An immediate consequence of this assumption is that the metric in such a Universe has the form

$$\mathrm{d}s^2 = \mathrm{d}t^2 - a(t)^2 \left[\frac{1}{1-kr^2} \mathrm{d}r^2 + r^2 \left(\mathrm{d}\theta^2 + \sin^2\theta \mathrm{d}\phi^2 \right) \right], \tag{7.1}$$

known as the Friedmann–Lemaître–Robertson–Walker (FLRW) metric. The function $a(t)$ is known as the scale factor, and the constant k takes one of the values 0,

$+1$, or -1, corresponding to a flat, positively curved, or negatively curved Universe, respectively.

In a flat and homogeneous Universe, the energy-momentum tensor in the right-hand side of Einstein's equations (6.1) takes the form of a perfect fluid,

$$(T^{\mu}{}_{\nu}) = \mathrm{diag}(\rho, p, p, p), \tag{7.2}$$

in a comoving reference frame, *i.e.*, a frame where r, θ, and ϕ are constant. The energy density ρ and the pressure p are related by an equation of state, $p = w\rho$, for some constant w, which depends on the specific type of energy. For example, for non-relativistic matter, $w = 0$, while for radiation, $w = 1/3$.

Inserting the metric (7.1) and the energy-momentum tensor (7.2) into Einstein's equations gives the so-called Friedmann equation,

$$H^2 \equiv \left(\frac{\dot{a}}{a}\right)^2 = \frac{8\pi G_{\mathrm{N}}\rho + \Lambda}{3} - \frac{k}{a^2}, \tag{7.3}$$

where we have the defined the Hubble rate H. The Hubble rate governs the expansion of the Universe through Hubble's law, $v = Hd$, where v is the relative velocity of two spacetime points separated by the distance d. It is useful to introduce the dimensionless constant $h = H/(100 \text{ km s}^{-1} \text{ Mpc}^{-1})$. Current observations give $h = 0.702 \pm 0.014$ at 68 % CL [40].

By defining the critical density

$$\rho_{\mathrm{c}} = \frac{3H^2}{8\pi G_{\mathrm{N}}}, \tag{7.4}$$

the Friedmann equation can be written as

$$\Omega + \Omega_\Lambda + \Omega_k = 1, \tag{7.5}$$

where $\Omega = \rho/\rho_{\mathrm{c}}$, $\Omega_\Lambda = \Lambda/(8\pi G_{\mathrm{N}}\rho_{\mathrm{c}})$, and $\Omega_k = -k/\dot{a}^2$. Furthermore, the density Ω can be divided into contributions from radiation, baryonic matter, and other forms of matter. Due to redshifting, radiation energy density decreases faster than matter density as the Universe expands. Today, the radiation energy density is negligible compared to the matter density. Also, observations indicate that the Universe is very close to being flat, *i.e.*, $\Omega_k \simeq 0$.

The Hot big bang model makes a number of predictions that have been successfully tested with observational data. One such example is nucleosynthesis, the creation of light elements at $t \simeq 100$ s. The observed abundances of ^{4}He, ^{3}He, D, and ^{7}Li agree well with the predictions of nucleosynthesis. Even more important is the observation of the cosmic microwave background radiation (CMBR), which is a relic from the time of recombination at $t \simeq 300\ 000$ years, when atoms were formed and the Universe became transparent to photons. Since that time, the CMBR has propagated essentially freely, providing an image of the Universe at the time of recombination. The anisotropies in the CMBR are of the order of 10^{-5},

in good agreement with the cosmological principle, and the correlations of these anisotropies provide a large amount of information regarding the energy content of the Universe.

Nucleosynthesis as well as the power spectrum of the CMBR depend sensitively on the relative contributions to the energy density Ω in the Universe. In particular, observations give information on the energy density from baryons as well as DM, to which we turn next.

7.2 The need for dark matter

There is a large body of experimental evidence for the existence of a dark component of the energy in the Universe, including observations of mass-to-light ratios [119], galaxy rotation curves [120], gravitational lensing effects [121], models of structure formation [122], and measurements of the anisotropy of the CMBR [40]. In principle, the DM sector could be made up of composite baryonic objects, such as black holes. However, it has been shown that such so-called massive compact halo objects (MACHOs) can make up at most a small fraction of the total DM density [123]. It has also been suggested that the observations that are interpreted as being due to DM could instead be results of deviations from Newton's gravitational law at large distance scales. Theories of this kind are known as modified Newtonian dynamics (MOND) [124]. However, it is hard to construct such theories that can account for all of the observations that the DM hypothesis can. In particular, the so-called Bullet cluster [125], which was observed in 2006 and consists of two colliding clusters of galaxies, displays a separation of the visible matter from the DM which is hard to describe using MOND theories [126]. Using the principle of Occam's razor, a DM sector seems to be the most plausible solution to the problem.

Simulations of structure formation indicate that the DM was non-relativistic at freeze-out, so-called cold DM (CDM)[1]. Dividing the matter part of the energy density in Eq. (7.5) into a baryonic part and a CDM part, $\Omega = \Omega_{\rm b} + \Omega_{\rm CDM}$ gives the ΛCDM model, which is the currently most widely accepted model of cosmology. A combined analysis of the WMAP seven-year data, baryon acoustic oscillations, and supernovae observations [40] applied to this model gives the best-fit values $\Omega_{\rm b} \simeq 0.05$, $\Omega_{\rm CDM} \simeq 0.23$, and $\Omega_\Lambda \simeq 0.73$. Hence, DM dominates the matter density, while the visible matter, *i.e.*, the stars and the interstellar medium, accounts for about 20 % only. The dark energy Λ, which is responsible for the observed acceleration of the expansion of the Universe [128], accounts for 73 % of the total energy density.

To date, all evidence for DM comes from gravitational observations, and therefore, the particle nature of the DM remains unknown. Establishing the nature of the DM is one of the major challenges of particle physics today. In order not to be in conflict with observations, the DM sector should mainly consist of non-baryonic

[1] There are still some potential problems with CDM, related to the structure formation, which have led to investigations of so-called warm DM [127]. The question of whether cold or warm DM gives the best description of structure formation is not yet resolved.

particles which do not interact electromagnetically. Also, any DM particle has to be able to reproduce the observed relic density. An important conclusion of these constraints is that none of the particles in the SM could constitute the DM.[2] Thus, the DM problem points to new physics beyond the SM.

7.3 Thermal production of dark matter

Given a particle species that satisfies the basic constraints on a DM candidate, *i.e.*, being stable, electrically neutral, and non-baryonic, the most important question is if there is some mechanism for producing it in the amount given by experimental data. A natural way to generate an abundance of a stable particle species is through thermal production in the early Universe.

In the thermal production picture, the particle species is in equilibrium with the thermal bath in the early Universe. Hence, the particle number density follows the Boltzmann distribution, $n \sim \mathrm{e}^{-m/T}$. In order for the equilibrium to be maintained, the interaction rate of the particle with the thermal bath has to be larger than the expansion rate of the Universe, *i.e.*, the Hubble rate. The interaction rate as well as the expansion rate are functions of the temperature of the thermal bath, which in turn is a function of time. At some point, the interaction rate falls below the expansion rate, and the particle drops out of thermal equilibrium and is frozen out at a constant density per comoving volume. From that point on, the number density of the particle is affected only by the expansion of the Universe. The value of the freeze-out density depends on the particle annihilation cross section σ_{ann} as well as its mass.

The process of thermal production can be more complicated in the case of coannihilations with other particles [130]. Typically, models for DM include a single stable DM particle and a number of heavier particles that interact with and can decay into the DM particle. Coannihilations occur when these heavier particles have masses close to the DM particle mass. Then, the thermal energy of the DM particles is large enough to convert them to the more massive particles, which would affect the abundance. In the general picture, the abundance does not depend on the DM pair annihilation rate only, but on all the coannihilation cross sections $\sigma_{\mathrm{ann}}(X_i X_j) = \sigma_{ij}$, for $i, j = 1, \ldots, n$.

The effects of coannihilations differ qualitatively depending on the relative sizes of these cross sections. For example, in the case that there is a single coannihilating particle with $\sigma_{12} \gg \sigma_{11}$, the second particle will annihilate with the DM particle, decreasing the DM abundance. On the other hand, if σ_{12} is very small, the two particle species act and freeze out essentially independently. Typically, the second particle species then decays into the DM particle, thus increasing the abundance.

[2] Although neutrinos interact only weakly, they are too light to make up more than a small fraction of the total DM density [129].

7.4 Weakly interacting massive particles

An important class of particle DM is constituted by weakly interacting massive particles (WIMPs). These are particles with an interaction strength typical for the weak interactions and masses that lie roughly in the GeV to TeV range. The reason for the importance of WIMPs is that they naturally reproduce the correct thermal relic density with only a few assumptions. The particular features of WIMPs are such that the relic DM density that is measured today can be reproduced without the need for unnatural fine-tunings of the parameters. This effect has been termed the "WIMP miracle".

Another reason for the popularity of WIMPs is that the most well-studied DM candidate, the neutralino, falls into this category. The neutralino appears in supersymmetric models, and is a combination of the neutral higgsinos and gauginos, which are fermionic superpartners of the Higgs scalars and gauge bosons, respectively. The stability of the neutralino is guaranteed if conservation of R-parity (see Ch. 5) is assumed, which is also motivated from other aspects of supersymmetric models [14].

In this thesis, we are mainly interested in DM candidates arising in UED models. These DM candidates fall into the WIMP category. Other WIMP candidates arise in different models of physics beyond the SM, *e.g.*, little Higgs models [131–134]. There are also DM candidates that are not WIMPs, such as axions [135], which appear in the Peccei–Quinn theory that attempts to solve the so-called strong CP problem [136], asymmetric DM, which connects the DM to the baryon asymmetry in the Universe [137], and keV sterile neutrinos, which would be warm DM candidates [127]. For a more comprehensive overview of particle DM candidates, see for example Ref. [9].

7.5 Kaluza–Klein dark matter

7.5.1 The lightest Kaluza–Klein particle

As discussed in Ch. 5, the conservation of KK parity in UED models guarantees the stability of the LKP. The mass of this particle is approximately $R^{-1} = \mathcal{O}(1)$ TeV, and in the case that it is a good DM candidate, it is typically a weakly interacting particle. This means that KKDM candidates are typically WIMPs.

The identity of the LKP is determined by the mass spectrum (see Sec. 5.4). In the MUED version of the five-dimensional model that is described in Sec. 5.5.1, the LKP is the first KK mode of the hypercharge gauge boson, the B^1 [70]. In the corresponding six-dimensional model, which is described in Sec. 5.5.2, the LKP is instead the first KK mode of the adjoint scalar corresponding to the hypercharge gauge boson, the B^1_{H} [72]. If the MUED assumption that the BLTs vanish at the cutoff scale is relaxed, the mass spectrum, and hence, the identity of the LKP, generally changes.

In general, the LKP could be any of the first-level KK modes. In the context of KKDM, we can restrict our attention to electrically neutral, non-baryonic particles. In the five-dimensional model, these are the first KK modes of the $U(1)_{\mathrm{Y}}$ gauge boson, B^1, the $SU(2)_{\mathrm{L}}$ gauge boson, Z^1, the neutral components of the Higgs boson, H^1 and $A^{0,1}$, the lightest neutrino ν^1, and the graviton, G^1. In the six-dimensional model, the adjoint scalars B^1_{H} and Z^1_{H} and the right-handed neutrino ν^1_{R} are also possible candidates.

It has been shown that the ν^1 direct detection cross section is in conflict with experimental limits, unless the mass of the ν^1 is very large [138]. However, it would then be far above the region favored by the relic density calculations. Thus, KK neutrinos as DM candidates have been ruled out by direct detection experiments.

KK gravitons could potentially be DM candidates, but are too weakly interacting to be considered as WIMPs. Therefore, a non-thermal production mechanism would be needed, and the phenomenology would be drastically different from that of WIMPs. As discussed in Sec. 5.5.1, the first KK excitation of the graviton is the LKP in some parts of the MUED parameter space. Then, the next-to-lightest KK particle would be unstable, but have very weak interactions with the LKP, and hence, a long lifetime. For a more thorough discussion on this topic, see for example the review in Ref. [89].

The KKDM candidates Z^1_{H} and ν^1_{R} in the six-dimensional model have not been discussed in the literature and we will not elaborate more upon them in this thesis.

Finally, the H^1 and $A^{0,1}$ particles have exactly the same DM properties regarding the relic abundance and the detection prospects. Therefore, we will only discuss the H^1, but all results can be directly carried over to the $A^{0,1}$.

7.5.2 The relic abundance

A common feature of different KKDM candidates is that coannihilations tend to play an important role for the relic abundance, since the first-level KK spectrum is quite degenerate. Hence, the abundance depends sensitively on the mass spectrum. It is usually calculated using either the MUED assumptions or a simplified parametrization, *e.g.*, varying a single common mass for all first-level particles in the range $1\ \% - 10\ \%$ above the LKP mass.

The relic abundance of B^1 DM has been calculated in Refs. [139, 140], taking all coannihilation processes involving first-level KK particles into account in the MUED model. The result is that the B^1 with a mass $m_{B^1} \simeq 500\ \mathrm{GeV} - 600\ \mathrm{GeV}$ could account for the observed DM. If the MUED assumptions are relaxed, the effects of coannihilations widen this range to $m_{B^1} \simeq 500\ \mathrm{GeV} - 1600\ \mathrm{GeV}$.

In Ref. [141], it was pointed out that second-level KK particles could have important effects on the abundance. For example, the second-level Higgs boson, having roughly twice the mass of the LKP, could be resonantly produced in the process $B^1 B^1 \to H^2$. The H^2 preferentially decays into SM particles, and therefore, this process contributes to a depletion of the DM density. These ideas were further investigated in Refs. [142, 143]. In Ref. [144], a complete calculation involving

KKDM candidate	**Mass range**
Five-dimensional UED, $S^1/\mathbb{Z}_2$	
B^1, MUED	500 GeV $\lesssim m_{B^1} \lesssim$ 600 GeV
B^1	500 GeV $\lesssim m_{B^1} \lesssim$ 1600 GeV
Z^1	1800 GeV $\lesssim m_{Z^1} \lesssim$ 2500 GeV
H^1	2000 GeV $\lesssim m_{Z^1} \lesssim$ 2700 GeV
Six-dimensional UED, $T^2/\mathbb{Z}_4$	
$B^1_{\rm H}$, MUED	100 GeV $\lesssim m_{B^1_{\rm H}} \lesssim$ 500 GeV

Table 7.1. Preferred mass regions according to the WMAP data for the KKDM candidates considered in this chapter.

second-level KK modes in intermediate as well as final states was performed. The result was that, in the MUED model, the preferred B^1 mass is pushed up to about 1.3 TeV. However, these results depend strongly on the KK mass spectrum, through the coannihilations as well as the resonance effects.

The relic density of a Z^1 LKP has been calculated in Ref. [145], taking coannihilations into account. It was found that the correct abundance is obtained for 1800 GeV $\lesssim m_{Z^1} \lesssim$ 2500 GeV, depending on the mass splittings to other first-level KK particles. Thus, the Z^1 LKP should have roughly twice the mass preferred for a B^1 LKP.

The relic density for the third and last possible candidate in five-dimensional UED models, the H^1, was calculated in Paper 4. Without coannihilations, the preferred mass is approximately $m_{H^1} \simeq 2$ TeV. In the case of a universal mass splitting for the first-level KK particles, coannihilations result in a higher value. For a relative mass splitting of 1 %, the preferred mass is instead $m_{H^1} \simeq 2.7$ TeV.

Finally, for the $B^1_{\rm H}$ in the six-dimensional MUED model, the calculation performed in Ref. [146] gives the preferred mass range 100 GeV $\lesssim m_{B^1_{\rm H}} \lesssim$ 500 GeV, depending on the value of the Higgs mass. For a low Higgs mass, $m_H \simeq 120$ GeV, the favored mass is $m_{B^1_{\rm H}} \simeq 200$ GeV, which corresponds to a slightly larger value for R^{-1}. Hence, for the $B^1_{\rm H}$ DM, the abundance constraints are in conflict with the general bounds on the six-dimensional MUED model that were summarized in Sec. 5.7.

In Table 7.1, we summarize the preferred mass regions for the different KKDM candidates.

7.6 Dark matter detection

There are currently a large number of running and planned experiments aiming to detect WIMPs and establish their properties. These experiments are generally divided into direct and indirect detection experiments. In this chapter, we only treat the detection of WIMPs in an astrophysical context. However, the production of

DM particles in high-energy colliders, such as the LHC, also plays an important and complementary role in the search for the particle identity of the DM. For a more comprehensive overview of DM detection methods, see one of the reviews on the subject, *e.g.*, Ref. [9].

The realistic DM detection prospects depend not only on the particle physics of a particular DM candidate, but also on astrophysical assumptions, in particular regarding the DM distribution. The currently available information on this distribution mainly comes from N-body computer simulations [122]. In the standard picture, the DM density follows a spherically symmetric distribution in the Milky way and other galaxies. The local DM density in the solar system is given by $\rho_0 \simeq 0.3$ GeV/cm^3. One of the most common choices for the parametrization of the profile, which fits simulation data well over large regions, is the Navarro–Frenk–White (NFW) profile [147], which is given by

$$\rho(r) = \frac{\rho_\mathrm{s}}{(r/r_\mathrm{s})^\gamma (1 + r/r_\mathrm{s})^{3-\gamma}}, \tag{7.6}$$

where $\gamma = 1$, the scale radius r_s is a free parameter, and $\rho_\mathrm{s} = \rho(r_\mathrm{s})$. The largest uncertainty is related to the behavior of the profile close to the galactic center, due to the finite resolution of the N-body simulations. The standard NFW profile has a r^{-1} behavior at this point, but simulations indicate that the density is in fact somewhat higher in this region. Other possibilities for the halo profile, which might fit the data in this region better, include a generalized NFW profile where γ is kept as a free parameter and the Einasto profile [148],

$$\rho(r) = \rho_\mathrm{s} \mathrm{e}^{-\frac{2}{\alpha}[(r/r_\mathrm{s})^\alpha - 1]}, \tag{7.7}$$

where α is an additional free parameter. In this thesis, we have assumed a standard NFW profile with a scale radius $r_\mathrm{S} = 20$ kpc in the Milky way.

7.6.1 Direct detection

The thermal WIMP production mechanism relies on WIMPs interacting with ordinary matter, and this fact can be used in order to search for them. The Earth moves through the DM halo with a speed of 230 km/s, and hence, WIMPs constantly traverse the Earth at this speed. Some of these WIMPs will scatter on nuclei, and such interactions can potentially be detected in laboratories by measuring the energy deposits in the target from the scattering WIMPs. This method is known as direct detection.

Due to the different kinds of possible interactions between WIMPs and quarks in nucleons, the direct detection prospects vary drastically with the particular WIMP candidate considered. On the WIMP-nucleus level, the interactions can be characterized as spin-dependent or spin-independent. Spin-independent interactions take place coherently between the WIMP and the whole nucleus, and the corresponding cross section is proportional to the square of the atomic number, A^2. This

means that, for a WIMP candidate having mainly spin-independent interactions, the interaction rate can be increased by using heavy target nuclei. Spin-dependent interactions, on the other hand, arise from the coupling of the WIMP to the spin of the nucleus, and the cross section is instead proportional to $J(J+1)$, where J is the angular momentum quantum number. For such interactions, it is not possible to enhance the cross section by using heavy target nuclei, and hence, spin-dependent scattering cross sections are harder to constrain than spin-independent ones. The constraints on spin-dependent cross sections are weaker than the constraints on spin-independent ones by several orders of magnitude.

The current strongest limits on the WIMP-proton spin-independent scattering cross section $\sigma_{\mathrm{WIMP,p}}$ are shown in Fig. 7.1, as exclusion regions in the m_{WIMP}-$\sigma_{\mathrm{WIMP,p}}$ plane. The strongest limits are set by the XENON100 [149] and CDMS II [150] experiments. Also shown are a number of claimed signals in different direct

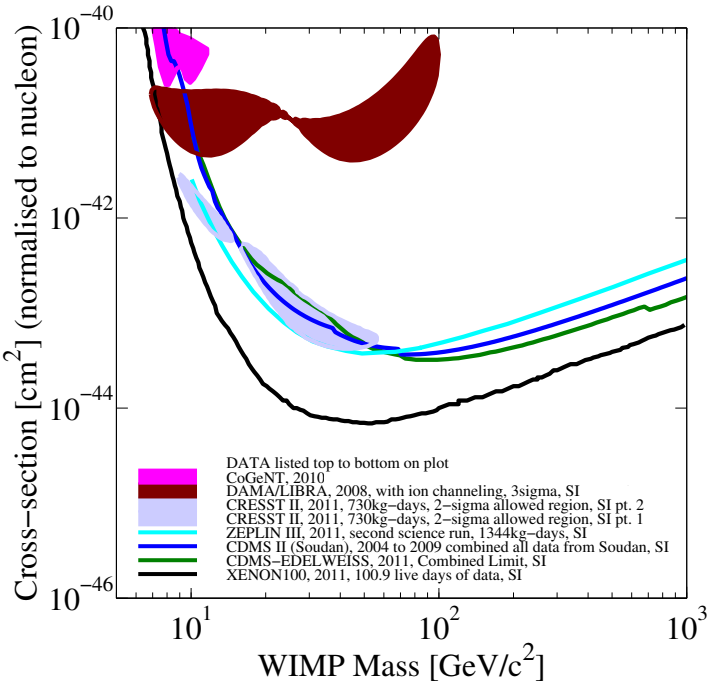

Figure 7.1. The strongest constraints on the spin-independent WIMP-proton interaction cross section as a function of the WIMP mass. Generated using the Dark matter limit plot generator [151].

detection experiments that could possibly be signals of DM. The oldest of these claims is made by the DAMA/NaI and the succeeding DAMA/LIBRA experiments, which have reported annual modulations in their event rates that are interpreted as signals from DM interactions [152]. An annual modulation in the signal is expected,

due to the orbit of the Earth around the Sun, which means that the speed of the Earth relative to the DM halo varies during the year. Later, in 2009, two events were observed in the CDMS II experiment [150]. According to the analysis made by the collaboration, the probability that two or more background events are observed in the signal region is 23 %. More recently, the CRESST-II [153] and CoGeNT [154] experiments have observed signals that could be due to a WIMP DM particle with a mass of the order of 10 GeV. Since these possible observations of DM are in conflict with other experimental limits, the issue of the validity of the results is still an open question.

The scattering of B^1 [138] and Z^1 [145] particles on nuclei is dominated by spin-dependent interactions, which means that their scattering cross sections are weakly constrained by direct detection experiments. For the B^1, the scattering cross section is more strongly constrained by indirect neutrino detection experiments, which are discussed in Sec. 7.6.2. For the Z^1, which has a higher preferred mass range, the direct detection rate as well as the indirect neutrino signal are suppressed, and no relevant bounds exist on the scattering cross section.

Since the H^1 is a scalar particle, it interacts only spin-independently. The Higgs boson interacts with quarks through Yukawa interactions and the couplings are proportional to the corresponding quark masses. Therefore, the H^1-quark scattering is negligible for all quark flavors except from the top quark. The heavy quarks contribute to the scattering only through loop-level interactions involving gluons in the nucleon, and the resulting H^1-nucleon scattering rate turns out to be several orders of magnitude below the sensitivities of current experiments.

Similar conclusions hold for the B^1_{H} scalar DM candidate. In Ref. [146], it was found that, due to suppressed couplings to quarks, the scattering rate is too low for current experiments.

7.6.2 Indirect detection

Another way to search for WIMPs is through their annihilations into SM particles. The annihilation products propagate away from the interaction point, and could potentially be detected in Earth- or space-based telescopes. Only a few particle species are stable over galactic scales, and the particles produced in WIMP annihilations will decay into these stable states. The most important particles that could be observed are photons, neutrinos, and different kinds of antimatter. Searching for DM through the detection of such particles is generally referred to as indirect detection.

Since the WIMPs annihilate in pairs, the annihilation rate in a given region of the Universe is proportional to the square of the local DM density. The fluxes of annihilation products is proportional to this rate, and thus, it is favorable to search for signals in the directions of regions where a high WIMP density is expected. Such regions include the galactic center, dwarf galaxies, and massive celestial bodies, such as the Sun and the Earth. However, these sources are generally plagued by

Final state	B^1	Z^1	H^1	$B^1_{\rm H}$
$\overline{u}u$	0.125	0.017	0	0
$\overline{d}d$	0.008	0.017	0	0
$\overline{\nu}\nu$	0.011	0.005	0	0
$\ell^+\ell^-$	0.183	0.005	0	0
HH	0.004	0.002	0.543	0.25
ZZ	0.004	0.002	0.237	0.25
W^+W^-	0.010	0.866	0.220	0.50

Table 7.2. Branching ratios into all final state channels for different KKDM particles. The branching ratios are computed in the limit of degenerate first-level KK masses. The branching ratios into fermions are not summed over generations.

large uncertainties due to other astrophysical processes, making it hard to properly estimate the background fluxes of particles.

The model-dependent quantities that determine the prospects for indirect detection searches are the WIMP pair annihilation cross section and the branching ratios into different final states. The branching ratios for the B^1, Z^1, H^1, and $B^1_{\rm H}$ are given in Table 7.2, computed in the limit of degenerate first-level KK masses and neglecting EWSB effects. The B^1 couples to the hypercharge of fermions, and hence, it has large branching ratios into charged leptons. The annihilation of the Z^1, which is a non-Abelian gauge boson, is dominated by the W^+W^- final state. For the H^1 and the $B^1_{\rm H}$, annihilations into fermion-antifermion pairs are helicity suppressed, and therefore, these particles annihilate only into bosons.

Neutrinos from dark matter annihilations in the Sun

As WIMPs travel through the solar system, a fraction of them will scatter elastically on nuclei in the Sun, and thereby lose energy. If the energy loss for such a WIMP is sufficiently large, its velocity will drop below the escape velocity of the Sun, and the WIMP will become gravitationally bound. This could lead to a DM density in the core of the Sun that is far higher than the average density. Hence, WIMP annihilation could be expected to be greatly enhanced in the solar core.

Since the Sun is a very hot and dense object, the only annihilation products that could escape its interior are neutrinos. In general, DM annihilations in the Sun produce neutrinos directly as well as indirectly, through decays or interactions of other annihilation products. Neutrinos from DM annihilations in the Sun can be searched for with Earth-based neutrino telescopes, such as AMANDA/IceCube [155], ANTARES [156], and Super-Kamiokande [157].

The capture rate of WIMPs in the Sun is proportional to the WIMP-proton cross section, which is the same quantity that is constrained by direct detection experiments. This means that the expected results in neutrino telescopes are correlated with the limits from direct detection experiments. An important consequence

of this is that, in the case that a DM candidate mainly has spin-independent interactions with nuclei, the constraints from direct detection experiments are already strong enough to rule out an observation of neutrinos from DM annihilations in the Sun [158]. Thus, in this context, only DM candidates which mainly interact spin-dependently are interesting. In particular, scalar DM candidates, such as the H^1 and adjoint scalars, only interact spin-independently.

On the other hand, for WIMPs that have mainly spin-dependent interactions, the constraints are sufficiently weak to allow for detection of neutrinos from DM annihilations in the Sun. This is true for the B^1, which has quite good prospects for indirect neutrino detection [1,159,160]. In fact, the strongest constraints on the spin-dependent cross section in the five-dimensional MUED model are placed by the IceCube collaboration [161].

In Paper 1, we found that the neutrino signals from the Z^1 are lower than those from the B^1, due to a lower scattering cross section on nuclei and the different distribution of final states shown in Table 7.2. Also, since the favored mass for the relic density is higher for the Z^1, and the WIMP-proton scattering cross section falls off rapidly with the WIMP mass, the prospects for this DM candidate in indirect neutrino detection experiments are not very good. Also, for the B^1 and the Z^1 in the six-dimensional model, the model-dependent quantities that are relevant for direct detection as well as neutrino detection experiments are approximately equal to the five-dimensional case.

Gamma ray astronomy

Another interesting annihilation product is photons, which have the advantage of not being affected by the galactic magnetic fields, so that they travel in straight lines and would point straight back at their sources. Since the DM particle is necessarily electrically neutral, it does not couple directly to the electromagnetic field, and therefore, photons are only emitted through radiative processes or the decays of other annihilation products, or through loop-level processes. The resulting photon energy spectrum can be divided into a monoenergetic line signal and a continuous part.

At loop-level, DM particles could pair-annihilate into the final states $\gamma\gamma$, γZ, and γH. In all three cases, the final-state particles are monoenergetic, with the photon energy given by

$$E_\gamma = m_{\mathrm{DM}} \left(1 - \frac{m_X^2}{4m_{\mathrm{DM}}^2} \right), \tag{7.8}$$

where $X = \gamma, Z, H$. The corresponding signals would be lines in the energy spectrum. The lines for γZ and γH annihilation would be slightly shifted towards a lower energy, but in practice, the relative shift is typically too small to be resolved in detectors, which have a finite resolution. Thus, all three signals would effectively contribute to a single line signal at $E_\gamma \simeq m_{\mathrm{DM}}$, giving a smoking-gun signature for DM self-annihilations.

The continuous component of the photon energy spectrum can be divided into primary and secondary photons. The primary photons are emitted as final state radiation from electrically charged annihilation products and could give an important contribution to the hard part of the spectrum. In contrast, the secondary photons, which are produced in the decays of other particles, contribute mainly to the soft end of the spectrum. The continuous spectrum extends up to the maximal energy $E_\gamma = m_{\rm DM}$. Hence, the detectability of the monoenergetic peak depends heavily on the relative contributions from the continuous and the monoenergetic components at this maximum energy.

Gamma rays from DM annihilations are being searched for in a number of experiments, the foremost being the Fermi satellite [162] and the Earth-based air Cherenkov telescopes (ACTs) H.E.S.S. [163], MAGIC [164], VERITAS [165], and CANGAROO-III [166]. For the DM candidates considered in this thesis, the energy range of Fermi, $E_\gamma \lesssim 300$ GeV, is typically too low, and hence, ACTs provide better prospects for detection of the gamma ray flux. ACTs search for high-energy gamma rays through the Cherenkov radiation that is emitted as the photons enter Earth's atmosphere.

The gamma ray spectrum from B^1 annihilations has some interesting features. Since the B^1 has a branching fraction of about 20 % into each charged lepton, the continuum spectrum is relatively large and features a sharp cutoff at $E_\gamma = m_{B^1}$ [167]. The monoenergetic peak from $\gamma\gamma$ annihilations can also be quite pronounced [168], whereas the additional contributions from the γZ and γH channels are relatively small [169].

In Paper 2 and 3, we calculated the gamma ray signals from Z^1 DM annihilations. For this candidate, the continuum spectrum is suppressed, whereas the peak signal can be quite large, even comparable to that from B^1, despite the larger mass preferred for the Z^1. This is due to the large number of diagrams coming from the gauge self-interactions of the non-Abelian Z^1 gauge boson.

Finally, the gamma ray spectrum for the H^1 was found in Paper 4 to be suppressed in the continuous as well as the monoenergetic part. Since the annihilation into leptons is helicity suppressed, the continuum spectrum is mainly due to secondary photons coming from the decays of other particles, which mainly contribute to the soft end of the spectrum.

Antimatter searches

A third important annihilation product is antimatter, such as positrons, antiprotons, and antideuterium. Here, we focus on positrons. In contrast to gamma rays, positrons can possibly be directly produced in WIMP self-annihilation processes. On the other hand, being electrically charged, the propagation of the positrons from the source to the detector are affected by the galactic magnetic fields, introducing a strong dependence on the modeling of this propagation. For positrons, the most important effects are space diffusion and energy loss due to synchrotron radiation and inverse Compton scattering [170].

The space-based satellite PAMELA [171], as well as the balloon-borne experiment ATIC [172], have reported excesses in their measured electron-positron spectra, which have been suggested to be due to DM annihilations. However, the validity of this interpretation is far from clear. The ATIC excess is not observed by the more recent Fermi experiment. The DM interpretation of the PAMELA results has the problem that, although there are DM models that can be made to fit the shape of the measured spectrum, the magnitude of the excess is larger than expected for DM annihilation products. This could possibly be due to local variations in the DM density, giving rise to a "boost factor" that would increase the fluxes. However, it is not clear whether or not such a mechanism could give rise to a boost factor which is large enough, and the origin of the PAMELA excess is still an unresolved matter.

Among the KKDM candidates, the B^1 has the most interesting features in relation to the positron signal. Since it annihilates directly into e^+e^- pairs (see Table 7.2), the corresponding positron flux has interesting spectral features, with a sharp cutoff at the compactification scale R^{-1} [64]. This shape of the spectrum has been shown to be possible to fit to the PAMELA data, although the predicted magnitude is too small [173]. The PAMELA data display no sharp cutoff, but the energy reach of the experiment extends only to about 300 GeV, below the preferred B^1 mass given in Table 7.1.

The Z^1, H^1, and B^1_{H} mainly annihilate into bosons, and have less interesting features from the point of view of the positron detection prospects.

Chapter 8

Summary and conclusions

In this first part of the thesis, we have described the SM of particle physics and the important fields of neutrino physics and dark matter. The general formalism of higher-dimensional quantum field theories has been introduced, as well as a number of specific models extending the SM through extra dimensions. Each of these models aims to resolve one or more of the problems with the SM. For the models of the UED type, we have focused on the possibility that the LKP could constitute the observed DM in the Universe. The ADD model, where the SM fields are confined to a brane, and only gravity can probe the extra dimensions, aims to solve the hierarchy problem between the electroweak scale and the Planck scale. Finally, in models where only sterile neutrinos propagate in the extra dimensions, there is a mechanism for generating small masses for the left-handed neutrinos. We have discussed existing limits on the models, as well as the potential to search for signals of them in the next generation of high-energy colliders, in particular at the LHC.

In Part II of the thesis, we present eight scientific papers, that investigate the models described in Part I, or generalizations of them. Below, we summarize the contents of each paper, stating the most important conclusions. More detailed results and discussions are found in the papers.

Paper 1 We studied KKDM in the context of non-minimal UED models with five and six dimensions. For both models, we studied the B^1 as well as the Z^1 as DM particles. We calculated the indirect signals from neutrinos coming from KKDM annihilations in the Sun, using numerical simulations of the neutrino propagation from the interior of the Sun to an Earth-based detector, properly taking interactions and flavor oscillations into account.

The main conclusions of this paper are:

- For the standard LKP candidate, the B^1, we approximately reproduced the results previously obtained in the literature, which imply that this

DM candidate could be indirectly observed in neutrino telescopes such as IceCube. Hence, the difference due to the proper three-flavor treatment of neutrino oscillations compared to previous approximative treatments is small.

- For the Z^1, on the other hand, the prospects are not so good.
- The corresponding LKP candidates give the same signals in the five- and the six-dimensional model.

Paper 2 We calculated the monoenergetic flux of gamma rays from annihilations of Z^1 particles, which are viable non-minimal KKDM candidates.

The main conclusions of this paper are:

- Due to the non-Abelian nature of the Z^1, there is a large number of diagrams in the bosonic sector contributing to the process, enhancing the cross section.
- Even though relic density calculations indicate that the mass of the Z^1 LKP should be larger than for the B^1 LKP, the fluxes at Earth are of the same order of magnitude.
- With a moderately large boost factor, the Z^1 LKP could possibly be detected in near-future ACT experiments.

Paper 3 We calculated the continuous component of the gamma ray energy spectrum from Z^1 annihilations.

The main conclusions of this paper are:

- Due to the large branching fraction of annihilations into W^+W^- pairs, the continuum spectrum is suppressed, especially close to the spectral endpoint at $E_\gamma = m_{Z^1}$.
- Due to this large suppression, the monoenergetic peak studied in Paper 2 has better prospects of being observable, and the combination of a non-observable continuum spectrum and an observable peak provide a signature for the Z^1 LKP.

Paper 4 We investigated the first-level KK Higgs boson in the non-minimal five-dimensional UED model as a DM candidate. We calculated the relic density and investigated the detection prospects for direct as well as indirect detection experiments.

The main conclusions of this paper are:

- The first-level Higgs boson could make up the DM if its mass $m_{H^1} \simeq$ 2 TeV. Coannihilations with other first-level KK particles could shift this value up to about 2.7 TeV.

- The direct detection rate of H^1 DM is several orders of magnitude below the sensitivities of current experiments, due to Yukawa-suppressed couplings to all quarks except for the top quark.
- The indirect detection rates are also suppressed, mainly due to the small Yukawa couplings and helicity suppression of H^1 annihilation into fermion-antifermion pairs.
- The same conclusions hold for the first KK mode of the pseudo-scalar Higgs component, A^0.

Paper 5 We investigated the generation of light-neutrino masses in a higher-dimensional model with only sterile fermions in the bulk. In particular, we considered the effects of introducing a high-energy cut on KK number, giving a renormalizable theory. Motivated by the Scherk–Schwarz mechanism, we employed a specific structure for the effective neutrino Majorana masses. We studied non-unitarity effects and possible LHC signatures of the model.

The main conclusions of this paper are:

- The only lepton-number violation in the model is due to a number of right-handed Majorana neutrinos at the top of the KK towers. These Majorana neutrinos could generate the small masses for the left-handed neutrinos.
- Due to the strong constraints on the non-unitarity parameters, an observation at the LHC seems to be ruled out.
- Mixing between the light neutrinos and the lower KK modes induces large non-unitarity effects. These effects could be observable in a future neutrino factory, demonstrating that such an experiment could provide complementary information on the existence of extra dimensions.

Paper 6 We analyzed the RG running behavior of neutrino parameters in extra dimensions. We studied two higher-dimensional models, the five-dimensional UED model and a model where the fermions are confined to a brane. In both cases, neutrino masses were described by the effective Weinberg operator, *i.e.*, the generation of the light-neutrino masses was assumed to occur at some high-energy scale.

The main conclusions of this paper are:

- As expected in higher-dimensional models, the running neutrino parameters follow a power-law behavior.
- Among the neutrino mixing angles, only θ_{12} displays a significant running. It only runs to larger values at higher energies, constraining the possible high-energy mixing patterns.
- The running is larger in the UED model than in the model where the fermions are confined to a brane.

- The possible high-energy values for the mixing parameters allowed for tri-bimaximal mixing.
- In both models, the running of the neutrino masses is universal, again with a significantly larger running in the UED model.

It should be noted that the recent results from the Daya Bay [31], and RENO [32] experiments, which indicate that $\theta_{13} \simeq 9^\circ$, rule out tri-bimaximal mixing at low energies. Since θ_{13} does not display any significant running in the two models that we consider, the same conclusion is true for those models.

Paper 7 We investigated the impact that recent LHC Higgs mass bounds have on the five-dimensional UED model, through the running of the Higgs self-coupling constant λ. In the small-mass region that remains, the enhanced running tends to drive λ to negative values, making the Higgs potential unstable.

The main conclusions of this paper are:

- The five-dimensional UED model can be valid at most up to the fifth KK level if the vacuum instability limit is to be avoided.
- This bound implies that it is not possible to achieve even approximate gauge coupling unification in the model.
- The regions of large power-law running for the fermion masses are also excluded.

Paper 8 We studied a generalization of the ADD model, where the internal space is hyperbolic rather than flat. This model could provide a more satisfactory solution to the hierarchy problem than the ADD model, where there is a large hierarchy between the fundamental Planck scale and the radius of the extra dimensions. Also, the model avoids the strong bounds on the size of the extra dimensions from astrophysics. We have investigated the LHC signals of the model in the jet $+ G$ and $\gamma + G$ channels, where G denotes any KK mode of the graviton.

The main conclusions of this paper are:

- In the jet channel, some regions of the parameter space, where the cross sections are typically of the order of 100 fb, could be probed by the LHC.
- The photon channel, on the other hand, is less promising.
- In general, the signals are similar to, and in some cases indistinguishable from, the signals of the ADD model.

There are a number of possible extensions and developments of these results. Regarding the investigations of KKDM in non-minimal UED models, it would be interesting to perform a more thorough study of the effects of the BLTs. Specifically,

it would be interesting to study how the coupling constants are affected by the BLTs and how they are correlated with the changes in the mass spectrum. For the studies of the effects of renormalization group running, it would be interesting to extend the work to higher-dimensional models. In particular, one could study the implications that the LHC Higgs bounds have on the six-dimensional UED model. Since the running is even more enhanced in six-dimensional models, the constraints on this model would probably be even stronger than on the five-dimensional one. In addition, with more data from the LHC, stronger bounds will be obtained also for the five-dimensional model. Finally, the recent LHC constraints on the ADD model could be carried over to the hyperbolic model. Since the signatures of the two models are similar, it should be possible to use the analyzes to rule out parts of the parameter space of this model as well.

Bibliography

[1] M. Blennow, H. Melbéus and T. Ohlsson, *Neutrinos from Kaluza–Klein dark matter in the Sun*, JCAP **01**, 018 (2010), 0910.1588.

[2] J. Bonnevier *et al.*, *Monoenergetic gamma-rays from non-minimal Kaluza–Klein dark matter annihilations*, Phys. Rev. **D85**, 043524 (2012), 1104.1430.

[3] H. Melbéus, A. Merle and T. Ohlsson, *Continuum photon spectrum from Z^1Z^1 annihilations in universal extra dimensions*, Phys. Lett. **B706**, 329 (2012), 1109.0006.

[4] H. Melbéus, A. Merle and T. Ohlsson, *Kaluza–Klein Higgs dark matter in universal extra dimensions*, (2012).

[5] M. Blennow *et al.*, *Signatures from an extra-dimensional seesaw model*, Phys. Rev. **D82**, 045023 (2010), 1003.0669.

[6] M. Blennow *et al.*, *Renormalization group running of the neutrino mass operator in extra dimensions*, JHEP **1104**, 052 (2011), 1101.2585.

[7] M. Blennow *et al.*, *RG running in UEDs in light of recent LHC Higgs mass bounds*, (2011), 1112.5339.

[8] H. Melbéus and T. Ohlsson, *Searches for hyperbolic extra dimensions at the LHC*, JHEP **08**, 077 (2008), 0806.1841.

[9] G. Bertone, *Particle dark matter: Observations, models and searches* (Cambridge University Press, 2010).

[10] Super-Kamiokande collaboration, Y. Fukuda *et al.*, *Evidence for oscillation of atmospheric neutrinos*, Phys. Rev. Lett. **81**, 1562 (1998), hep-ex/9807003.

[11] SNO collaboration, Q. R. Ahmad *et al.*, *Measurement of the rate of $\nu_e + d \to p + p + e^-$ interactions produced by ^8B solar neutrinos at the Sudbury neutrino observatory*, Phys. Rev. Lett. **87**, 071301 (2001), nucl-ex/0106015.

[12] KamLAND collaboration, K. Eguchi *et al.*, *First results from KamLAND: Evidence for reactor anti-neutrino disappearance*, Phys. Rev. Lett. **90**, 021802 (2003), `hep-ex/0212021`.

[13] KamLAND collaboration, S. Abe *et al.*, *Precision measurement of neutrino oscillation parameters with KamLAND*, Phys. Rev. Lett. **100**, 221803 (2008), `0801.4589`.

[14] S. P. Martin, *A supersymmetry primer*, `hep-ph/9709356`.

[15] P. Langacker, *Grand unified theories and proton decay*, Phys. Rept. **72**, 185 (1981).

[16] O. Klein, *Quantum theory and five-dimensional theory of relativity*, Z. Phys. **37**, 895 (1926).

[17] T. Kaluza, *On the problem of unity in physics*, Sitzungsber. Preuss. Akad. Wiss. Berlin (Math. Phys.) **1921**, 966 (1921).

[18] J. Polchinski, *String theory. Vol. 2: Superstring theory and beyond* (Cambridge University Press, 1998).

[19] Particle Data Group, C. Amsler *et al.*, *Review of particle physics*, Phys. Lett. **B667**, 1 (2008).

[20] M. Peskin and D. Schroeder, *Quantum field theory* (Addison-Wesley, 1995).

[21] S. Weinberg, *The quantum theory of fields. Vol. II: Modern applications* (Cambridge University Press, 1996).

[22] ATLAS collaboration, G. Aad *et al.*, *Combined search for the standard model Higgs boson using up to 4.9 fb^{-1} of pp collision data at $\sqrt{s}$ = 7 TeV with the ATLAS detector at the LHC*, Phys. Lett. **B710**, 49 (2012), `1202.1408`.

[23] CMS collaboration, S. Chatrchyan *et al.*, *Combined results of searches for the standard model Higgs boson in pp collisions at $\sqrt{s}$ = 7 TeV*, (2012), `1202.1488`.

[24] TEVNPH (Tevatron new phenomena and Higgs working group), CDF and D0 collaboration, *Combined CDF and D0 Search for standard model Higgs boson production with up to 10.0 fb^{-1} of data*, (2012), `1203.3774`.

[25] ALEPH, CDF, D0, DELPHI, L3, OPAL, SLD collaborations, the LEP electroweak working group, the Tevatron electroweak working group, and the SLD electroweak and heavy flavour groups, *Precision electroweak measurements and constraints on the Standard Model*, (2010).

[26] LEP working group for Higgs boson searches, ALEPH collaboration, DELPHI collaboration, L3 collaboration, OPAL collaboration, R. Barate *et al.*, *Search for the standard model Higgs boson at LEP*, Phys. Lett. **B565**, 61 (2003), hep-ex/0306033.

[27] B. A. Dobrescu and E. Poppitz, *Number of fermion generations derived from anomaly cancellation*, Phys. Rev. Lett. **87**, 031801 (2001), hep-ph/0102010.

[28] R. Davis, Jr., D. S. Harmer and K. C. Hoffman, *Search for neutrinos from the Sun*, Phys. Rev. Lett. **20**, 1205 (1968).

[29] MINOS collaboration, P. Adamson *et al.*, *Improved search for muon-neutrino to electron-neutrino oscillations in MINOS*, Phys. Rev. Lett. **107**, 181802 (2011), 1108.0015.

[30] T2K collaboration, K. Abe *et al.*, *Indication of electron neutrino appearance from an accelerator-produced off-axis muon neutrino beam*, Phys. Rev. Lett. **107**, 041801 (2011), 1106.2822.

[31] Daya Bay collaboration, F. An *et al.*, *Observation of electron-antineutrino disappearance at Daya Bay*, (2012), 1203.1669.

[32] RENO collaboration, S. B. Kim, *Observation of reactor electron antineutrino disappearance in the RENO experiment*, (2012), 1204.0626.

[33] S. M. Bilenky and S. T. Petcov, *Massive neutrinos and neutrino oscillations*, Rev. Mod. Phys. **59**, 671 (1987).

[34] E. K. Akhmedov, *Neutrino physics*, (1999), hep-ph/0001264.

[35] T. Ohlsson, *Dynamics of quarks and leptons: Theoretical studies of baryons and neutrinos*, (2000), Ph.D. Thesis.

[36] T. Schwetz, M. Tórtola and J. Valle, *Global neutrino data and recent reactor fluxes: status of three-flavour oscillation parameters*, New J. Phys. **13**, 063004 (2011), 1103.0734.

[37] T. Schwetz, M. Tórtola and J. Valle, *Where we are on θ_{13}: addendum to 'Global neutrino data and recent reactor fluxes: status of three-flavour oscillation parameters'*, New J. Phys. **13**, 109401 (2011), 1108.1376.

[38] P. Harrison, D. Perkins and W. Scott, *Tri-bimaximal mixing and the neutrino oscillation data*, Phys. Lett. **B530**, 167 (2002), hep-ph/0202074.

[39] KATRIN collaboration, A. Osipowicz *et al.*, *KATRIN: A next generation tritium beta decay experiment with sub-eV sensitivity for the electron neutrino mass*, (2001), hep-ex/0109033.

[40] WMAP collaboration, E. Komatsu *et al.*, *Seven-Year Wilkinson Microwave Anisotropy Probe (WMAP) observations: Cosmological interpretation*, Astrophys. J. Suppl. **192**, 18 (2011), 1001.4538.

[41] W. Rodejohann, *Neutrino-less double beta decay and particle physics*, Int. J. Mod. Phys. **E20**, 1833 (2011), 1106.1334.

[42] P. Minkowski, $\mu \to e^- \gamma$ *at a rate of one out of 1-billion muon decays?*, Phys. Lett. **B67**, 421 (1977).

[43] R. N. Mohapatra and G. Senjanović, *Neutrino mass and spontaneous parity nonconservation*, Phys. Rev. Lett. **44**, 912 (1980).

[44] M. Magg and C. Wetterich, *Neutrino mass problem and gauge hierarchy*, Phys. Lett. **B94**, 61 (1980).

[45] T. P. Cheng and L. F. Li, *Neutrino masses, mixings and oscillations in SU(2) × U(1) models of electroweak interactions*, Phys. Rev. **D22**, 2860 (1980).

[46] G. B. Gelmini and M. Roncadelli, *Left-handed neutrino mass scale and spontaneously broken lepton number*, Phys. Lett. **B99**, 411 (1981).

[47] G. Lazarides, Q. Shafi and C. Wetterich, *Proton lifetime and fermion masses in an SO(10) model*, Nucl. Phys. **B181**, 287 (1981).

[48] R. Foot *et al.*, *Seesaw neutrino masses induced by a triplet of leptons*, Z. Phys. **C44**, 441 (1989).

[49] E. Ma, *Pathways to naturally small neutrino masses*, Phys. Rev. Lett. **81**, 1171 (1998), hep-ph/9805219.

[50] R. N. Mohapatra and J. W. F. Valle, *Neutrino mass and baryon-number nonconservation in superstring models*, Phys. Rev. **D34**, 1642 (1986).

[51] S. Antusch *et al.*, *Unitarity of the leptonic mixing matrix*, JHEP **10**, 084 (2006), hep-ph/0607020.

[52] S. Antusch, J. P. Baumann and E. Fernández-Martínez, *Non-standard neutrino interactions with matter from physics beyond the standard model*, Nucl. Phys. **B810**, 369 (2009), 0807.1003.

[53] M. Masip and A. Pomarol, *Effects of SM Kaluza–Klein excitations on electroweak observables*, Phys. Rev. **D60**, 096005 (1999), hep-ph/9902467.

[54] T. G. Rizzo and J. D. Wells, *Electroweak precision measurements and collider probes of the standard model with large extra dimensions*, Phys. Rev. **D61**, 016007 (2000), hep-ph/9906234.

[55] N. Arkani-Hamed, A. G. Cohen and H. Georgi, *(De)constructing dimensions*, Phys. Rev. Lett. **86**, 4757 (2001), `hep-th/0104005`.

[56] C. T. Hill, S. Pokorski and J. Wang, *Gauge invariant effective Lagrangian for Kaluza–Klein modes*, Phys. Rev. **D64**, 105005 (2001), `hep-th/0104035`.

[57] K. R. Dienes, E. Dudas and T. Gherghetta, *Grand unification at intermediate mass scales through extra dimensions*, Nucl. Phys. **B537**, 47 (1999), `hep-ph/9806292`.

[58] T. Appelquist, H. C. Cheng and B. A. Dobrescu, *Bounds on universal extra dimensions*, Phys. Rev. **D64**, 035002 (2001), `hep-ph/0012100`.

[59] N. Arkani-Hamed, S. Dimopoulos and G. R. Dvali, *The hierarchy problem and new dimensions at a millimeter*, Phys. Lett. **B429**, 263 (1998), `hep-ph/9803315`.

[60] N. Arkani-Hamed, S. Dimopoulos and G. R. Dvali, *Phenomenology, astrophysics and cosmology of theories with sub-millimeter dimensions and TeV scale quantum gravity*, Phys. Rev. **D59**, 086004 (1999), `hep-ph/9807344`.

[61] L. Randall and R. Sundrum, *An alternative to compactification*, Phys. Rev. Lett. **83**, 4690 (1999), `hep-th/9906064`.

[62] L. Randall and R. Sundrum, *A large mass hierarchy from a small extra dimension*, Phys. Rev. Lett. **83**, 3370 (1999), `hep-ph/9905221`.

[63] G. Servant and T. M. P. Tait, *Is the lightest Kaluza–Klein particle a viable dark matter candidate?*, Nucl. Phys. **B650**, 391 (2003), `hep-ph/0206071`.

[64] H. C. Cheng, J. L. Feng and K. T. Matchev, *Kaluza–Klein dark matter*, Phys. Rev. Lett. **89**, 211301 (2002), `hep-ph/0207125`.

[65] T. Appelquist *et al.*, *Proton stability in six-dimensions*, Phys. Rev. Lett. **87**, 181802 (2001), `hep-ph/0107056`.

[66] T. Appelquist *et al.*, *Neutrinos vis-a-vis the six-dimensional standard model*, Phys. Rev. **D65**, 105019 (2002), `hep-ph/0201131`.

[67] B. A. Dobrescu and E. Ponton, *Chiral compactification on a square*, JHEP **03**, 071 (2004), `hep-th/0401032`.

[68] G. Burdman, B. A. Dobrescu and E. Ponton, *Six-dimensional gauge theory on the chiral square*, JHEP **02**, 033 (2006), `hep-ph/0506334`.

[69] H. Georgi, A. K. Grant and G. Hailu, *Brane couplings from bulk loops*, Phys. Lett. **B506**, 207 (2001), `hep-ph/0012379`.

[70] H. C. Cheng, K. T. Matchev and M. Schmaltz, *Radiative corrections to Kaluza–Klein masses*, Phys. Rev. **D66**, 036005 (2002), `hep-ph/0204342`.

[71] J. A. Cembranos, J. L. Feng and L. E. Strigari, *Exotic collider signals from the complete phase diagram of minimal universal extra dimensions*, Phys. Rev. **D75**, 036004 (2007), `hep-ph/0612157`.

[72] E. Ponton and L. Wang, *Radiative effects on the chiral square*, JHEP **11**, 018 (2006), `hep-ph/0512304`.

[73] G. Burdman, B. A. Dobrescu and E. Ponton, *Resonances from two universal extra dimensions*, Phys. Rev. **D74**, 075008 (2006), `hep-ph/0601186`.

[74] B. A. Dobrescu, K. Kong and R. Mahbubani, *Leptons and photons at the LHC: Cascades through spinless adjoints*, JHEP **07**, 006 (2007), `hep-ph/0703231`.

[75] H. C. Cheng, K. T. Matchev and M. Schmaltz, *Bosonic supersymmetry? Getting fooled at the CERN LHC*, Phys. Rev. **D66**, 056006 (2002), `hep-ph/0205314`.

[76] A. Datta, K. Kong and K. T. Matchev, *Discrimination of supersymmetry and universal extra dimensions at hadron colliders*, Phys. Rev. **D72**, 096006 (2005), `hep-ph/0509246`.

[77] T. Flacke, A. Menon and D. J. Phalen, *Non-minimal universal extra dimensions*, Phys. Rev. **D79**, 056009 (2009), `0811.1598`.

[78] ATLAS collaboration, G. Aad *et al.*, *Search for diphoton events with large missing transverse momentum in 1 fb^{-1} of 7 TeV proton-proton collision data with the ATLAS detector*, (2011), `1111.4116`.

[79] K. Nishiwaki *et al.*, *A bound on universal extra dimension models from up to 2 fb^{-1} of LHC data at 7 TeV*, Phys. Lett. **B707**, 506 (2012), `1108.1764`.

[80] G. Belanger *et al.*, *Higgs phenomenology of minimal universal extra dimensions*, (2012), `1201.5582`.

[81] C. Lin, *A search for universal extra dimensions in the multi-lepton channel from $p\bar{p}$ collisions at $\sqrt{s}$ = 1.8 TeV*, FERMILAB-THESIS-2005-69.

[82] M. Baak *et al.*, *Updated status of the global electroweak fit and constraints on new physics*, (2011), `1107.0975`.

[83] T. Appelquist and H. U. Yee, *Universal extra dimensions and the Higgs boson mass*, Phys. Rev. **D67**, 055002 (2003), `hep-ph/0211023`.

[84] I. Gogoladze and C. Macesanu, *Precision electroweak constraints on universal extra d imensions revisited*, Phys. Rev. **D74**, 093012 (2006), `hep-ph/0605207`.

[85] U. Haisch and A. Weiler, *Bound on minimal universal extra dimensions from* $\bar{B} \to X_s\gamma$, Phys. Rev. **D76**, 034014 (2007), `hep-ph/0703064`.

[86] A. Freitas and U. Haisch, $\bar{B} \to X_s\gamma$ *in two universal extra dimensions*, Phys. Rev. **D77**, 093008 (2008), `0801.4346`.

[87] J. F. Oliver, J. Papavassiliou and A. Santamaria, *Universal extra dimensions and* $Z \to b\bar{b}$, Phys. Rev. **D67**, 056002 (2003), `hep-ph/0212391`.

[88] A. J. Buras, M. Spranger and A. Weiler, *The impact of universal extra dimensions on the unitarity triangle and rare K and B decays*, Nucl. Phys. **B660**, 225 (2003), `hep-ph/0212143`.

[89] D. Hooper and S. Profumo, *Dark matter and collider phenomenology of universal extra dimensions*, Phys. Rept. **453**, 29 (2007), `hep-ph/0701197`.

[90] P. Horava and E. Witten, *Eleven-dimensional supergravity on a manifold with boundary*, Nucl. Phys. **B475**, 94 (1996), `hep-th/9603142`.

[91] H. Murayama and J. D. Wells, *Graviton emission from a soft brane*, Phys. Rev. **D65**, 056011 (2002).

[92] G. F. Giudice, R. Rattazzi and J. D. Wells, *Quantum gravity and extra dimensions at high-energy colliders*, Nucl. Phys. **B544**, 3 (1999), `hep-ph/9811291`.

[93] N. Kaloper *et al.*, *Compact hyperbolic extra dimensions: Branes, Kaluza–Klein modes and cosmology*, Phys. Rev. Lett. **85**, 928 (2000), `hep-ph/0002001`.

[94] N. Straumann, *General relativity with applications to astrophysics* (Springer-Verlag, 2004).

[95] T. Han, J. D. Lykken and R. J. Zhang, *On Kaluza–Klein states from large extra dimensions*, Phys. Rev. **D59**, 105006 (1999), `hep-ph/9811350`.

[96] E. A. Mirabelli, M. Perelstein and M. E. Peskin, *Collider signatures of new large space dimensions*, Phys. Rev. Lett. **82**, 2236 (1999), `hep-ph/9811337`.

[97] J. L. Hewett, *Indirect collider signals for extra dimensions*, Phys. Rev. Lett. **82**, 4765 (1999), `hep-ph/9811356`.

[98] S. Nussinov and R. Shrock, *Some remarks on theories with large compact dimensions and TeV-scale quantum gravity*, Phys. Rev. **D59**, 105002 (1999), `hep-ph/9811323`.

[99] T. G. Rizzo, *More and more indirect signals for extra dimensions at more and more colliders*, Phys. Rev. **D59**, 115010 (1999), `hep-ph/9901209`.

[100] K. M. Cheung and W. Y. Keung, *Direct signals of low scale gravity at e^+e^- colliders*, Phys. Rev. **D60**, 112003 (1999), hep-ph/9903294.

[101] C. Balazs *et al.*, *Collider tests of compact space dimensions using weak gauge bosons*, Phys. Rev. Lett. **83**, 2112 (1999), hep-ph/9904220.

[102] N. Delerue, K. Fujii and N. Okada, *Higgs pair production at a linear e^+e^- collider in models with large extra dimensions*, Phys. Rev. **D70**, 091701 (2004), hep-ex/0403029.

[103] J. Gao *et al.*, *Signature of large extra dimensions from Z boson pair production at the CERN Large Hadron Collider*, Phys. Rev. **D80**, 016008 (2009), 0903.2551.

[104] D. Kapner *et al.*, *Tests of the gravitational inverse-square law below the dark-energy length scale*, Phys. Rev. Lett. **98**, 021101 (2007), hep-ph/0611184.

[105] S. Hannestad and G. G. Raffelt, *Stringent neutron star limits on large extra dimensions*, Phys. Rev. Lett. **88**, 071301 (2002), hep-ph/0110067.

[106] Fermi-LAT collaboration, B. Berenji, E. Bloom and J. Cohen-Tanugi, *Limits on large extra dimensions based on observations of neutron stars with the Fermi-LAT*, JCAP **1202**, 012 (2012), 1201.2460.

[107] S. Cullen and M. Perelstein, *SN1987A constraints on large compact dimensions*, Phys. Rev. Lett. **83**, 268 (1999), hep-ph/9903422.

[108] ATLAS collaboration, CERN preprint ATLAS-CONF-2011-096 (2011).

[109] ATLAS collaboration, G. Aad *et al.*, *Search for new phenomena with the monojet and missing transverse momentum signature using the ATLAS detector in $\sqrt{s}$ = 7 TeV proton-proton collisions*, Phys. Lett. **B705**, 294 (2011), 1106.5327.

[110] CMS collaboration, CERN preprint CMS-PAS-EXO-11-059 (2011).

[111] CMS collaboration, S. Chatrchyan *et al.*, *Search for new physics with a monojet and missing transverse energy in pp collisions at $\sqrt{s}$ = 7 TeV*, Phys. Rev. Lett. **107**, 201804 (2011), 1106.4775.

[112] ATLAS collaboration, G. Aad *et al.*, *Search for extra dimensions using diphoton events in 7 TeV proton-proton collisions with the ATLAS detector*, (2011), 1112.2194.

[113] CMS collaboration, S. Chatrchyan *et al.*, *Search for signatures of extra dimensions in the diphoton mass spectrum at the Large Hadron Collider*, (2011), 1112.0688.

[114] CMS collaboration, S. Chatrchyan *et al.*, *Search for large extra dimensions in dimuon and dielectron events in pp collisions at* $\sqrt{s} = 7$ *TeV*, (2012), 1202.3827.

[115] R. Contino *et al.*, *Graviton loops and brane observables*, JHEP **0106**, 005 (2001), hep-ph/0103104.

[116] K. R. Dienes, E. Dudas and T. Gherghetta, *Light neutrinos without heavy mass scales: A higher-dimensional seesaw mechanism*, Nucl. Phys. **B557**, 25 (1999), hep-ph/9811428.

[117] F. del Aguila and J. A. Aguilar-Saavedra, *Distinguishing seesaw models at LHC with multi-lepton signals*, Nucl. Phys. **B813**, 22 (2009), 0808.2468.

[118] N. Haba, S. Matsumoto and K. Yoshioka, *Observable seesaw and its collider signatures*, Phys. Lett. **B677**, 291 (2009), 0901.4596.

[119] F. Zwicky, *Spectral displacement of extra galactic nebulae*, Helv. Phys. Acta **6**, 110 (1933).

[120] V. C. Rubin, N. Thonnard and W. K. Ford, Jr., *Rotational properties of 21 Sc galaxies with a large range of luminosities and radii, from NGC 4605 (R = 4 kpc) to UGC 2885 (R = 122 kpc)*, Astrophys. J. **238**, 471 (1980).

[121] J. A. Tyson, G. P. Kochanski and I. P. Dell'Antonio, *Detailed mass map of CL0024+1654 from strong lensing*, Astrophys. J. **498**, L107 (1998), astro-ph/9801193.

[122] B. Moore and J. Diemand, Simulations of cold dark matter haloes, Particle dark matter: Observations, models and searches, edited by G. Bertone, pp. 14–37, Cambridge University Press, 2010.

[123] EROS-2 collaboration, P. Tisserand *et al.*, *Limits on the Macho content of the galactic halo from the EROS-2 survey of the magellanic clouds*, Astron. Astrophys. **469**, 387 (2007), astro-ph/0607207.

[124] M. Milgrom, *A modification of the Newtonian dynamics as a possible alternative to the hidden mass hypothesis*, Astrophys. J. **270**, 365 (1983).

[125] D. Clowe *et al.*, *A direct empirical proof of the existence of dark matter*, Astrophys. J. **648**, L109 (2006), astro-ph/0608407.

[126] P. Natarajan and H. Zhao, *MOND plus classical neutrinos not enough for cluster lensing*, (2008), 0806.3080.

[127] M. Shaposhnikov, Sterile neutrinos, Particle dark matter: Observations, models and searches, edited by G. Bertone, pp. 228–248, Cambridge University Press, 2010.

[128] Supernova Cosmology Project, S. Perlmutter *et al.*, *Measurements of* Ω *and* Λ *from 42 high-redshift supernovae*, Astrophys. J. **517**, 565 (1999), astro-ph/9812133.

[129] WMAP collaboration, D. Spergel *et al.*, *First year Wilkinson Microwave Anisotropy Probe (WMAP) observations: Determination of cosmological parameters*, Astrophys. J. Suppl. **148**, 175 (2003), astro-ph/0302209.

[130] K. Griest and D. Seckel, *Three exceptions in the calculation of relic abundances*, Phys. Rev. **D43**, 3191 (1991).

[131] N. Arkani-Hamed, A. G. Cohen and H. Georgi, *Electroweak symmetry breaking from dimensional deconstruction*, Phys. Lett. **B513**, 232 (2001), hep-ph/0105239.

[132] N. Arkani-Hamed *et al.*, *Phenomenology of electroweak symmetry breaking from theory space*, JHEP **08**, 020 (2002), hep-ph/0202089.

[133] N. Arkani-Hamed *et al.*, *The minimal moose for a little Higgs*, JHEP **08**, 021 (2002), hep-ph/0206020.

[134] N. Arkani-Hamed *et al.*, *The littlest Higgs*, JHEP **07**, 034 (2002), hep-ph/0206021.

[135] P. Sikivie, Axions, Particle dark matter: Observations, models and searches, edited by G. Bertone, pp. 204–227, Cambridge University Press, 2010.

[136] R. D. Peccei and H. R. Quinn, *CP conservation in the presence of instantons*, Phys. Rev. Lett. **38**, 1440 (1977).

[137] D. E. Kaplan, M. A. Luty and K. M. Zurek, *Asymmetric dark matter*, Phys. Rev. **D79**, 115016 (2009), 0901.4117.

[138] G. Servant and T. M. P. Tait, *Elastic scattering and direct detection of Kaluza–Klein dark matter*, New J. Phys. **4**, 99 (2002), hep-ph/0209262.

[139] F. Burnell and G. D. Kribs, *The abundance of Kaluza–Klein dark matter with coannihilation*, Phys. Rev. **D73**, 015001 (2006), hep-ph/0509118.

[140] K. Kong and K. T. Matchev, *Precise calculation of the relic density of Kaluza–Klein dark matter in universal extra dimensions*, JHEP **01**, 038 (2006), hep-ph/0509119.

[141] M. Kakizaki *et al.*, *Significant effects of second KK particles on LKP dark matter physics*, Phys. Rev. **D71**, 123522 (2005), hep-ph/0502059.

[142] M. Kakizaki *et al.*, *Relic abundance of LKP dark matter in UED model including effects of second KK resonances*, Nucl. Phys. **B735**, 84 (2006), hep-ph/0508283.

[143] M. Kakizaki, S. Matsumoto and M. Senami, *Relic abundance of dark matter in the minimal universal extra dimension model*, Phys. Rev. **D74**, 023504 (2006), hep-ph/0605280.

[144] G. Belanger, M. Kakizaki and A. Pukhov, *Dark matter in UED: The role of the second KK level*, JCAP **1102**, 009 (2011), 1012.2577.

[145] S. Arrenberg *et al.*, *Kaluza–Klein dark matter: Direct detection vis-a-vis LHC*, Phys. Rev. **D78**, 056002 (2008), 0805.4210.

[146] B. A. Dobrescu *et al.*, *Spinless photon dark matter from two universal extra dimensions*, JCAP **0710**, 012 (2007), 0706.3409.

[147] J. F. Navarro, C. S. Frenk and S. D. White, *The Structure of cold dark matter halos*, Astrophys. J. **462**, 563 (1996), astro-ph/9508025.

[148] J. Einasto, *Dark matter*, (2009), 0901.0632.

[149] XENON100 collaboration, E. Aprile *et al.*, *Dark matter results from 100 live days of XENON100 data*, Phys. Rev. Lett. (2011), 1104.2549.

[150] CDMS-II collaboration, Z. Ahmed *et al.*, *Dark matter search results from the CDMS II experiment*, Science **327**, 1619 (2010), 0912.3592.

[151] A. Desai, Dmtools, http://dmtools.brown.edu/, 2012.

[152] DAMA collaboration, R. Bernabei *et al.*, *First results from DAMA/LIBRA and the combined results with DAMA/NaI*, Eur. Phys. J. **C56**, 333 (2008), 0804.2741.

[153] G. Angloher *et al.*, *Results from 730 kg days of the CRESST-II dark matter search*, (2011), 1109.0702.

[154] C. Aalseth *et al.*, *Search for an annual modulation in a P-type point contact germanium dark matter detector*, Phys. Rev. Lett. **107**, 141301 (2011), 1106.0650.

[155] IceCube collaboration, R. Abbasi *et al.*, *Multi-year search for dark matter annihilations in the Sun with the AMANDA-II and IceCube detectors*, Phys. Rev. **D85**, 042002 (2012), 1112.1840.

[156] ANTARES collaboration, G. Lim, *First results on the search for dark matter in the Sun with the ANTARES neutrino telescope*, (2009), 0905.2316.

[157] Super-Kamiokande collaboration, T. Tanaka *et al.*, *An indirect search for WIMPs in the Sun using 3109.6 days of upward-going muons in Super-Kamiokande*, Astrophys. J. **742**, 78 (2011), 1108.3384.

[158] F. Halzen and D. Hooper, *Prospects for detecting dark matter with neutrino telescopes in light of recent results from direct detection experiments*, Phys. Rev. **D73**, 123507 (2006), `hep-ph/0510048`.

[159] D. Hooper and G. D. Kribs, *Probing Kaluza–Klein dark matter with neutrino telescopes*, Phys. Rev. **D67**, 055003 (2003), `hep-ph/0208261`.

[160] T. Flacke *et al.*, *Kaluza–Klein dark matter and neutrinos from annihilation in the Sun*, (2009), `0908.0899`.

[161] IceCube collaboration, R. Abbasi *et al.*, *Limits on a muon flux from Kaluza–Klein dark matter annihilations in the Sun from the IceCube 22-string detector*, Phys. Rev. **D81**, 057101 (2010), `0910.4480`.

[162] Fermi-LAT collaboration, `http://fermi.gsfc.nasa.gov/`.

[163] H.E.S.S. collaboration, A. Abramowski *et al.*, *Search for a dark matter annihilation signal from the galactic center halo with H.E.S.S*, Phys. Rev. Lett. **106**, 161301 (2011), `1103.3266`.

[164] MAGIC collaboration, J. Aleksic *et al.*, *Searches for dark matter annihilation signatures in the Segue 1 satellite galaxy with the MAGIC-I telescope*, JCAP **1106**, 035 (2011), `1103.0477`.

[165] VERITAS collaboration, V. A. Acciari *et al.*, *VERITAS search for VHE gamma-ray emission from dwarf spheroidal galaxies*, Astrophys. J. **720**, 1174 (2010), `1006.5955`.

[166] S. Kabuki *et al.*, *CANGAROO-III search for gamma rays from Centaurus A and the Omega Centauri region*, Astrophys. J. **668**, 968 (2007), `0706.0367`.

[167] L. Bergström *et al.*, *Gamma rays from Kaluza–Klein dark matter*, Phys. Rev. Lett. **94**, 131301 (2005), `astro-ph/0410359`.

[168] L. Bergström *et al.*, *Two photon annihilation of Kaluza–Klein dark matter*, JCAP **0504**, 004 (2005), `hep-ph/0412001`.

[169] G. Bertone *et al.*, *Gamma ray lines from a universal extra dimension*, JCAP **1203**, 020 (2012), `1009.5107`.

[170] P. Salati, F. Donato and N. Fornengo, Indirect dark matter detection with cosmic antimatter, Particle dark matter: Observations, models and searches, edited by G. Bertone, pp. 521–546, Cambridge University Press, 2010.

[171] PAMELA collaboration, O. Adriani *et al.*, *An anomalous positron abundance in cosmic rays with energies 1.5-100 GeV*, Nature **458**, 607 (2009), `0810.4995`.

[172] J. Chang *et al.*, *An excess of cosmic ray electrons at energies of 300-800 GeV*, Nature **456**, 362 (2008).

[173] D. Hooper and K. M. Zurek, *The PAMELA and ATIC signals from Kaluza–Klein dark matter*, Phys. Rev. **D79**, 103529 (2009), 0902.0593.

Part II

Scientific papers

1

Paper 1

Mattias Blennow, *Henrik Melbéus*, and Tommy Ohlsson
Neutrinos from Kaluza–Klein dark matter in the Sun
Journal of Cosmology and Astroparticle Physics **01**, 018 (2010)

2

Paper 2

Johan Bonnevier, *Henrik Melbéus*, Alexander Merle, and Tommy Ohlsson

Monoenergetic gamma-rays from non-minimal Kaluza–Klein dark matter annihilations

Physical Review D **85**, 043524 (2012)

Paper 3

Henrik Melbéus, Alexander Merle, and Tommy Ohlsson
Continuum photon spectrum from $Z^1\,Z^1$ annihilations in universal extra dimensions
Physics Letters B **706**, 329-332 (2012)

3

Paper 4

Henrik Melbéus, Alexander Merle, and Tommy Ohlsson
Higgs Kaluza–Klein dark matter in universal extra dimensions
Manuscript

4

Paper 5

Mattias Blennow, *Henrik Melbéus*, Tommy Ohlsson, and He Zhang
Signatures from an extra-dimensional seesaw model
Physical Review D **82**, 045023 (2010)

5

Paper 6

Mattias Blennow, *Henrik Melbéus*, Tommy Ohlsson, and He Zhang
Renormalization group running of the neutrino mass operator in extra dimensions
Journal of High Energy Physics **04**, 052 (2011)

6

Paper 7

Mattias Blennow, *Henrik Melbéus*, Tommy Ohlsson, and He Zhang
RG running in UEDs in light of recent LHC Higgs mass bounds
Submitted for publication.

7

Paper 8

Henrik Melbéus and Tommy Ohlsson
Searches for hyperbolic extra dimensions at the LHC
Journal of High Energy Physics **08**, 077 (2008)

8